DIVERGENT FUNCTIONS OF NLRP7 IN EMBRYOGENESIS, INFLAMMATION AND ONCOGENESIS

by

Aybüke Garipcan

B.S., Biology, Ankara University, 2009

M.S., Bioengineereing, Hacettepe University, 2011

Submitted to the Institute for Graduate Studies in
Science and Engineering in partial fulfillment of
the requirements for the degree of
Doctor of Philosophy

Graduate Program in Molecular Biology and Genetics

Boğaziçi University

2019

"It is good to have an end to journey toward; but it is the journey that matters, in the end." Ursula K. Le Guin

ACKNOWLEDGEMENTS

I would like to sincerely thank my supervisor Prof. Nesrin Özören for giving me the opportunity to conduct this work under her supervision. She encouraged and supported me to follow my curiosity throughout my PhD studies from the beginning until the very end.

I am truly grateful to Asst. Prof. T.Tamer Önder for allowing me to perform iPSC studies and providing me with his precious guidance during my studies. I am also thankful to Assoc. Prof. N.C.Tolga Emre for monitoring my progresses, for his valuable time and advices. I would also like to thank Prof. Devrim Gozuacik and Assoc. Prof. Umut Sahin for sparing their valuable time to evaluate my thesis.

Besides, I would like to express my special thanks to my former project partners, Duygu Demiroz-Bas and Mustafa Yalcinkaya for teaching me many of the techniques I know and for their intellectual contributions to my thesis. I also thank to my current project partners, Burcu Ozcimen for her great effort and support with iPSC studies and Ilke Suder for helping me with iPSC studies. Also, I want to thank Efe Elbeyli for helping me with bioinformatic analyses.

I would also thank to my former lab members, Serkan Ugurlu and Alican Sahillioglu for their friendship and helping me with the techniques. I would like to thank our special project students Orhun Kulekci, Ozan Kucukkase, Alper Cevirgel, Aybeg Gonenc and especially Onur Eskiocak for their friendship and help. I also thank to former and current AKIL members, Seda Yasa, Elif Eren, Hulusi Onur Kuzucu, Olay Artik, Ozen Kaya, Aylin Alkan, Ozan Oztas and Davod Khalafkhany. I would specially like to thank all MBG family for sharing their knowledge with me and providing me a beautiful work environment.

I am more than grateful to my sisters and brothers in the lab, Mustafa Yalcinkaya, Ekin Ece Erkan, Acelya Yilmazer, Aysin Akpinar, Beren Aylan, Mesut Berber, Can Gurkaslar and Kubra Zirhlioglu, Emre Kirgin who glamorized these years of work with a lot of encouragement, intellectual contribution, friendship and welfare. They were always by my side with their precious scientific and emotional support and always will be.

I am deeply indebted to my parents Husne Alici, Umit Alici for their tremendous love and endless support in every decision I have made. A very special thanks goes to my sister Elif Alici and my brother Burak Alici for transforming even the most stressful times into joyful moments with their energy, support and love. I also thank to Garipcan family for their sincere love and support. Lastly, I would like to express my deepest gratitude to the hero behind this thesis, my beloved Bora. He was there all the time for me to make my entire life beautiful and to make my dreams come true with his guidance, patience and love.

ABSTRACT

DIVERGENT FUNCTIONS OF NLRP7 IN EMBRYOGENESIS, INFLAMMATION AND ONCOGENESIS

NLRP7 is a novel protein about which we have limited information. To date, mutations in NLRP7 gene have been associated with recurrent Complete Hydatidiform Mole (RCHM) and NLRP7 is accepted to be the first causative gene for RHM. CHM is a gestational disease characterized by hyper trophoblast proliferation with no embryo formation. Furthermore, NLRP7 expression was found to be elevated in testicular seminoma, endometrium cancer and embryonal carcinoma. Yet, the possible mechanisms of action of NLRP7 in these biological conditions or pathways have not been enlightened. In this thesis, we generated patient derived induced Pluripotent Stem Cells (iPSC) to address the role of NLRP7 in HM. We revealed that inadequate NLRP7 levels expedited the differentiation of iPSCs towards the trophoblasts through BMP4. Recovery of NLRP7 expression or BMP pathway inhibition decelerated excessive differentiation of patient iPSCs to trophoblasts. Also, as NLRP7 is an NOD Like Receptor Family member, it is expected to play a role in innate immunity. We have found that infection of human monocytic cells with *Pseudomonas aeruginosa* activated the NLRP7 inflammasome followed by increased IL-1β secretion. Clearly, stable overexpression of NLRP7 is correlated with increased secretion of pro-inflammatory cytokines such as; TNF-alpha, IL-6, i-309. In addition, to elucidate the possible proto-oncogenic role of NLRP7 in tumorogenesis, we performed xenograft experiments in vivo. We found that stable expression of NLRP7 in the endometrial cancer cell line (Hec1a) resulted in increased tumor growth. Furthermore, potential interaction partners of NLRP7 were identified after co-immunoprecipitation followed by mass spectrometry. Our results shed further light to the overlapping and diverging molecular pathways regulated by NLRP7 in embryogenesis, inflammation and oncogenesis.

ÖZET

NLRP7'NİN EMBRYOGENEZ, ENFLAMASYON VE ONKOGENEZDEKİ FARKLI FONKSİYONLARI

NLRP7 hakkında kısıtlı bilgiye sahip olduğumuz yeni bir proteindir. Bu güne kadar, NLRP7 mutasyonları rekürren komplet Hidatidiform mole (RKHM) sebep olan ilk gen olarak belirlenmiştir. RKHM embryo oluşumu gözlenmeyen ve hipertrofik trophoblast proliferasyonu ile takip eden hamilelikler olarak tanımlanmıştır. Bunun yanı sıra, NLRP7'nin gen ifadesi testiküler seminoma, endometriyum ve embiryonal karsinomalarda fazla bulunmuştur. Fakat, NLRP7'nin bu yolaklardaki muhtemel çalışma mekanizması henüz aydınlatılamamıştır. Bu tezde, NLRP7'nin RHM'deki görevini ortaya çıkarmak üzere hastaya özel indüklenmiş pluripotent kök hücreler (iPKH) geliştirilmiş ve yetersiz NLRP7 seviyelerinin BMP4 yolakları üzerinden iPKH'lerin trofoblastlara farklılaşmasını arttırdığını ortaya çıkarılmıştır. NLRP7'nin gen ifadesinin geri kazandırılması veya BMP yolaklarının baskılanması hastadan elde edilen hücrelerdeki artmış trofoblast farklılaşmasını geri çevirebilmiştir. Bunun yanı sıra NLRP7'nin NOD benzeri alıcılar ailesi üyesi olması sebebiyle doğuştan gelen bağışıklık sisteminde de görev alması beklenmektedir. Bu calişmada *Pseudomonas aeruginosa*'nın NLRP7 inflamazomunu aktive ederek IL-1β salımına sebep olduğu bulunmuştur. Sürekli NLRP7 ekspresyonu TNF-alpha, IL-6, i-309 gibi pro-inflamatuar sitokinlerin salımıyla korelasyon göstermiştir. Bunun yanı sıra NLRP7'nin potansiyel proto-onkogenik rolünü ortaya çıkarmak için *in-vivo* tümör zenogreft deneyleri gerçekleştirilmiştir. Sürekli NLRP7 ifade eden endometriyum kanser hücrelerinde tümör oluşumunun arttığı gösterilmiştir. Bu hücrelerde yapılan beraber immün çöktürme sonucunda gercekleştirilen kütle spektreskopisi NLRP7'nin potansiyel etkileşim ortaklarını ortaya çıkarmıştır. Sonuçlarımız, NLRP7'nin embiryogenezde, enflamasyonda ve onkogenezde, kesişen ve farklılık gösteren moleküler yolaklarda görev aldığını ortaya koymuştur.

TABLE OF CONTENTS

LIST OF FIGURES

LIST OF TABLES

LIST OF SYMBOLS

°C	Degree Celcius
h	Hour
g	Gram
g	Gravity
kDa	Kilodalton
L	Liter
M	Molar
mg	Miligram
mM	Milimolar
mm	Milimeter
ml	Mililiter
min	Minute
ng	Nanogram
rpm	Revolutions per Minute
sec	Second
V	Volt
α	Alpha
β	Beta
γ	Gamma
κ	Kappa
μg	Microgram
μm	Micrometer
μM	Micromolar
μl	Microliter

LIST OF ACRONYMS/ABBREVIATIONS

Ab	Antibody
AD	Acidic Transactivation Domain
ALRs	Absent in melanoma 2 (AIM2)-like receptors
AP	Alkaline Phosphatase
APC	Antigen Presenting Cell
APS	Ammonium Persulfate
ASC	Apoptosis Associated Speck-Like Protein Containing CARD
ATP	Adenosine Triphosphate
BMP4	Bone morphogenic protein4
BSA	Bovine Serum Albumin
CARD	Caspase Activation and Recruitment Domain
CAS9	CRISPR Associated Protein 9
Caspase	Cysteine-Aspartic Protease
cDNA	Complementary DNA
CDX2	Caudal Type Homeobox 2
CLR	C-type Lectin Receptor
CRISPRi	Clustered Regularly Interspaced Short Palindromic Repeats Interference
DAMP	Danger Associated Molecular Patterns
DC	Dendritic Cell
dH_2O	Distilled water
ddH_2O	Double-distilled water
DMEM	Dulbecco's Modified Eagle Mediım
DMSO	Dimethyl Sulfoxide
DNA	Deoxyribonucleic Acid
EDTA	Ethylenediaminetetraacetic Acid
EGFP	Enhanced Green Florescent Protein
ELISA	Enzyme-Linked Immunosorben Assay

FBS	Fetal Bovine Serum
FC	Flow Cytometry
GFP	Green Fluorescence Protein
HBS	Hepes Buffer Saline
HEK293	Human Embryonic Kidney Cells
HM	Hydatidiform Mole
HLA	Human Leukocyte Antigen
IFN	Interferon
IgG	Immunoglobulin G
IκBα	Nuclear factor of kappa light polypeptide gene enhancer in B-cells inhibitor, alpha
IL	Interleukin
KRT7	Cytokeratin7
LB	Luria Broth
LRR	Leucin Reach Repeat
LPS	Lipopolysaccharide
MHC	Major Histocompatibility Complex
MOI	Multiplicity of infection
mRNA	Mesenger RNA
NACHT	Present in NAIP, CIITA, HET-E, and TP1
NaCl	Sodium Chloride
NEAA	Non-esential Amino Acid
NF-κB	Nuclear factor kappa B
NLR	NOD-Like Receptor
NOD	Nucleotide-binding Oligamerization Domain
OCT4	octamer-binding transcription factor 4
OD	Optical Density
PAMP	Pathogen Associated Molecular Pattern
PBS	Phosphate Buffer Saline
PBS-T	Phosphate Buffer Saline and Tween 20
PCR	Polymerase Chain Reaction

PFA	Paraformaldehyde
PMA	Phorbol 12-Myristate 13-Acetate
PRR	Pattern Recognition Receptor
PVDF	Polyvinylidene fluoride
PYD	Pyrin Domain
RLR	RIG-I-like Receptor
RNA	Ribonucleic Acid
RT	Room Temperature
RT-PCR	Reverse Trascriptase PCR
qPCR	Quantitative PCR
SDS	Sodium Dodecyl Sulfate
SDS-PAGE	SDS-Polyacrylamide Gel Electrophoresis
sgRNA	Single Guide RNA
TBS	Tris Buffered Saline
TBST	Tris Buffered Saline and Tween 20
TEMED	N,N,N',N'-Tetramethyl ethylenediamine
TLR	Toll Like Receptor
TNF	Tumor Necrosis Factor
TRP	Trypsin
Tween 20	Polysorbate
v	Volume
w	Weight
WB	Western Blot
WT	Wild Type

1. INTRODUCTION

1.1. Inflammasome

Pathogen recognition receptors (PRRs) of the innate immune cells (macrophages, dendritic cells and neutrophils) are responsible for the detection of pathogen associated molecular patterns (PAMPs) (such as LPS, flagellin) of the invading pathogens or danger associated molecular patterns (DAMPs) (such as ATP, uric acid crystlas) of the damaged cells. These molecules trigger immune responses via pro-inflammatory cytokine secretion such as TNF-α, IL-1β secretion by the innate immune cells to fight the infection. To start the immune response for the clearance of infection, maturation of IL-1β occurs in multi molecular complexes called "inflammasome" [1]. Inflammasomes consist of a sensor protein, which recognizes PAMPs or DAMPs, an adaptor protein ASC and caspase 1 or caspase 5. Upon inflammasome formation in response to pathogens, danger signals or impaired immune response, pro caspase 1 is activated to pro inflammatory cytokines (IL-1β, IL-18) without the need for inflammasome formation [2]. Recent studies show that caspase-11 is able to process pro-IL-1β and induce pyroptosis [3]. NLR protein family members are located in the cytoplasm and assigned for the recognition of invading pathogens or danger signals. NLRs commonly contain a pyrin domain (PYD) or a caspase activation and recruitment domain (CARD), nucleotide binding and oligomerization domain (NOD or NACHT) and leucine rich repeat (LRR) domain. The PYD or CARD domains are responsible for the interactions with ASC or caspase-1, while NACHT mediates oligomerization and LRR senses PAMPs or DAMPs [4]. NACHT/NOD domain as known to contain an ATP binding cassette, thus the oligomerization is ATP driven. In addition to their role of NLRs in immune system, NLRs can also participate in non immune pathways such as proliferation, regulation of cell death or expression of major histocompatibility complex (MHC) [5].

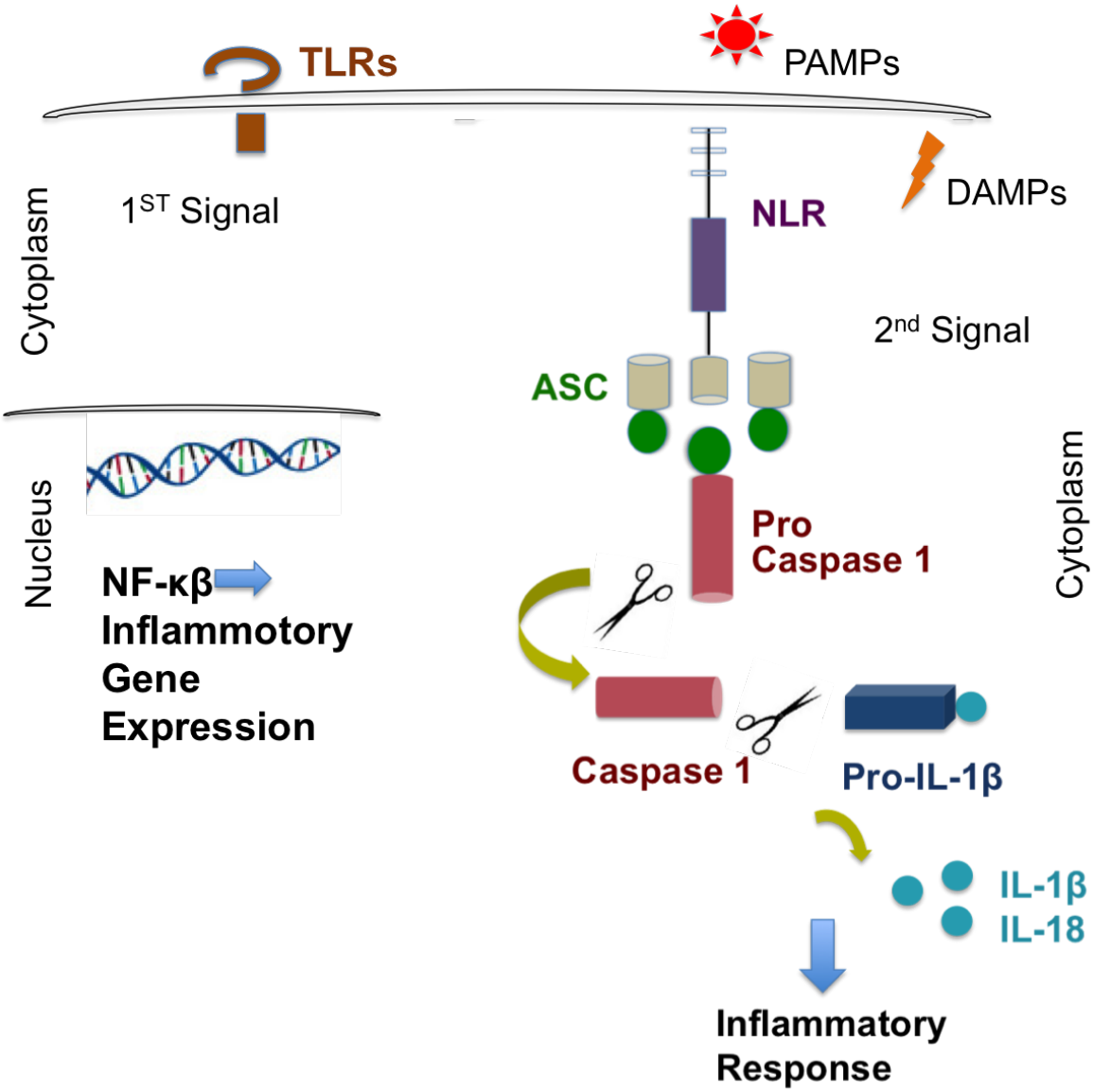

Figure 1.1. Inflammasome activation. Priming singnal drives pro-inflammatory gene expression and activation signal results in inflammasome assembly thereby IL-1β, IL-18 secretion.

1.2. NLRP7

Nucleotide-binding domain and leucine-rich repeat containing gene family member with a pyrin domain 7 (NLRP7, PYPAF3, NALP7, PAN7, NOD12, CLR19.4 and HYDM) belongs to the Nod Like Receptor family. The human NLRP7 gene is located

in locus 19q13.24. The total length of NLRP7 3 different transcript variants can be generated via alternative splicing. All of the isoforms have the characteristic domains of NLRs, which are PYD (pyrin domain), NACHT/NOD (domain present in NAIP, CIITA, HET-E, TP-1), NAD (NACHT-associated domain) and LRR (Leucin Rich Repeat) domains. The NLRP7 gene is found only in humans, chimpanzee, marmoset, rhesus macaque and orangutan and absent in all other species [6].

The first literature data about NLRP7 was published by Kinoshita *et al.* in which they claimed that NLRP7 is an anti inflammatory protein and inhibits IL-1β secretion [7]. They also proposed that NLRP7's mRNA expression is not only specific for immune system cells; it is also expressed in the nervous system and testis. Seven years later, Khare *et al.* showed that NLRP7 is a pro inflammatory protein that forms inflammasomes with ASC and Caspase-1 upon stimulation with microbial acetylated lipoproteins [8]. Its interaction with ASC and Caspase-1 was later verified by Duygu Demiroz Bas in our lab (Master Thesis, 2012) and Pinheiro *et al.* [9]. Another study showed that NLRP7 co-localizes to the Golgi apparatus and the microtubule-organizing center in PBMCs. Messaed et. al suggested that in NLRP7 mutant PBMCs IL-1β processing was not affected but its secretion was diminished, which was linked to its probable role in the trafficking of IL-1β [10]. Also, NLRP7 has been reported to form an inflammasome upon infection with *Mycobacterium bovis* Beijing Strain. Activation of the NLRP7 inflammasome was shown to result in pyroptosis and increased expression of tumor necrosis factor alpha (TNF-α), Chemokine (C-C motif) ligand 3 (CCL3) and IL-1β mRNAs [11]. A recent paper has suggested that NLRP7 is constitutively ubiquitinated and degraded in the endolysosome. Upon stimulation with Toll-like receptor (TLR) agonist bacterial lipopolysaccharide (LPS) and the synthetic acylated lipopeptide Pam3CSK4, STAMBP (the deubiquitinase enzyme) deubiquitinates NLRP7 and inhibits its degradation. Thus, NLRP7 becomes stable and forms inflammasomes which leads to IL-1β secretion. They have also reported a small-molecule inhibitor of STAMBP deubiquitinase activity, BC-1471, to inhibit IL-1β secretion dependent on the NLRP7 inflammasome [12].

In 2006, NLRP7 mutations in women were associated with familial recurrent hydatidiform moles (FRHM), recurrent spontaneous abortions, stillbirths and intrauterine growth retardation. NLRP7 has been accepted to be first maternal effect gene identified in humans. After this publication, many genetic studies were reported showing NLRP7 mutations in FRHM patients. So far, 214 NLRP7 alternative transcripts and at least 59 hereditary mutations have been identified were found to result in familial recurrent hydatidiform moles (FRHM) [13]. These mutations lead to stop codons, small deletions or insertions (less than 20-bp), splicing mutations and large deletions. However, HM can develop via homozygous, compound heterozygous and heterozygous NLRP7 genotypes and also in the lack of NLRP7 mutations, which all show the multifactorial properties of HM [14]. Nacht/NOD domain of NLRP7 was identified to be responsible of the self- oligo-merization of the protein. They showed that certain mutations of NLRP7 linked with hydatidiform moles prevent its oligomerization and therefore cause improper function of NLRP7 [15].

In 2014, Mahadevan *et al.* proposed another non-inflammatory role for NLRP7, where NLRP7 takes a role in the differentiation of human embryonic stem cells into trophoblast cells via interaction with YY-1, a transcription factor. Reduced NLRP7 expression levels in human embryonic stem cells apparently result in changes of DNA methylation, which lead them to differentiate into trophoblasts [16].

Until now, NLRP7 has been showN to localize in Golgi, microtubule organizing center, nuclei, cortical region of oocyte and 2-cell stage embryos with KHDC3L until morula stage then NLRP7 is distributed to the cytoplasm [6, 10, 17].

NLRP7 has been also shown to interact with ZBTB16 which is a transcriptional repressor [18]. ZBTB16 and NLRP7 co-localized in the cytoplasm in juxtanuclear aggregates in overexpression system. However, mutations of NLRP7 observed in HM did not changed interaction potential with ZBTB16. Rather, they showed that when NLRP7 overexpressed, ZBTB16 changed its localization from nucleus to cytoplasm.

Moreover, high expression levels of NLRP7 have been associated with testicular seminoma and embryonal carcinoma [**?**]. Also NLRP7 has a role in the progression of endometrial cancers [19]. NLRP7 was postulated to have a potential role in the proliferation of germ line cells [20].

NLRP7 has been also found to contribute *in vitro* decidualization of endometrial stromal cells. Interestingly, Huang *et al.* showed that NLRP7 promoted the transcription activity of progesterone receptor (PR) and the native NLRP7 relocalized to the nucleus after *in vitro* decidualization of endometrial stromal cells. As a result, they speculated that NLRP7 could be a transcription cofactor of PR [21]. A rare variant of NLRP7 gene has been associated with ulcerative colitis [22].

In 2005, NLRP7 has been found to be highly expressed in undifferentiated embryonal carcinomas along with POU5F1 that encodes OCT3/4, NANOG, DPPA-4 (developmental pluripotency-associated 4) and GAL (Galanin/GMAP Prepropeptide) [**?**] Qin *et al.*, reported that NLRP7 was upregulated in naive pluripotent stem cells along with the genes such as DNMT3L, ID1, NODAL [**?**]. In concerdance with Qin *et al.* and Kilens *et al.*, determined differentially expressed gene candidates overexpressed in epiblast and human induced naive pluripotent stem cells (hiNPSCs) by singe cell RNA-Seq. According to their findings, NLRP7 was found to be upregulated in epiblast and hiNPSCs along with the genes related to RNA binding, such as the DPPA family or the KH-domain proteins KHDC1L, OOEP and KHDC3L. They suggested that those genes might take crucial role in naive pluripotency by mRNA processing [23].

Although the information in the literature about NLRP7 protein and its possible biological functions has growing over the last five years, there are still many questions to answer. Clearly, NLRP7 appears to have critical contributions in several biological functions but comprehensive and detailed understanding of prevalent pathways and mechanisms is still missing.

1.3. Maternal Effect Proteins in NLR Family

Maternal effect genes encode for proteins deposited into oocytes that are required for embryonic development [24]. Mutations in such genes result in embryonic phenotypes that reflect the genotype of the mother rather than that of the offspring [25]. In mice models, null phenotypes of a majority of these genes result in arrested development at very early embryonic time points [26]. NLRP7 gene was the first identified maternal effect gene in humans. In 2006, mutations of NLRP7 was found to be responsible for familial biparental hydatidiform mole (FBHM) [27] which is discussed in the following section in detail. KHDC3L (c6orf221 or ECAT1) was found to be the second causative gene of FRHM. [28] Later, KHDC3L was shown to contribute subcortical maternal complex (SCMC) which is consist of NLRP5, OOEP, KHDC3L and TLE6 in humans.

NLRP5 (mouse ortholog, *Mater*) has been also identified as a maternal effect gene. Xu showed that maternal depletion of NLRP5 blocked early embryogenesis in rhesus macaque monkeys (*Macaca mulatta*) [29]. One publication claimed that mutations in NLRP5 was associated with reproductive wastage and multilocus imprinting disorders in humans [30].

Another NLR family member, Nlrp2 has been referred as a maternal effect gene. Maternal depletion of Nlrp2 caused early embryonic arrest in mouse [31]. In 2009, two patient with Beckwith–Wiedemann syndrome (BWS), which is characterized as fetal overgrowth and human imprinting disorder resulting from the deregulation of a number of genes, was reported to carry NLRP2 mutations [32].

In contrast to mice models of maternal effect genes, embryos of affected women with NLRP7 mutations do not arrest at a very early stage, but rather undergo excessive differentiation and commitment to extraembryonic lineages in vivo.

1.4. Hydatidiform Mole

Molar pregnancy or HM is a subtype of gestational trophoblastic disease along with choriocarcinoma, invasive mole, and placental site trophoblastic tumour. HM can be explained as a pregnancy with no or little embryo and abnormal trophoblast proliferation (both cytotrophoblasts and syncytiotrophoblasts). HM can be classified as partial (excessive trophoblasts with improper embryo) or complete hydatidiform moles (excessive trophoblasts with no embryo) [33]. Partial HM (PHM) usually has maternal and paternal origin with triploid karyotype due to fertilization of an egg with two sperm. On the other hand, complete HM (CHM) has only paternal origin with diploid karyotype (fertilization of an empty ovum by two haploid sperm) while familial recurrent CHMs represent biparental karyotype (FBCHM). Although, the genome of FBCHM consists of both paternal and maternal genomes, gene expression patterns show lack of maternal genome as observed in sporadic androgenetic CHM. DNA methylation at differentially methylated regions (DMRs) of FBCHM substantially displays altered pattern. CHM has a higher risk of malignant transformation to gestational choriocarcinoma (15 percent of CHM) than PHM. Recurrent hydatidiform moles are defined as more than one molar pregnancy in the same patient [34].

In 2006, due to mutations in the NLRP7 gene are identified as the first causative gene for FBCHM. 48-80 percent of patients with recurrent HM (RHM) carry NLRP7 mutations in homozygous or compound heterozygous state. So far, 214 NLRP7 alternative transcripts have been identified and more than 59 hereditary mutations were found to result in familial recurrent hydatidiform moles (FRHM) [14]. Stop codons, small deletions or insertions (less than 20-bp), splicing mutations and large deletions have been identified in the NLRP7 gene of patients with CHM. However, CHM can develop via homozygous, compound heterozygous and heterozygous NLRP7 genotypes and also in the lack of NLRP7 mutations in the coding sequence, which together show the multifactorial genotypes and phenotypes of HM. It is already accepted in the field that NLRP7 is a maternal effect gene and its mutations cause abnormal DNA methylations in imprinted genes. However, recent study showed that DNA methylation

patterns differed at both imprinted and non-imprinted loci in patient born to a mother with NLRP7 mutation [35]. Also Sills *et al.* showed that embryos derived from *in vitro* fertilized oocytes carrying NLRP7 mutation were arrested at or before blastocyst stage [36]

Recently, KHDC3L mutations were also found to be responsible for 10-14 percent of RHM in patients with no NLRP7 mutations [37].

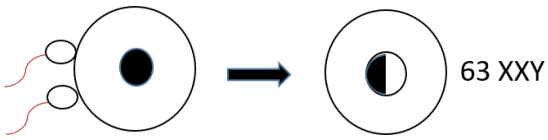

Figure 1.2. Karyotype of Partial Hydatidiform Moles.

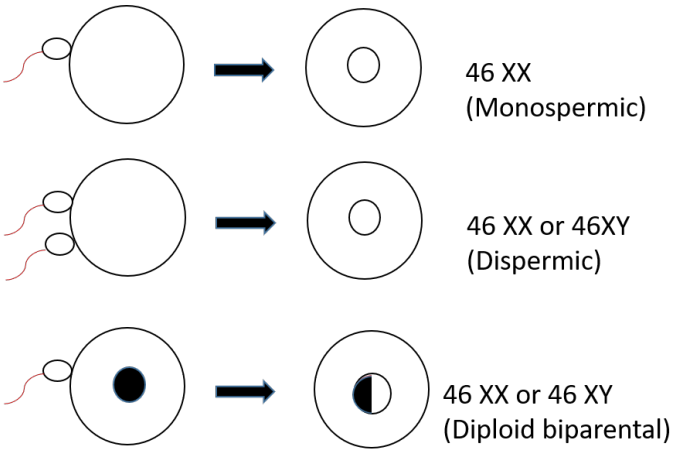

Figure 1.3. Karyotypes of Complete Hydatidiform Moles..

1.4.1. Trophoblast Linage Commitment in Humans

During early embryogenesis, the first cell fate decision is made between the inner cell mass (ICM), precursor of embryo and trophectoderm, progenitor of the placenta. Most of our knowledge about this process is based on mouse experiments. At the

blastocyst stage, some of the cells are allocated to outher layer of blastomere whilst the remaining cells are located in inner sites. This polarization of the cells is presumed as the first signs of differentiation occurring in the blastocyst. Upregulation of caudal type homeobox 2 (Cdx2) and downregulation of Oct4 in proximal cells generating trophectoderm (TE) diverge from Oct4 and Nanog expressing ICM. Cdx2 expression is evident in the outer layer as of 8 cell stage embryos [38]. TE cells of mouse can also be characterized with GATA binding protein 2 (Gata2), human chorionic gonadotropin beta (hCG-β) expressions [39]. However, mouse trophoblast linage commitment differs from that of human and may not represent early human embryogenesis. As mentioned, mouse TE does not express Oct4 and tightly regulated reverse expression pattern of Oct4 and Cdx2 governs the differentiation route towards ICM or TE [40]. Instead, even the expression of OCT4 is lower than ICM, human TE express OCT4 along with CDX2 [41]. The timing of CDX2 expression also differs for human TE, they gain CDX2 expression at blastocyst stage and it is relatively later than mouse cells (8 cell stage). Moreover, human TE cells isolated from blastocysts can be reverted towards ICM-like cells as those cells express NANOG under certain culture conditions implying that cells are not fully committed to trophectoderm in human [42]. On the other hand, the ability of reversible differentiation capability of human TE cells was not observed in mouse TE cells.

Human trophectoderm consists of three main population which are cytotrophoblast (CTB), syncytiotrophoblast (STB) or extravillous trophoblast cells (EVT) [43]. Among these populations, CTBs are mononucleated and expresses CDX2, EGFR and P63 in human TE. CTBs are mostly accepted as trophoblast stem cell population which are proliferative and capable to differentiate to either STB or EVT after implantation. Unlike CTB, STB is deficient in proliferation as they are formed by the fusion of cytotrophoblasts [43]. STB is responsible for gas and nutrient exchange between fetus and mother. These cells serve as the main source of placental hormones and growth factors such as human chorionic gonadotrophin (hCG), placental growth factor (PGF), placental lactogen (hPL) [44]. EVT, which are assigned to model maternal vascular remodeling, is orginated from migrating cytotrophoblast to endometrium. Although,

surface expression of HLA-G expression is particular to EVT, cytotrophoblast cells can contain soluble HLA-G protein [45].

In addition to aforementioned trophoblast subtype specific markers that are widely accepted, several other markers are evident and dedicated to TE linage. Insulin like protein-4 (INSL4), (or Early placenta insulin-like peptide ,EPIL), is a placenta specific marker predominantly expressed by syncytiotrophoblast and cytotrophoblasts [46]. Placental growth Factor (PGF or PIGF) is thought be has roles in trophoblast differentiation and proliferation and expressed mainly by syncytiotrophoblast [47, 48]. Human pregnancy-specific glycoproteins (PSG) take role in immune modulation during pregnancy and syncytiotrophoblast differentiation [49]. Keratin 7 (KRT7) is a widely used pan-trophoblast markers [50].

So far, many experiments were conducted to make explicit human trophoblast differentiation. Inaccessibility of early embryo due to ethical considerations or inability to maintain isolated trophoblast cells *in vitro* prevented to further enlighten human placental development.

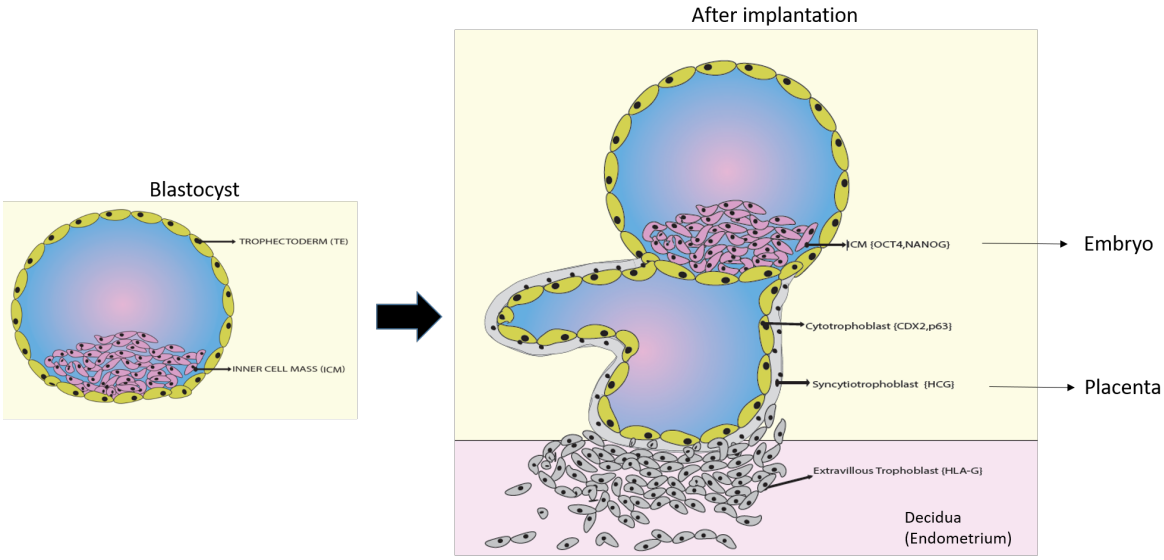

Figure 1.4. Early human embryonic development.

1.5. IPSC Disease Modeling

The derivation of human embryonic stem cells from the embryos is a controversial issue due to ethical considerations and these concerns are restricting the scientific studies. Therefore, reprogramming of somatic cells to be converted to a specific type of stem cells called induced pluripotent stem cells (iPS) provide a unique opportunity to study disease pathology and allows drug screening to develop cell based therapy. iPS cells can be generated from any patient by using Yamanaka factors (OCT 3/4, SOX2, KLF4, c-Myc) and can differentiate into many cell types [51].

Thus far, animals have been used to model different diseases. However, in many cases they may not reflect the accurate results due the differences in between species. Besides, not all animals have the genes that are expressed in humans [52]. For example, NLRP7 protein is a primate specific gene, which makes it impossible to study in animal models except primates and knock in models, which are very expensive procedures. Therefore, IPSCs offer a unique platform to mimic the cells in human disease. Previously published studies of iPS-disease modeling established that iPSCs disease models can be used to reveal disease mechanisms, drug effects and develop new therapeutic agents and patient specific cell therapies [53, 54].

1.5.1. Trophoblast Derivation from Human Embryonic Stem Cells

The first lineage differentiation occurs at blastocyst stage of developing embryo towards inner cell mass (ICM) or trohectoderm (TE). Pathways governing early embryogenesis mostly revealed in mouse. However, early embryogenesis with first cell fate commitment in humans are still recondite event due to ethical restrictions in studying with human embryos. Although, mouse experiments present preliminary aspects on how human cells of pre-implantation embryos decide on differentiation route through TE or ICM, those studies on mouse may not resemble exactly early human embryogenesis due to crucial discrepancies between human and mouse embryogenesis with regard to complex disposition of human embryogenesis and placen-

tation. Several groups were able to isolate trophoblast cells from human placenta and propagate them *in vitro*. Studies with primary trophoblast cells mostly discovered different characteristics of trophoblast subtypes namely, cytotrophoblasts, extra villous trophoblasts and syncytiotrophoblasts. Yet, those studies can not explain prior mechanisms behind trophoblast differentiation. At this stage, establishment of human trophoblast cells from pluripotent stem cells ensure great opportunity to elucidate early embryogenesis and trophoblast differentiation. In 2002, Xu *et al.* stated that hESC expressed trophoblast specific genes when exposed to bone morphogenic protein 4 (BMP4) [55]. Since then, many groups attempted to derivehESC to trophoblast cells by using BMP4 [**?**, 43, 56]. However, several groups claimed that extraembryonal tissues cannot be derived from embryonal cells and trophoblasts generated by BMP4 exposure do not represent proper trophoblast characteristics. These doubts on BMP4 is able to convert cells to trophoblast-like phenotype, is most probably raised from uncertain trophoblast specific features. Lee *et al.*, in 2016, determined four criteria specific to trophoblast cells isolated from human placenta that are expression of trophoblast protein markers and C19MC miRNAs, HLA class I profile, and methylation status of ELF5 promoter [50]. Then, they assessed an embryonal carcinoma (EC) cell line, and trophoblast-like cells induced from BMP4-exposed hESC whether they were capable of meeting these criteria. According to their results, although those cells displayed some features of trophoblasts, they could not totally resemble to primary trophoblast cells. Of note, most of the studies intending to reveal specific features of human trophoblast cells were based on primary isolation of trophoblast cells which were already differentiated. Thus, none of these studies explained first cell fate decision during early embryogenesis. Recently, 3 different publications from Michael Roberts *et al.* unveiled that BMP4 was able to convert hESC towards trophoblast-phenotype when used in combination with ALK/4/5/7 inhibitor, A83-01 (A) and PD173074 (P) FGF2 signaling inhibitor. 24 hours of BMP4/A/P (BAP) treated cells exhibited trophoblast like phenotype by progressive expression of trophoblast specific markers such as; HLA-G, KRT7, CGB, PGF, CDX2 [57]. They also noted that although cell showed trophoblastic characteristics, BMP4 + A83-01+ PD173074 or BMP4+PD173074 treatments resulted in different outcomes regarding to levels of placenta specific hormone

secretion or gene expression [58]. Most recent publication from the same group depicted that continuous BAP exposure rather than 24 hours were able to generate syncytiotrophoblasts coincided with syncytiotrophoblasts isolated from human placenta [59].

2. HYPOTHESIS AND PURPOSE

Hydatidiform mole (HM) is a gestational trophoblastic disease, characterized as a pregnancy with no or little embryo and abnormal trophoblast proliferation. NLRP7 mutations were identified as the first causative gene malformations for HM. Although many genetic studies were reported certain NLRP7 mutations in HM patients, underlying mechanism of HM caused by NLRP7 mutations are still elusive. Analyses based on gene expression databases by using Gene Expression Omnibus (GEO) repository showed that NLRP7 is highly expressed in iPS cells (iPSCs). Concurrently, a recent paper stated that NLRP7 has a role in differentiation of embryonic stem cells into trophoblast cells. Moreover, high expression levels of NLRP7 in endometrium cancers, testicular seminomas and embryonal carcinoma have been reported [**?**, 19, 20]. Therefore we aimed to clarify the functions of NLRP7 in embryogenesis, inflammation and oncogenesis in this PhD study. Accordingly, our specific aims are divided into three sections. For the first part, our purpose is to elucidate the contribution of NLRP7 in HM pathology. Effects of NLRP7 on proliferation in certain cancer cells may have a link with its role in stem cell differentiation. Our initial studies and the data presented in the literature led us to hypothesize that improper expression of NLRP7 may cause HM via differentiation of excessive number of stem cells into trophoblast cells. In order to examine this hypothesis, we decided to utilize iPS cells from a patient who carry NLRP7 heterozygous deletion that generated in the scope of this Ph.D thesis. iPSCs disease modeling technique gave us the chance to mimic hydatidiform moles via differentiation of iPSCs into trophoblast cells by using BMP4.

The second part of the thesis included the characterization of NLRP7 as a member of the inflammasome macromolecular complex. Our group previously showed that NLRP7 is a pro-inflammatory protein and contributes inflammasome assembly by interacting with ASC, Caspase1 and Caspase5 in overexpression conditions. In the literature, NLRP7 inflammasome was found to be activated by *Acholeplasma laidlawii*, *Staphylococcus aureus* and *Mycoplasma bovis*. Here, we investigated novel stimulants

of NLRP7 inflammasome.

In the last part, NLRP7 involvement in oncogenesis was assessed. In the literature, three publications have claimed that NLRP7 has oncogenic roles in testicular seminoma, endometrium cancer and embryonal carcinoma [**?**, 19, 20]. With the light of the studies of Mahadevan *et al.* and our bioinformatics analysis which both indicate that NLRP7 expression is relatively high in embryonic stem cells, we hypothesize that the high expression levels of NLRP7 may have promote proliferation [16]. Thus, NLRP7 overexpression in endometrial cancer cell line (Hec1a) was examined to detect its tendency to promote tumor formation by tumor xenograft experiment in SCID mice. Moreover potential interaction partners of NLRP7 were determined via mass spectrometry.

Elucidating the functions of NLRP7 in human early embryogenesis, inflammation and oncogenesis has critical importance to enlighten the relationship between different pathologies and signaling pathways (such as HM, cancer, embryonic cell differentiation). Tergeting NLRP7 or its partners will ensure certain cancer therapy or provide cell based therapy with iPSCs to prevent HM and related abortions in close future.

3. MATERIALS

3.1. Cell Lines

3.1.1. THP1 Monocytic Cell Line

The THP1 acute monocytic leukemia cell line was kindly provided by Prof. Ahmet Gül from the Istanbul University, (Istanbul, Turkey) and grown in RPMI-1640 including 10% FBS, 1x MEM Non-Essential Aminoacids, 100 U/ml penicillin and 100 μg/ml streptomycin.

3.1.2. Human Embryonic Kidney Cell Line (HEK293FT)

The HEK293FT cell line was kindly provided by Prof. Maria Soengas from the Spanish National Cancer Research Center (CNIO, Madrid, Spain) and grown in DMEM supplemented with 10% FBS, 1x MEM Non-Essential Aminoacids, 100 U/ml penicillin and 100 μg/ml streptomycin.

3.1.3. HEC1A Endometrial Cancer Cell Line

The HEC1A cell line was purchased from the American Type Culture Collection, Virginia, USA and grown in McCoy's 5A modified media including 10% FBS, 1x MEM Non-Essential Aminoacids, 100 U/ml penicillin and 100 μg/ml streptomycin.

3.1.4. Tera-2 Embryonal Carcinoma Cell Line

The tERA-2 cell line was purchased from the American Type Culture Collection, Virginia, USA and grown in McCoy's 5A modified media including 15% FBS, 1x MEM Non-Essential Aminoacids, 100 U/ml penicillin and 100 μg/ml streptomycin.

3.1.5. Swan71 Throphoblast Cell Line

The Swan71 cell line was purchased from the American Type Culture Collection, Virginia, USA and grown in DMEM supplemented with 10% FBS, 2mM L-Glutamine, 1x MEM Non-Essential Aminoacids, 100 U/ml penicillin and 100 μg/ml streptomycin.

3.1.6. F0 Myeloma Cells

F0 myeloma cell line (CRL-1646) was kindly provided by Fatıma Yücel Ph. D. from TUBİTAK Marmara Research Center, (Gebze, Turkey) and grown in DMEM supplemented with 20% FBS, 2mM L-Glutamine, 1x MEM Non-Essential Aminoacids, 100 U/ml penicillin and 100 μg/ml streptomycin..

3.2. Chemicals, Plastics and Glassware

Chemicals purchased from either Sigma (USA), Applichem (Germany) or Merck (Germany) and plastics from TPP (Switzerland), Axygen (USA), or VWR (USA) were used throughout these studies. Before using, glassware, tips and tubes were sterilized by autoclaving at 121°C for 20 minutes.

3.3. Buffers and Solutions

3.3.1. Molecular cloning

Table 3.1: Enzymes used in cloning.

Enzymes/Buffers	**Supplier**
BsmBI FD	Fermantes, USA
EcoRI	NEB, USA
Gateway LR Clonase II Enzyme Mix	ThermoFisher, USA
FastAP	Fermantes, USA

Table 3.1. Enzymes used in cloning (cont.).

FastDigest Buffer	Fermantes, USA
NotI	NEB, USA
T4 DNA Ligase	NEB, USA
T4 DNA Ligase buffer	NEB, USA
T4 PNK	NEB, USA
SalI HF	NEB, USA
XbaI	NEB, USA

3.3.2. Cell Culture

Table 3.2: Cell Culture Chemicals.

Chemicals	**Supplier/ Recipe**
ATP	Sigma, USA
DMSO	AppliChem, Germany
Dulbecco's Modified Eagled Medium	Gibco Invitrogen, USA
Fetal Bovine Serum	Gibco Invitrogen, USA
Gentamicin	Sigma, USA
LPS	Sigma, USA
McCoy's 5A (modified) Medium	Gibco Invitrogen, USA
MEM Non-essential amino acid 100X	Gibco Invitrogen, USA
Penicillin/Streptomycin	Gibco Invitrogen, USA
PBS 10X	80 gr NaCl 2gr KCl 2.4 gr KH_2PO_4 14.4 gr Na_2HPO_4 Add ddH_2O up to 1 lt (pH:7.2)

Table 3.2. Cell Culture Chemicals. (cont.).

PMA	Sigma, USA
Puromycine	Sigma, USA
RPMI Media 1640	Gibco Invitrogen, USA
0.05% TRP with EDTA	0.154 gr EDTA 0.5 gr Trypsin 8 gr NaCl 0.4 gr KCl 0.06 gr KH_2PO_4 1gr Glucose 0.048 gr Na_2HCO_3 Add ddH_2O up to 1 lt Adjust pH to 8 and filter

3.3.3. Transfection and Transduction

Table 3.3: Transfection and Transduction Reagents.

Reagents	**Supplier/ Recipe**
$CaCl_2$	Merck, USA
2X HBS Buffer	50 mM HEPES pH 7.0 280 mM NaCl 1.5 mM Na_2HPO_4
HEPES	Gibco Invitrogen, USA
Polybren	Sigma, USA

3.3.4. Western Blotting

Table 3.4: Chemicals used in WB.

Solutions/Chemicals	**Recipe/Supplier**
Acrylamide: Bisacrylamide	30 gr Acrylamide 0.8 gr Bisacrylamide in 100 ml ddH_2O
Ammonium Persulfate	10 % APS (w/v)
Blocking Solution	5 % Non-fat milk in TBS-T
Bovine Serum Albumin Fraction V	Roche, Germany
Cell Lysis Buffer	0.2 % NP-40 142 mM KCl 5 mM MgCl2 10 mM Hepes 1 mM EDTA
6X Laemmli Sample Buffer	1.2 gr SDS
	6 mg Bromophenol Blue 4.7 ml Glycerol 1.2 ml 0.5 M Tris pH 6.8 500 μl β-mercaptoethanol Add ddH_2O up to 10 ml
Methanol	Merck, USA
2-Propanol	Merck, USA
Protease Inhbitor Cocktail	Roche, Germany
Protein Ladder (PI-26617)	Pierce, USA
PVDF membrane	Merck, USA
SDS	Sigma-Aldrich, USA
10 % Resolving Gel	333 ml Acrylamide: Bisacrylamide 10 ml 10 % SDS 200 ml 1.875 M Tris pH 8.8 Add ddH_2O up to 1 lt

Table 3.4. Chemicals used in WB (cont.).

Running Buffer	1X Tris-Glycine Buffer 0.1 % SDS
15 % Resolving Gel	500 ml Acrylamide: Bisacrylamide 10 ml 10% SDS 200 ml 1.875 M Tris pH 8.8 Add ddH_2O up to 1 lt
4 % Stacking Gel	3.3 ml Acrylamide: Bisacrylamide 6.3 ml 0.5 M Tris-HCl pH 6.8 250 μl 10 % SDS Add ddH_2O up to 25 ml
10X TBS	90 gr NaCl 121.14 gr Tris-Base Add ddH_2O up to 1 lt pH:7.5
TBS-T	1X TBS 0.1 % Tween-20
TEMED	Merck, USA
Transfer Buffer	39 mM Glycine 48 mM Tris-Base 0.0625 % SDS pH:9.2
10X Tris-Glycine Buffer	15 gr Tris-Base 72 gr Glycine Add ddH_2O up to 500 ml
TWEEN-20	Sigma-Aldrich, USA
WesternBright ECL HRP substrate	Advansta, USA
WesternBright Sirius HRP substrate	Advansta, USA

3.3.5. ELISA

Table 3.5: Solutions used in ELISA.

Solutions	**Recipe**
Reagent Diluent	1% BSA in 1X PBS
Stop Solution	2N H_2SO_4
Subsrate Solution	1:1 mixture of Color Reagent A (H_2O_2) and Color Reagent B (Tetrametylbenzidine)
Wash Buffer	0.05 % Tween-20 in 1X PBS

3.3.6. Culture of Bacteria

Table 3.6: Chemicals used in culture of bacteria.

Chemicals	**Recipe/Supplier**
Ampicillin	AppliChem, Germany
Chloramphenicol	Sigma-Aldrich, USA
Kanamycin	Sigma-Aldrich, USA
LB Agar	1 L LB medium 15 g Agar
LB Medium	10 g Tryptone 5 g Yeast Extract 5 g NaCl
20X M9 salts	70 g $Na_2HPO_4 \bullet 7H_2O$ 30 g KH_2PO_4 5 g NaCl 10 g NH4Cl ddH2O up to 500 ml

Table 3.6. Chemicals used in culture of bacteria (cont.).

Modified LB	50 ml 20X M9 salts 10 ml 20% glucose 1X kanamycin 1X chloramphenicol

3.3.7. Protein Purification

Table 3.7: Buffers used in protein purification.

Buffers/Chemicals	**Supplier/ Recipe**
Coomassie Blue Solution	0.1 % Coomassie Brilliant Blue R-250 10 % Acetic Acid 50 % Methanol
Destainin Solution	40 % Methanol 10 % Acetic acid
Dough's Solution	167 mM Tris-HCl (pH 6.8) 0.5 % SDS 10 % Sucrose 25 μl/ml β-mercaptoethanol 0.01 % Bromophenol Blue
Elution Buffer	50 mM Tris-HCl 150 mM NaCl 0.1 mM EDTA pH 7.5
IPTG	Roche, Germany

3.4. Fine Chemicals

3.4.1. Plasmids

Table 3.8: Plasmids.

Plasmids	**Provider**
pcDNA3-Flag-NLRP7	AKIL, Bogazici University
pcDNA3-GFP-NLRP7	AKIL, Bogazici University
pcDNA3-HA-NLRP7	AKIL, Bogazici University
pcDNA3-Myc-NLRP7	AKIL, Bogazici University
pcDNA3-hASC	Nunez Lab, University of Michigan
pcDNA3-Procaspase-1	Nunez Lab, University of Michigan
pet30a-NLRP7	AKIL, Bogazici University
pet30a-NLRP7-PYD	AKIL, Bogazici University
pet30a-NLRP7-NACHT	AKIL, Bogazici University
pet30a-NLRP7-LRR	AKIL, Bogazici University
pCMV6-NLRP2 (RC201357)	Origene, USA
pENTR1A-noCCDB	Tamer Onder Lab, Koc University
pENTR1A-noCCDB-NLRP7	AKIL, Bogazici University
pENTR1A-noCCDB-NLRP7-PYD	AKIL, Bogazici University
pENTR1A-noCCDB-NLRP7-NACHT	AKIL, Bogazici University
pENTR1A-noCCDB-NLRP7-LRR	AKIL, Bogazici University
pENTR1A-noCCDB-NLRP2	AKIL, Bogazici University
plex307	GenReg, Bogazici University
plex307-empty	AKIL, Bogazici University
plex307-NLRP7	AKIL, Bogazici University
plex307-NLRP2	AKIL, Bogazici University
pCW-Cas9	GenReg, Bogazici University
pLKO5.sgRNA.EFS.GFP	GenReg, Bogazici University

3.4.2. Primers

Table 3.9: Primers for RT-qPCR.

Primer ID	**Sequence (5'-3')**	**Application**
BMP4-F	TCCTGGTAACCGAATGCTGA	RT-qPCR
BMP4-R	CCTGAATCTCGGCGACTTTT	RT-qPCR
CDX2-F	GCCAAGTGAAAACCAGGACG	RT-qPCR
CDX2-R	TCCTCCGGATGGTGATGTAG	RT-qPCR
cFOS-F	CCGGGGATAGCCTCTCTTA	RT-qPCR
cFOS-R	GTGGGAATGAAGTTGGCACT	RT-qPCR
CGB-F	GTCAACACCACCATGTGTGC	RT-qPCR
CGB-R	GGTAGTTGCACACCACCTGA	RT-qPCR
δNp63-F	CTGGAAAACAATGCCCAGA	RT-qPCR
δNp63-R	AGAGAGCATCGAAGGTGGAG	RT-qPCR
GABRP-F	GTGGGAAACAGGCTCATCCG	RT-qPCR
GABRP-R	GTTCCAGTCCACGCACAGAG	RT-qPCR
GAPDH-F	GGAGCGAGATCCCTCCAAAAT	RT-qPCR
GAPDH-R	GGCTGTTGTCATACTTCTCATGG	RT-qPCR
HLA-G-F	CTCTCAGGCTGCAATGTGAA	RT-qPCR
HLA-G-R	CATGAGGAAGAGGGTCATGG	RT-qPCR
ID1-F	CAGCCAGTCGCCAAGAAT	RT-qPCR
ID2-R	ACAGACAGCGCACCACC	RT-qPCR
INSL4-F	CCCCATGCCTGAGAAGACAT	RT-qPCR
INSL4-R	GTTGTTGGAGGTTGACACCATT	RT-qPCR
KLF4-F	ACCTACACAAAGAGTTCCCATC	RT-qPCR
KLF4-R	TGTGTTTACGGTAGTGCCTG	RT-qPCR
LIF-F	CCATAATGAAGGTCTTGGCG	RT-qPCR
LIF-R	AGGTACACGACTATGCGGTA	RT-qPCR

Table 3.9. Primers for RT-qPCR (cont.).

Primer ID	**Sequence (5'-3')**	**Application**
NANOG-F	CATGAGTGTGGATCCAGCTTG	RT-qPCR
NANOG-R	CCTGAATAAGCAGATCCATGG	RT-qPCR
NLRP2-F	GCTGCTGTGTTGGTTGTCAG	RT-qPCR
NLRP2-R	GCAGTTCCAAAGCACCAAGG	RT-qPCR
NLRP7-F	TAAGGAATGCGACTGTGAACATC	RT-qPCR
NLRP7-R	TGCTAACTCCGAGTCTTCTTCT	RT-qPCR
PGF-F	TCCTACGTGGAGCTGACGTT	RT-qPCR
PGF-R	CACCTTTCCGGCTTCATCTTC	RT-qPCR
POU5F1-F	GGCTCGAGAAGGATGTGGT	RT-qPCR
POU5F1-R	GCCTCAAAATCCTCTCGTTG	RT-qPCR
PSG4-F	CCAGGGTAAAGCGACCCATT	RT-qPCR
PSG4-R	AAGAATATTGTGCCCGTGGGTT	RT-qPCR
TFAP2A-F	CGGAGGGCGAAGTCTAAAA	RT-qPCR
TFAP2A-R	GTTGGCAGCTTTACGTCTC	RT-qPCR
TFAP2C-F	GGCCCAGCAACTGTGTAAAG	RT-qPCR
TFAP2C-R	ATGTTCGTCTCCAAGACTGG	RT-qPCR
YY1-F	AAGAAGTGGGAGCAGAAGCA	RT-qPCR
YY1-R	GGTCAATGCCAGGTATTCCT	RT-qPCR
ZFP42-F	TGGAGCCTGTGTGAACAGAAC	RT-qPCR
ZFP42-R	CTGGCTCATGTTTTCCTGCCT	RT-qPCR

Table 3.10: shRNA Oligos.

Guide	**Sequence (5'-3')**	**Vector**
SH1-F	CTAGAGAGATGAATCTCACGGAATTGTCCACA-CCACAATTCCGTGAGATTCATCTCTTTTTG	KH1
SH1-R	AATTCAAAAAGAGATGAATCTCACGGAATTGT-GGTGTGGACAATTCCGTGAGATTCATCTCT	KH1
SH2-F	CTAGAGTGTTCCTGGAGAATTACATGGCCACA-CCCCATGTAATTCTCCAGCAACACTTTTTG	KH1
SH2-R	AATTCAAAAAGTGTTCCTGGAGAATTACATGG-GGTGTGGCCATGTAATTCTCCAGCAACACT	KH1
SH3-F	CTAGAGTCAGAGGGTCACATGTTAACACCACA-CCTGTTAACATGTGACCCTCTGACTTTTTG	KH1
SH3-R	AATTCAAAAAGTCAGAGGGTCACATGT TAACA-GGTGTGGTGTTAACATGTGACCCTCTGACT	KH1

Table 3.11: Cloning Primers.

Gene	**Sequence (5'-3')**	**Vector**
NLRP7-F	ATTTGTCGACATGACATCGCCC-CAGCTAG	pENTR1A no ccDB (w48-1)
NLRP7-R	TTATGCGGCCGCTTATCAGCAA-AAAAAGTCACAG	pENTR1A no ccDB (w48-1)
NLRP7/PYRIN-F	ATTTGTCGACATGTCGCCCCAG-CTAGAG	pENTR1A no ccDB (w48-1)
NLRP7/PYRIN-R	TTATGCGGCCGCTTATCAATCT-ATTTCTTGCAC	pENTR1A no ccDB (w48-1)
NLRP7/NACHT-F	AGGTGTCGACATGCCCAGGAAG-CTAACACC	pENTR1A no ccDB (w48-1)

Table 3.11. Cloning Primers (cont.).

Gene	Sequence (5'-3')	Vector
NLRP7/NACHT-R	TTATGCGGCCGCTTATCACTCA-AAGGCACGCAT	pENTR1A no ccDB (w48-1)
NLRP7/LRR-F	AGGTGTCGACATGTTCTGTCTT-GCTTTC	pENTR1A no ccDB (w48-1)
NLRP7/LRR-R	TTATGCGGCCGCTTATCAGATT-TCCAAATTAGT	pENTR1A no ccDB (w48-1)
NLRP2-F	TTACGTCGACAATGGTGTCTTC-GGCGCAGAT	pENTR1A no ccDB (w48-1)
NLRP2-R	TAATGCGGCCGCTTATCAGATC-ATGAAGTCATGAGAA	pENTR1A no ccDB (w48-1)

3.4.3. Antibodies

Table 3.12: Antibodies.

Antibody	Source	Supplier	Dilution
ACTIN (D6A8)	Cell Signalling Technologies, USA	Rabbit	WB: 1:2000
Anti-mouse IgG AlexaFluor488	ThermoFisher Scientific, USA	Donkey	IF: 1:500
Anti-mouse IgG AlexaFluor568	ThermoFisher Scientific, USA	Donkey	IF: 1:500
Anti-rabbit IgG AlexaFluor555	ThermoFisher Scientific, USA	Donkey	IF: 1:500
Anti-mouse IgG HRP	Cell Signalling Technologies, USA	Mouse	WB: 1:2000

Table 3.12. Antibodies (cont.).

Antibody	**Source**	**Supplier**	**Dilution**
Anti-rabbit IgG HRP	Cell Signalling Technologies, USA	Rabbit	WB: 1:2000
Caspase-1 (P10) (A19)	Santa Cruz Biotechnology, USA	Mouse	WB: 1:1000
Caspase-1 (P20) (Bally-1)	Adipogen Life Sciences, USA	Mouse	WB: 1:1000
CDX2 (EPR2764Y)	Abcam, UK	Rabbit	WB: 1:1000 IF: 1:250
HLA-G (4H84)	Santa Cruz Biotechnology, USA	Mouse	WB: 1:1000 IF: 1:100
KRT7 (M7018)	Dako, DNK	Mouse	WB: 1:1000 IF: 1:100
OCT3/4 (C-10)	Santa Cruz Biotechnology, USA	Mouse	WB: 1:1000 IF: 1:100
NLRP2 (PA5-29196)	ThermoFisher Scientific, USA	Rabbit	WB: 1:1000
NLRP7 (C-8)	Santa Cruz Biotechnology, USA	Mouse	WB: 1:1000 IF: 1:100
NLRP7 (Homemade)	AKIL, TUR	Rabbit	WB: 1:1000 IF: 1:100
Pro-IL-1β (3A6)	Cell Signalling Technologies, USA	Rabbit	WB: 1:1000

3.5. Kits

Table 3.13: Kits.

Kits	**Supplier**
DC Protein Assay Kit	Bio-Rad, USA
Direct-zol RNA Miniprep Kit	Zymoresearch
Human CG beta (HCG) DuoSet	R&D Systems, USA
Human IL-β DuoSet	R&D Systems, USA
Human IL-6 DuoSet	R&D Systems, USA
Human PGF Quantikine ELISA Kit	R&D Systems, USA
Human TNF-α DuoSet	R&D Systems, USA
Nucleobond Xtra Plus EF Plasmid Isolation Kit	Macherey Nagel, Germany
Nucleospin Gel and PCR Clean-up Kit	Macherey Nagel, Germany
Nucleospin Plasmid Kit	Macherey Nagel, Germany
SensiFAST cDNA Synthesis Kit	Bioline, UK

3.6. Equipments

Table 3.14: Equipments.

Autoclaves	MAC601, Eyela, Japan ASB260T, Astekk, UK
Centrifuges	Allegra X22-R, Beckman, USA Himac CT4200C, Hitachi Koki, Japan J2-MC Centrifuge, Beckman, USA J2-21 Centrifuge, Beckman, USA
Freezers	2021D, Uğur, Turkey 4250T, Uğur, Turkey

Table 3.14. Equipments (cont.).

Flow cytometer	BD Accuri C6, USA
Incubator	Hepa ClassII Forma Series, Thermo, USA
Heat Block	VWR, USA
Laminar Flow Cabinets	Class II ., Tezsan, Turkey
Micropipettes	Gilson, USA
Microscopes	Zeiss, Acio Observer, Germany Zeiss, Axio Observer Z1, Germany Nikon, Eclipse TS100, Netherlands
Microwave Oven	Arçelik, Turkey
pH Meter	Hanna Instruments, USA
Pipettors	VWR, USA
Plate Reader	VersaMax, Molecular Devices, USA
Power supply	Power Pac Universal, BIO-RAD, USA
SDS-PAGE Electrophoresis System	Mini-Protean 4Cell, BIO-RAD, USA
SDS-PAGE Transfer System	Trans-blot Semi-Dry, USA
Sonicator	SonoPlus, Bandelin, Germany
Spectrophotometer	Nanodrop ND-100 Thermo, USA
Shakers	Polymax 1010, USA Polymax 1040, USA Heildophl, Germany
Vortex	Fisons Whirli Mixer, UK GmcLab, Gilson, USA
Water Bath	GFL, Germany
Water filter	UTES, Turkey
Western Blot Visualization	Syngene GBOX, UK

4. METHODS

4.1. Cell Culture

4.1.1. Maintenance of HEK293FT Cell line

Human Embryonic Kidney cells were cultured in DMEM (41966, Gibco, Life Technologies, USA) supplemented with 10% Fatal Bovine Serum (FBS Gibco, Life Technologies, USA) and Penicillin (100U/mL)-Streptomycin (100μg/mL) (Gibco, Life Technologies, USA) at 37°C, 5% CO_2 and humidified atmosphere. Cells were frozen in DMEM 41966 with 10% DMSO and 10% FBS and stored at -80°C.

4.1.2. Maintenance of THP-1 Cell line

Acute monocytic leukemia THP-1 cells were maintained in RPMI (1460, Gibco, Life Technologies, USA) supplemented with 10% FBS (Gibco, Life Technologies, USA), 2 mM L-Glutamine, 1X MEM Non-Essential Amino acids, 100 U/ml penicillin and 100 μg/ml streptomycin at 37°C and 5% CO2 incubator. Cells were frozen RPMI (1460, Gibco, Life Technologies, USA) with 10% DMSO and 10% FBS and stored at -80°C.

4.1.3. Maintenance of Hec1-a Cell line

Human endometrial cancer cell line Hec-1a was maintained in McCoy's Modified Medium 5A supplemented with 10% Fetal Bovine Serum (FBS), 2 mM L-Glutamine, 1X Non-Essential Amino acids (NEAA), 100 U/ml penicillin and 100 μg/ml streptomycin. Hec-1a cells were grown at 37°C and 5% CO2 incubator. Cells were frozen in McCoy's Modified Medium 5A with 10% DMSO and 10% FBS and stored at -80°C. All the solutions used in cell culture are purchased from Invitrogen, Gibco.

4.1.4. Maintenance of TERA-2 Cell line

Testicular seminoma line Tera-2 was purchased from American Type Culture Collection. Tera-2 cells were grown in McCoy's Modified Medium 5A supplemented with 15% FBS, 2 mM L-Glutamine, 1X MEM Non-Essential Amino acids, 100 U/ml penicillin and 100 μg/ml streptomycin at 37°C and 5% CO2 incubator. Cells were frozen in McCoy's Modified Medium 5A with 15% DMSO and 10% FBS and stored at –80°C.

4.1.5. Maintenance of iPS Cells

iPS cells were cultured on a monolayer of mitomycin-C treated mouse embryonic fibroblast (MEF) feeder cells with hES media in DMEM-F12 (Stemcell Technologies, USA) supplemented with FGF2 (10ng/ml), 1X MEM Non-Essential Amino acids, 1% L-gulatimine (Gibco, Life Technologies, USA), 20% KnockOut Serum Replacement (KnockOut SR Gibco, Life Technologies, USA), 0.1% β-mercapoethanol (for cell culture,Gibco, Life Technologies, USA) and Penicillin (100U/mL)-Streptomycin (100μg/mL) (Gibco, Life Technologies, USA) at 37°C, 5% CO_2 and humidified atmosphere. Cells were frozen in DMEM 41966 with 10% DMSO and 10% FBS and stored at -80°C.

4.2. Cloning

4.2.1. Generation of PENTR1-A NO CCDB - NLRP7

Full lenght NLRP7 were amplified from pcDNA3-Flag-NLRP7 by using Q5 polymerase (NEB) with SalI and NotI restriction sites added primers (Forward: 5' ATTTGT CGACATGACATCGCCCCAGCTAG 3' Reverse: 5' TTATGCGGCCGCTTATCAGC AAAAAAAGTCACAG 3') that were synthetized by Macrogen Korea. Then, NLRP7 was ligated into SalI and NotI digested pENTR1A no ccDB (w48-1) in a 3:1 insert/vector molar ratio. Ligation mix was transformed into Stbl3 bacteria.

4.2.2. Generation of pLEX307-NLRP7

After verification via sequencing of pENTR1A no ccDB (w48-1) / NLRP7 vector as mentioned above, NLRP7 was transferred to lentiviral pLEX-307 vector to generate stably NLRP7 expressing cell lines. Gateway® LR Clonase® II Enzyme mix was used for this purpose. The LR reaction was set up in 50ng pENTR1A no ccDB (w48-1)/ NLRP7 vector, 150ng pLEX-307 vector and 2 l LR Clonase® II Enzyme mix at 25°C for 1 hour. At the end of incubation time, 1l Proteinase K solution was added to reactions and the samples incubated at 37°C for 10 minutes. 1l of reaction was transformed into Stbl3 bacteria. After verification by colony PCR, positive colonies were sequenced.

4.2.3. Generation of PENTR1-A NO CCDB-NLRP2

NLRP2 was cloned into pENTR1A no ccDB (W48-1) to transfer NLRP2 into pLEX-307 (lentiviral mammalian expression vector) by LR reaction. First, NLRP2 cDNA (NLRP2 (NM-017852) Human cDNA ORF clone) was purchased from Origine (USA) and NLRP2 was amplified from commercial plasmid by PCR using SalI and NotI restriction sites added primers. SalI and NotI double digested PCR products were ligated into double digested pENTR1A no ccDB (W48-1) vector that was digested before for NLRP7 cloning into the same vector and positive colonies were verified by colony PCR. Then, positive colonies were sent to sequencing. After sequencing, no SNP or frame shift containing pENTR1A no ccDB (W48-1)/NLRP2 vector was kept to transfer NLRP2 into pLEX-307 vector by LR reaction.

4.3. Development of Stable Cell Lines

4.3.1. Calcium Phosphate Transfection Method in HEK293FT Cells

The cells were seeded one day before transfection into the plates in number depending on purpose and incubated overnight at 37°C, 5% CO2. At the day of transfec-

tion, plasmids were mixed in an eppendorf tube then $CaCl_2$ and 2X HEPES Buffered Saline (HBS) solution were added onto the mix and incubated 10 minutes. Then, the mixture was added drop wise onto cells and the cells were incubated at 37oC, 5% CO_2 incubator. On the following day, transfection efficiency was measured with control GFP plasmid or the fluorescent protein itself.

4.3.2. Lentivirus Production and Transduction

Expression constructs (1500ng) were transfected to 8x10^5 HEK293FT cells together with virus packaging vectors (250ng VSV-g, 750ng pDELTA) by calcium phosphate method explained above. After two days, the supernatants of the cells containing the viral particles were collected and filtered with 0.45 μM filters. Polybreen (4 μg/ml) added the virus particle mixture and added drop by drop onto 8x10^5 cells seeded the day before infection. One day later, virus-containing medium was replaced with fresh medium. After a week, cells were selected with puromycin (1-2 μg/ml).

4.3.3. Recovery of NLRP7 in NLRP7/2Δ IPSCs

NLRP7 or GFP expressing pLEX-307 vectors were transfected to 293FT cells at a density of 2,5x10^6 in 10cm dishes to produce lentiviruses using Fugene (Promega) according to manufacturer‘s protocol. Virus containing medium were collected with 24h intervals for 2 days.

4.3.3.1. Virus Precipitation. 50% PEG-8000 (Sigma) solution in PBS was autoclaved to dissolve and sterilize. After spinning the viral supernatant to disregard dead cells, 40 mL of viral supernatant was loaded a syringe with a 0.45 micron filter and filtered onto 10ml of 50% PEG-8000 in 50 ml falcon tube mixed by inversion. The mixture was stored overnight (or upto 10 days) at °C4 in the dark. The tube was centrifuged at 2500 rpm for 20 minutes. The supernetant was disregarded by leaving a small volume of it (100μl). The tube was centrifuged again at 1200 rpm for 5 minutes and the supernetant was disregarded. Then, 400μl PBS was added and the pellet was dissolved

by pipetting. Each 100μl was aliquoted and stored at 80 °C. iPSCs were infected with obtained viruses two times for 16h.

4.3.4. Generation of NLRP7 Knock-down Cell lines

Three different oligonucleotides targeting NLRP7 SH1, SH2 and SH3 were synthesized by Macrogen Korea. Each pair of oligos were phosphorylated and annealed with 10μM Oligo forward and Oligo reverse, 1μl T4 PNK (NEB), 1l 10X T4 ligation buffer (NEB) and 6,6μl ddH2O. The reaction was put into 37°C for 30 minutes, then 95°C for 5 minutes and then decreased down to 25°C at 5°C/minute. Afterwards, the ligation reaction was done with 2μl EcoRI and XbaI double digested KH1 vector (50ng), 1μl diluted oligo duplex (1:200) from previous step, 1μl 10X T4 DNA ligase buffer, 1 T4 DNA ligase and 5μl ddH2O in room temprature for 10 minutes. Then 5μl of ligation reaction was transformed into Stbl3 bacteria.

4.4. Generation of NLRP7 Knock-out Cell Lines via CRISPR technology

Clustered Regularly Interspaced Short Palindromic Repeat (CRISPR) / CAS9 RNA guided Nucleases (CRISPR/CAS9 system) was used to knock out NLRP7. For this purpose, different target sequences from the first and second exons of the gene of interest were designed in 20-nucleotide length. Then, these target sequences cloned into LentiCRSPR V.2 vector (AddGene 49535) at BsmBI site by Seda Yasa. After successful cloning steps including colony PCR, sequencing, LentiCRSPR virus particles were produced in HEK293 cell line via calcium phosphate transfection with packing plasmids pVSVg (AddGene 8454) and psPAX2 (AddGene 12260) of 1:9 ratio. When the viruses were produced, different cell lines were infected to transduce cells. At last, transduced cells were selected by puromycin.

4.5. Western Blotting

Harvested cells in lysis buffer were centrifuged at 13000 rpm for 30 minutes at 4°C. Supernatant of the cells was suspended with 6X Laemmli sample buffer (1,2 g SDS, 6.0 mg bromophenol blue, 4.7 ml glycerol, 1.2 ml 0,5M Tris pH 6.8, 0.93g DTT, qsp 10 ml water). Then the samples were boiled at 95°C for 10 minutes. SDS gel was poured with 10% resolving gel and 4% stacking gel with 1,5mm thickness. When the polymerization steps were done, the gel was put into a vertical electrophoresis tank and the tank was filled with 1X running buffer (0,9 g Tris-Base, 4,32 g Glycin, 0,1% SDS, ddH2O qsp 3L). Then samples were loaded to the wells of acrylamide gels, samples were run at 80V when the proteins enter the resolving gel, and voltage was set to 120V. Semidry transfer was performed by using Blotting papers (Sigma-Aldrich, USA) and PVDF membrane (Millipore, Ireland) which were cut into proper size. PVDF membrane was activated in methanol and then the filter papers and PVDF membrane were wetted in cold transfer buffer (1,47 g Glycin, 2,91 g Tris, 0,0625% SDS, ddH2O qsp 500 ml). 2 filter papers followed with PVDF membrane were placed to semidry transfer machine, and then the gel was put on the PVDF membrane following with 2 more filter paper. Transfer was performed 10V for 45 minutes. After transfection, the PVDF membrane was blocked with 5% BSA in TBS-T solution (0,9 g NaCl, 10 ml 1M Tris-base pH7,5, 1ml Tween-20, ddH_2O. qsp 1L) for 1 hour at RT by shaking and then incubated with primary antibody which is prepared by dissolving primary antibody with 1:1000 ratio in 5% BSA with sodium azide. Then, unbound and non-specific antibodies were washed three times with TBS-T for 5 minutes. Next the membrane was incubated with 1:2000 HRP-coupled secondary antibody at RT for 1 hour. After repeating three wash step with TBS-T for 5 minutes, membrane was visualized with Stella Raytest machine by using enhanced chemiluminescence system. Densitometry analysis of western blot results was performed with ImageJ v.1.42q software. All measurements were repeated three times.

4.6. Generation of Antibodies aganist NLRP7

4.6.1. IPTG Induction

pET30-NLRP7 vector was transformed into Rosetta DE3 pLysS E. coli bacteria, inoculated into 5 ml Terrific Broth containing kanamycin and chloramphenicol and incubated at 37°C for overnight. On the next day, 5 ml bacterial culture was added into 250 ml Terrific Broth containing kanamycin and chloramphenicol and shaked at 37°C. When OD_{600} was between 0.6-1, 250 μl 1 M IPTG was given to bacterial culture and shaked overnight at 23°C.

4.6.2. NLRP7 Protein Purification from SDS-Gel

Bacterial culture was centrifuged at 7500 g for 10 minutes and the bacterial pellet was suspended with 1X PBS containing 1% Triton X-100. The bacterial suspension was sonicated 10 times, 3 seconds 3x50% power program in ice and centrifuged at 4500 g for 5 minutes. Sonication and centrifugation steps were repeated two more times and the bacterial pellet was collected each time. Triton X-100 makes proteins precipitate more as inclusion body and preliminary purification was achieved and the pellet was finally dissolved into 1X PBS. Dough's Solution was added to the final bacterial suspension and boiled at 90 °C for ten minutes. Then, the protein solution was loaded into 10% polyacrylamide gel with two wells (one small well for ladder and other large well for protein lysate). After electrophoresis for a certain time, the gel was cut from above 100 kDa and below 130 kDa, excised gel was crushed well with elution buffer (50 mM Tris-HCl, 150 mM NaCl, 0.1 mM EDTA pH 7.5) and homogenized gel-buffer solution was shaked at 30°C overnight. On the next day, the solution was centrifuged at 10000g for 10 minutes and the supernatant containing proteins was collected at -20°C. Protein concentration was quantified by comparing with BSA standards via SDS-PAGE.

4.6.3. Immunization

His-tagged NLRP7 purified from gel slices was injected to 5 Balb/c mice and one rabbit for immunization every 15 days during a 45 day procedure. 50 μg NLRP7 was injected with Freud Adjuvant Complete for the first injection and Freud Adjuvant Incomplete for further injections. The injection volume was 400 μl (200 μl+200 μl adjuvant) for rabbit injections and 200 μl (100 μl+100 μl adjuvant) for mice injections. After the injection procedure, blood was taken into tubes containing sodium citrate glucose from animals and blood serum containing our antibodies was obtained by centrifugation at 13000 rpm for 15 minutes. Finally, blood serum was tested via ELISA and Western Blotting and anti-NLRP7 polyclonal serum aliquots were stored at -20 ^{2}C for further studies.

4.6.4. Monoclonal Antibody production via Hybridoma Technology

Monoclonal NLRP7 antibodies were produced via classical Hybridoma Technology which allows fusion of antibody-producing mouse B cells from Balb/c mice with immortal human myelomas in tissue culture conditions. Before fusion procedure, 6000 feeder cells (primary mouse peritoneal macrophages) per well were seeded into 96 well plate. These feeder cells were isolated from different Balb/c mouse by injecting 5 ml DMEM with intraperitoneal injection and taking DMEM back containing blood cells. Then, the cell suspension was centrifuged at 2000 g for 2 minutes, the bigger white cells (peritoneal macrophages) were counted and seeded.

On the next day, our immunized mice were sacrificed and their spleens were isolated for fusion procedure. Single spleen cell suspension was obtained by dissociating isolated spleen mechanically in 1X PBS. Spleen cells were washed two times with 1X PBS by centrifugation at 900 rpm for 10 minutes. In parallel, F 0 myelomas were washed two times. Both cells were counted and they were mixed with 1:5 F 0 myeloma: Spleen cell ratio and centrifuged at 2000 g for 2 minutes. Then, cell pellet was dissolved with 1 ml pre-warmed PEG slowly in 60 seconds and waited for 60 seconds at 37°C.

Then, 4 ml DMEM without FBS and antibiotics was added to the suspension slowly in 2-3 minutes and then 20 ml DMEM without FBS and antibiotics was added slowly in 2-3 minutes. Finally, 20 ml DMEM with 20% FBS was added to the suspension slowly in 2- 3 minutes and waited the mixture at 37°C for 1 hour. After one hour incubation, cells were centrifuged at 2000 g for 2 minutes, suspended with 50 ml DMEM (10% FBS and 1X HAT) and 100 μl cell suspension per well was seeded into 96 well plate containing feeder cell. Ten days after the fusion step, colonies were selected by visual inspection and screened using ELISA.

4.7. Gene Expression Analysis

4.7.1. RNA Extraction

The cells ($1x10^6$) were seeded in a well of 6 well culture dishes. Following to certain treatments, cells were washed with 1 ml PBS and RNA extraction kit (Zymo, USA) was used according to manufacturer,s protocol. Briefly, cells were washed with PBS were lysed with 300 μl Tri reagent (MRC gene, USA). Those lysates were mixed with equal volume of absolute Ethanol. After mixing, RNA solutions were load on the RNA columns. Any contaminant DNA was removed with DNase application. After several washing steps, RNA was eluted with RNase free dH_2O. Extracted RNA was quantified with NanoDrop 2000 (Thermo Scientific, USA) and stored at -80 °C.

4.7.2. cDNA Synthesis

cDNA was synthesized by Sensifast cDNA synthesis kit (Bioline, England) as described by the manufacturer. 1 μg total RNA was mixed with oligo (dt), 5x reaction mix containing and reverse transcriptase enzyme in 20 μl reaction volume. cDNA was synthesized at 46 °C for 20 minutes and reverse transcriptase was inactivated at 95 °C for 1 minute. Produced cDNA was diluted 1:5 and used as template in further qPCR analysis.

4.7.3. Quantitative Reverse Transcription PCR (RT-qPCR)

SYBR Premix Ex Taq (Takara), a SYBR qPCR master mix for real-time RT-PCR (qPCR) were used. 10μl master mix, 2μl cDNA, final 0,5 mM dNTP, are used for all PCRs. Reaction conditions are: 95°C 5 minutes; 35 cycles of 95°C 10 seconds, 61°C 15 seconds, melting 60°C to 94°C, Every 1.0°C. qPCR results were anaylzed by Δ ΔCt method for relative quantifications.

Table 4.1: qPCR Reaction Components.

Conponent	**Volume (μl**
SensiFast SYBR Mastermix (Bioline)	5
Forward primer (10 μM)	0.25
Reverse primer (10 μM)	0.25
1:5 Diluted cDNA	2
dH_2O	2.5
Total	**10**

Table 4.2: qPCR Conditions.

Temperature°C	**Time**	**Cycle**
95	5 min	1
95	10 sec	35
61.5	10 sec	
72	10sec	

4.8. Trophoblast Differentiation

4.8.1. MEF Conditioned Medium Preparation

1 x 106 MEFs were cultured on 10cm plates, in complete MEF medium (10% FBS, DMEM). Next day, the MEF medium was changed with 12 ml 20% KSR hESC medium containing 4 ng/ml bFGF, and incubate for 24 hours at 37°C, 5% CO2. MEF-CM from the plates was collected after 24 hours and 0.22 μM filter sterilized. MEF-CM was used fresh by adding bFGF or stored at -80°C.

4.8.2. Cell Seeding for Trophoblast Differentiation

IPS cells were seeded 2.4 $\times$ 104 cells per square centimeter on matrigel coated plates. On the next day, medium was changed to conditioned medium by a monolayer of γ-irradiated MEF feeder cells containing FGF2 (4 ng/mL).

4.8.3. BAP Treatment

Next day of the seeding, the medium was changed to BMP4 (10 ng/mL), the ALK4/5/7 inhibitor A83-01 (1 μM), and the FGF2-signaling inhibitor PD173074 (0.1 μM) containing (BAP). hESC basal medium not conditioned with MEF feeder cells. Control cultures were grown in the presence of FGF2 and in the absence of BAP. After 24h BAP exposure, medium was changed to MEF-CM with FGF2 (10 ng/mL). Culture medium was replenished daily. For cBAP groups, BAP containing medium was replenished daily. After 4-5 days, cells were trypsinized and transferred to 0.1% gelatin-coated culture dishes. For gene expression studies, half of the cells were collected when the cells were trypsinized.

4.9. Enzyme-linked immunosorbent assays (ELISA)

ELISA is performed with RD DuoSet ELISA Development kit. Diluted to appropriate concentration of samples and standards (100 μl) are transferred on 96 well-plate and incubated overnight at room temperature. The next day, wells are aspirated and washed three times with wash buffer (400 μl) (0.05% Tween 20 in PBS, pH 7,2) and any remaining liquid is removed completely at last wash. The plate is blocked with reagent diluents (300 μl) (1% BSA in PBS pH 7,2-7,4) 1 hour at room temperature. Washing is repeated as mentioned above. Then primary antibody (100 μl) in Reagent Diluent are added to the plate and incubated 2 hours at room temperature. The biotinylated detection antibody (100 μl) is added and incubated 2 hous at room temperature. After washing steps, 100 μl of Streptavidin-HRP is incubated 20 minutes at room temperature by avoiding the plate in direct light. Substrate Solution (100 μl) (1:1 Color Reagent A (H_2O_2): Color Reagent B (Tetramethylbenzidine)) is incubated 20 minutes at room temperature on dark. Stop Solution (50 μl) (2M H_2SO_4) is added and mixed to stop the reaction and optical density of the samples was detected by subtracting the readings at 530 nm from readings at 450 nm within 30 minutes.

4.10. Live Infection

Glycerol stocks of *Staphylococcus aureus* and *Pseudomnas aeruginosa* were taken from -80°C and grown in 10 ml fresh LB broth overnight at 37°C on an orbital shaker.Next day, bacterial cultures were diluted in 1:50 ratio with LB broth and grown until their optical densities were reached to 1 at 600 nm. Then, bacterial cultures were centrifuged at 5000 rpm for 10 minutes at 4°C and washed with cold PBS twice. After washing steps, bacterial pellets were suspended with RPMI-1640 including 10% FBS and 1% MEM-NEA without any antibiotics in certain volumes which were determined according to the count of THP-1 cells and the multiplicity of infection (MOI). When the optical density at 600 nm equals to 1, the bacterial cultures of *S. aureus* and *P. aeruginosa* has 10^7 and 2x10^8 CFU/ml, respectively. Cells were infected with S.aureus (MOI:50) and P.aeruginosa (MOI:10) for 2 hours and then medium replenished with

gentamycin containing medium to remove remaining bacteria for 30 minutes. Medium was collected for analysis of secreted cytokines at the certain time points.

4.11. Cytokine Array

THP1-NLRP7 and THP1 control cells were differentiated with 10 μM PMA for 3 hours and then cells were cultured 48 hours. After 48 hours, the cell supernatant of THP1-NLRP7 and THP1-empty cells was collected. Then, array membranes were incubated with 1X Array blocking buffer for 30 min at RT and after 1 ml of serum for each sample was added onto the membrane and incubate overnight at 4°C. On the next day, the membranes were washed with 1X Array wash buffer I for 5 min three times and with 1X Array wash buffer II for 5 min three times. Then, 1 ml of 1X Biotin-Conjugated Anti-Cytokines was given to each membrane and incubated for 2 hours at RT. The membranes were washed again as mentioned above and 2 ml of 1X HRP-Conjugated Streptavidin was given for 2h incubation at RT. Again, washing steps were repeated, (1:1) mixture of Detection Buffer C and Detection Buffer D was put on the membranes and cytokines were detected by chemiluminescence via CCD cameras of Stella imaging system. In order to analyze the signals of the dot blots each positive control spots (biotin-conjugated IgG) were used to normalize spot densities. Each dot blot signal belonging to a certain cytokine was normalized by dividing them to average of positive signals. Then, fold change in cytokine secretions was calculated by dividing normalized cytokine signals of THP1-NLRP7 sample to THP1-empty ones.

4.12. Membrane-Based Human Inflammation Antibody Array

THP1 cells stably expressing NLRP7 and control THP1 cells were infected with live *P. aeruginosa* in MOI:10. The supernatants were collected and kept at 4°C. The secreted cytokines were detected via Abcam Human Inflammation Antibody Array - Membrane (ab134003). The array membranes were incubated with 1X Array blocking buffer for 30 min at room temperature. After blocking of the membranes, 1 ml of serum for each sample was added onto the membrane and the membranes were incu-

bated overnight at 4°C on an orbital shaker. On the next day, the membranes were washed with 1X Array wash buffer I for 5 min three times and with 1X Array wash buffer II for 5 min two times. Then, 1 ml of 1X Biotin-Conjugated Anti-Cytokines was given to each membrane and the membranes were incubated for 2 hours at room temperature. Then, the membranes were washed again as mentioned above and 2 ml of 1X HRP-Conjugated Streptavidin was given to membranes. After 2h incubation at room temperature, washing steps were repeated. After last washing step, 1:1 mixture of Detection Buffer C and Detection Buffer D was put on the membranes and cytokines were detected by chemiluminescence via CCD cameras of SynGene imaging system. The intensity of each dot was determined via ImageJ and normalized to control dots to obtain comparative cytokine secretions.

4.13. Flow Cytometry

Cells were dispersed by trypsinization and fixed with 4% PFA. Then, the cells were incubated in 500μl of 0.2% TritonX in PBS for 20 min for permeabilization and washed with 1X PBS for 3 times. Then, the cells were blocked in 500 μl of blocking buffer (3% BSA and 5% donkey serum in PBS) for 30min at RT. Cells were centrifuged at 600g for 5 min and supernatant were removed. 1:100 diluted 1°AB and 0,4 μg/ml mouse IgG in blocking buffer were added onto cells and incubated 1hour at RT. Then, cells were washed with 1X PBS for 3 times. The PBS were aspirated. The cells were incubated with 1:500 diluted 2°AB for 30min at RT. After 3 washing steps with PBS, cells were analyzed on an Accuri C6 flow cytometer system (Accuri Cytometers). Final data were prepared in FlowJo software.

4.14. Immunoprecipitation

To perform Immunoprecipitation (IP), 7x106 cells were transfected with 1μg pcDNA3-Flag-NLRP7 plasmid via X-treme GENE HP DNA Transfection Reagent as explained above. After two days of transfection cells were harvested by scraping and washed with cold PBS 3 times. To lyse the cells 0,2% NP40 lysis buffer (0,2%

NP-40, 142 mM, 5mM KCl, 5 mM MgCl2, 10 mM HEPES, 1 mM EDTA, 1 Roche Complete Mini Protease Inhibitor Coktail tablet) was used. The cells were lysed for 30 minutes incubation on ice while vortexing gently and periodically. Then, 30 minutes-centrifugation were performed at 13000 RPM at 4oC. Meanwhile 50 μl of Protein A/G Agarose beads were washed with lysis buffer 3 times. 500 μl of the supernatant was added onto washed Protein A/G Agarose beads. The bead-supernatant mix was incubated on shaker for pre-clearing at room temperature for 30 minutes. Then, centrifugation of the samples was performed for 15 seconds at 13000 RPM at to discard non-specific binding. New 50 μl of Protein A/G Agarose beads were washed with lysis buffer 3 times. Subsequently, pre-cleared lysates and 10 μg antibody (anti-NLRP7 or anti-IgG) were added onto new beads. The bead-supernatant mix was incubated on shaker at 4oC for overnight.

One day after the process mentioned above, the beads containing the antibody-protein complexes were washed three times with lysis buffer and centrifuged 30 second at 6500 RPM. Filtered 4x leamli buffer was added to supernatant and boiled at 95 °C for ten minutes to proceed to SDS-Page. When the pull down of NLRP7 was verified, the samples were analyzed with mass spectrometry.

4.15. Immunostaining

The cells were seeded onto coverslips and next day the cover slips were placed into wells of 12-well plate. Then they were washed with 1X PBS. The cells fixed in 500μl of 4% PFA (kept at +4°C) for 20-30min at RT and washed with 1X PBS for 3 times. The cells were incubated in 500μl of 0.2% TritonX in PBS for 30min for permeabilization and washed with 1X PBS for 3 times. Then, the cells were blocked in 500 μl of blocking buffer (3% BSA and 5% donkey serum in PBS) for 2hours at RT. Next day the blocking buffer was aspirated. The cover slips were closed onto 12μl of 1°AB diluted with PBS and incubated overnight at +4°C. The cover slips were placed into wells of 12-well plate and washed with 1X PBS for 3 times. The PBS were aspirated and closed onto 12μl of 2°AB diluted with PBS. The cover slips were incubated for 3h at +4°C in dark.

The cells were washed again with 1X PBS for 3 times then 100μl of DAPI (1:10000 diluted in PBS) were added. The edges of the cover slip were enclosed with a colorless nail polish. The slides were kept in dark at +4°C. Images were taken by confocal microscope (Leica TCS SP8, USA). Images were processed via ImageJ.

4.16. Statistical Analysis

Statistical analyses were performed by Graphpad Prism 6.0. (San Diago, USA). qPCR and ELISA results were implemented to 2way ANOVA followed by Sidak's multiple comparison test. The bars are presented as the mean ±SD. P values of ¡ 0.05 are considered statistically significant and represented as follows: *p $\leq$ 0.05, **p<0.01, ***p<0.001, ****p<0.0001. All the experiments were conducted at least three times unless indicated otherwise.

5. RESULTS

5.1. Bioinformatic Analysis of NLRP7 Gene Expression

Previous to our study, NLRP7 expression was reported in testicular seminomas, endometrium cancer tissues, human macrophages, THP1 cell line, BMDM, peripheral mononuclear cells, bronchial epithelial Beas2B cells, H9 hESCs and pre-implantation embryos. In addition to the literature, NLRP7 expressing tissues were assessed via Gene Expression Omnibus (GEO) repository. These datasets show the changes in gene expression profile of the gene of interest for a certain published study. Interestingly, NLRP7 expression was identified to be high in induced pluripotent stem cells, especially in IPSCs derived from gronulosa cells when compared to primary papilla cells, foreskin cells (Figure 5.1) [60]. Moreover, human primary cytotrophoblasts, when cultured *in vitro* for the differentiation to syncytiotrophoblasts, expressed more NLRP7 than their first isolated forms. Although NLRP7 levels were not changed in response to Estrogen exposure (Figure 5.2) [61]. Moreover, NLRP7 expression was found to be increased in plasmacytoid dendritic cells (Figure 5.3) [62] and also metaphase II oocytes (Figure 5.4) [63].

5.2. Patient Specific IPSC Derived Hydatidiform Mole Disease Modeling with NLRP7 Deletions

5.2.1. Generation and characterization of patient specific IPSCs

To generate HM-specific human iPSCs, fibroblast cells were obtained from a patient via skin biopsy with a prior diagnosis of HM. The patient was previously reported to carry 60kb deletion which encompasses both *NLRP7* and its adjacent gene, *NLRP2*, in a heterozygous state [64]. Later, Reddy *et al.* investigated this deletion belonging to same patient and identified the borders of the deletion from exon 1 to intron 5 of *NLRP7* (Figure 5.5 and 5.6). Also, unrelated healthy individual was assigned as a

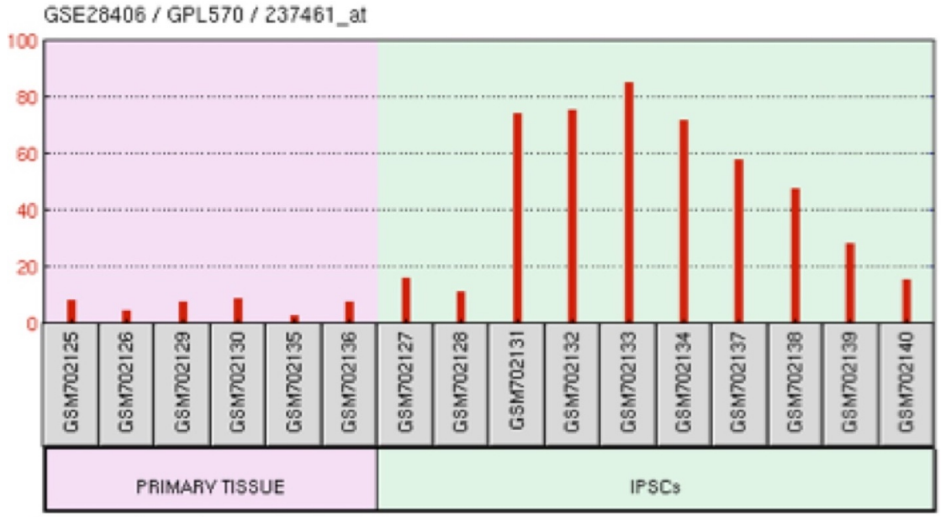

GSM702125	primary dermal papilla cells	male
GSM702126	primary dermal papilla cells	male
GSM702127	induced pluripotency cells from DPC	male
GSM702128	induced pluripotency cells from DPC	male
GSM702129	primary granulosa cells	female
GSM702130	primary granulosa cells	female
GSM702131	induced pluripotency cells from granulosa cells	female
GSM702132	induced pluripotency cells from granulosa cells	female
GSM702133	induced pluripotency cells from granulosa cells	female
GSM702134	induced pluripotency cells from granulosa cells	female
GSM702135	primary foreskin cells	male
GSM702136	primary foreskin cells	male
GSM702137	induced pluripotency cells from foreskin cells	male
GSM702138	induced pluripotency cells from foreskin cells	male
GSM702139	induced pluripotency cells from foreskin cells	male
GSM702140	induced pluripotency cells from foreskin cells	male

Figure 5.1. Human iPSCs showed higher NLRP7 expression. NLRP7 Expression profiling by array in "Characteristic expression of major histocompatibility complex and immune privilege genes in human pluripotent stem cells and the derivatives" study Profile: GSE28406 [**?**]

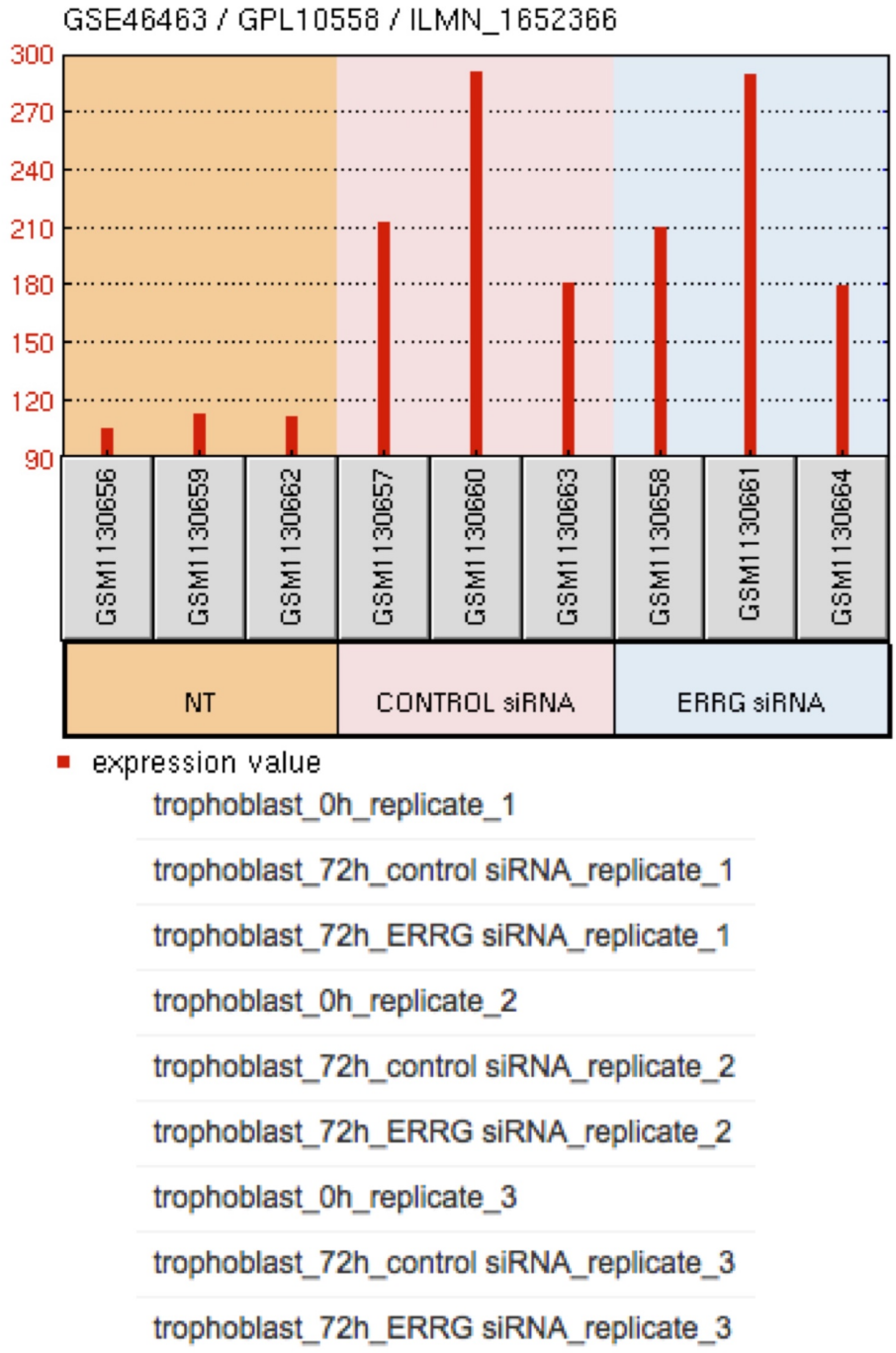

Figure 5.2. NLRP7 expression profiling by array in "Estrogen-Related Receptor γ (ERRγ) Regulates Oxygen-Dependent Expression of Voltage-gated Potassium (K+) Channels and Tissue Kallikrein during Human Trophoblast Differentiation". Profile:GSE46463 [**?**]

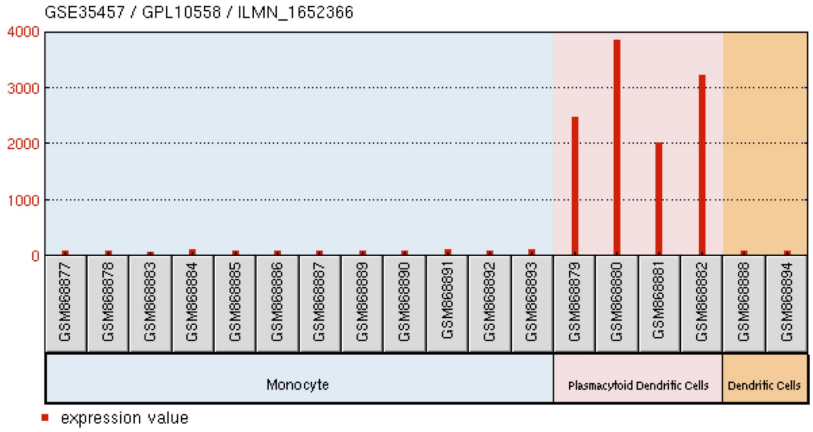

GSM868877	monocyte
GSM868878	monocyte
GSM868879	plasmacytoid dendritic cell
GSM868880	plasmacytoid dendritic cell
GSM868881	plasmacytoid dendritic cell
GSM868882	plasmacytoid dendritic cell
GSM868883	monocyte
GSM868884	monocyte
GSM868885	monocyte
GSM868886	monocyte
GSM868887	monocyte
GSM868888	dendritic cell
GSM868889	monocyte
GSM868890	monocyte
GSM868891	monocyte
GSM868892	monocyte
GSM868893	monocyte
GSM868894	dendritic cell

Figure 5.3. Plasmacytoid dendritic cells expressed eleveted levels of NLRP7 in comparison to monocytes or dendritic cells. NLRP7 expression profiling by array in "human monocyte and dendritic cell subtypes". Profile:GSE35457 [**?**]

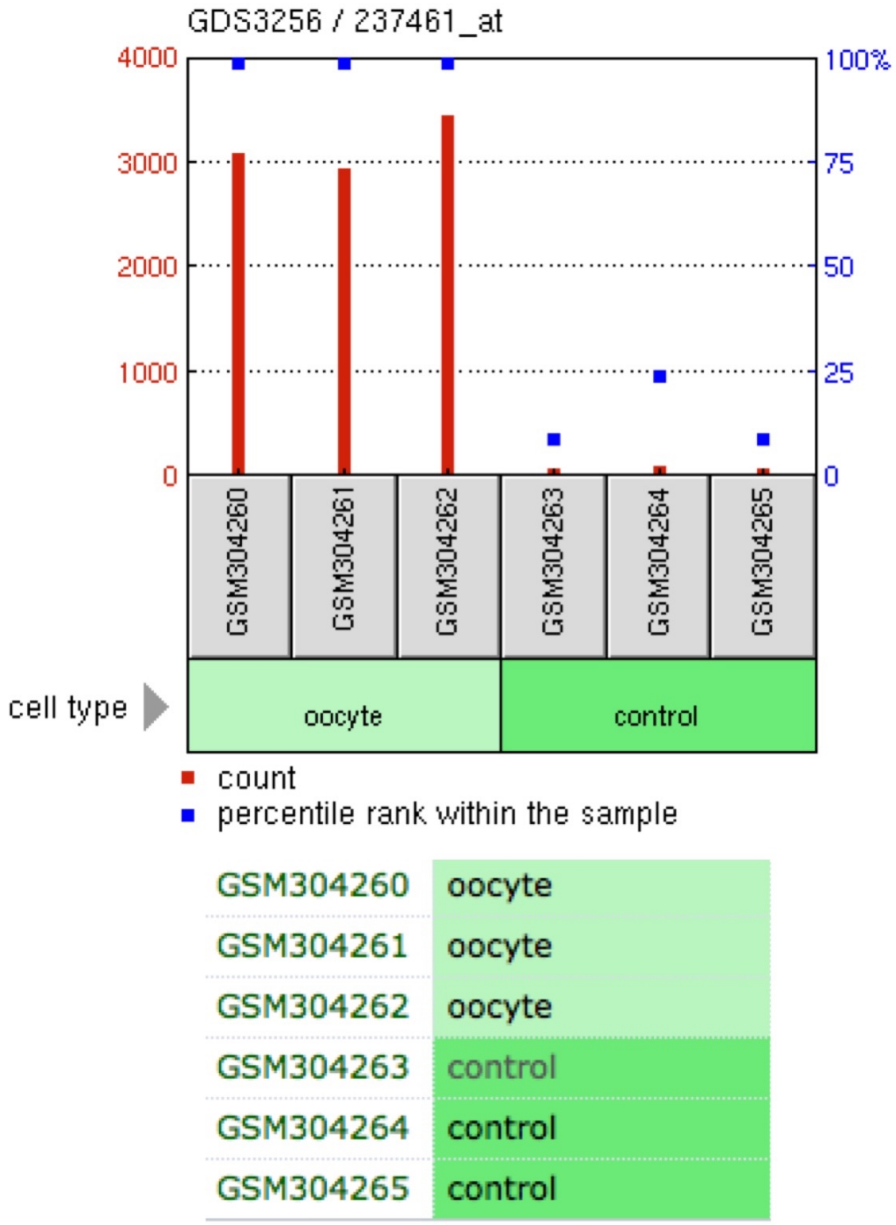

Figure 5.4. Metaphase II stage oocytes express high levels of NLRP7 in comparison to control tissues (kidney, liver,lung etc. NLRP7 expression profiling by array in "Metaphase II stage oocytes matured *in vivo*". Profile:GDS3256 [**?**].

control (WT) [65].

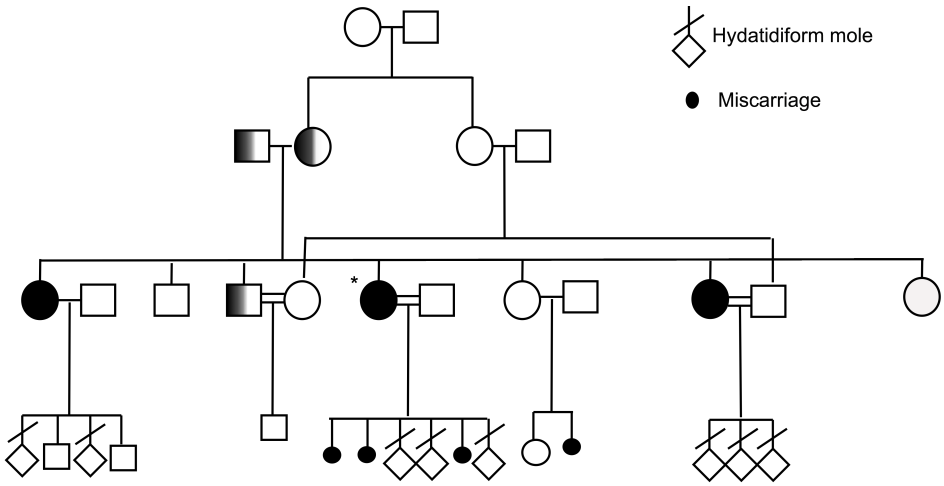

Figure 5.5. Family pedigree of the HM patient (marked by the asterisk) in this study.

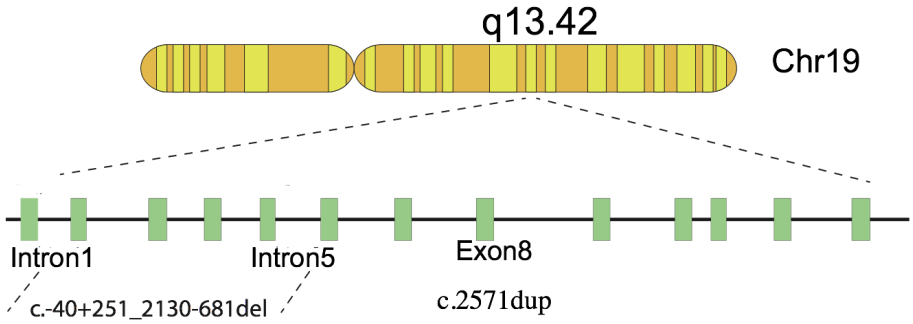

Figure 5.6. Schematic and coordinates of the deletion and the single base pair duplication on NLRP7 gene in patient cells used in this study.

After propagation of fibroblasts cells, they were converted to iPSCs by using episomal non-integrating approach by Burcu Özçimen and Tamer Önder, Koc University. ES-like colonies were selected based on their morphology (Figure 5.7). Then, EBNA PCR was performed to verify the endosomal expression of integration free plasmids. The plasmids, used for reprogramming, were not integrated to genome (Figure 5.8). To show pluripotency properties, the cells stained with stem cell markers including OCT3/4, NANOG and SSEA-4. Both HM patient-derived (HM) and WT cells were positive for pluripotency markers; OCT4, NANOG (Figure 5.9). For further charac-

terization of the IPSCs, teratoma formation assay was performed in SCID mice and revealed that the iPSCs were able to give rise to all three of the embryonic germ-layers, namely endoderm, ectoderm, mesoderm (Figure 5.10). Cytogenetic analysis was exhibited normal karyotypes (Figure 5.11). Concurrently, we determined mRNA and protein expressions of NLRP7 to affirm NLRP7 deficit in the HM patient at the molecular level. Although deletion was claimed to be heterozygous, mRNA levels of NLRP7 were quite low (Figure 5.12). Low mRNA expression of NLRP7 in HM iPSCs corresponded with barely detected protein levels. However, we could not detect such deficiency in both mRNA and protein levels of NLRP2 (Figure 5.13).

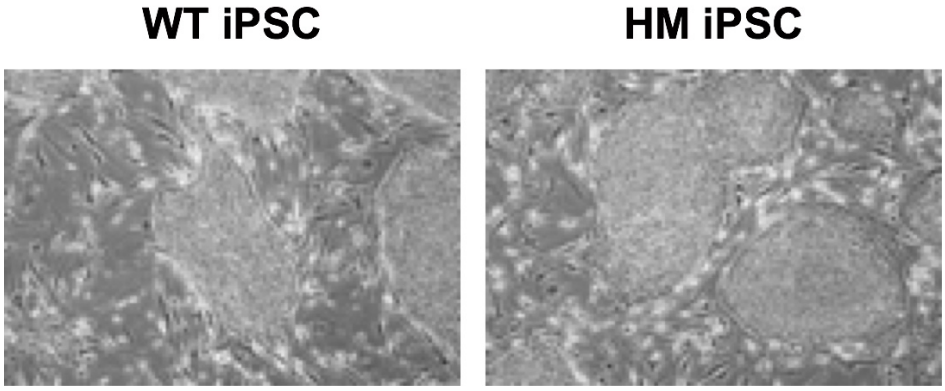

Figure 5.7. Hydatidiform Mole Disease modelling - IPSC Characterization. Colony morphologies of established iPSCs were visualized on mouse embryonic feeder cells. The cells displayed expected colony morphology resembling to stem cells.

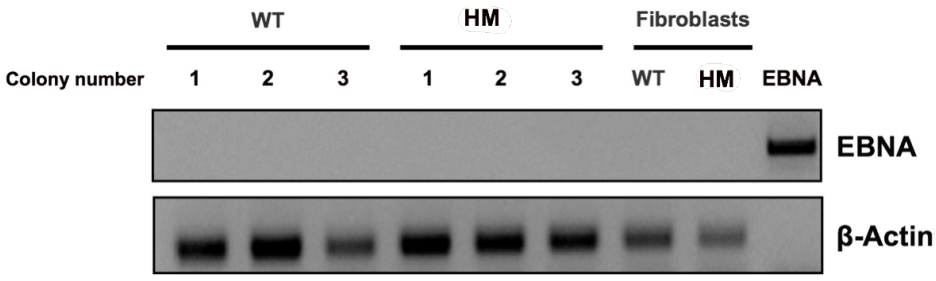

Figure 5.8. iPSC Characterization. EBNA PCR from the genome of three different colonies for each group was verified that plasmids containing reprogramming genes did not integrate to the genome.

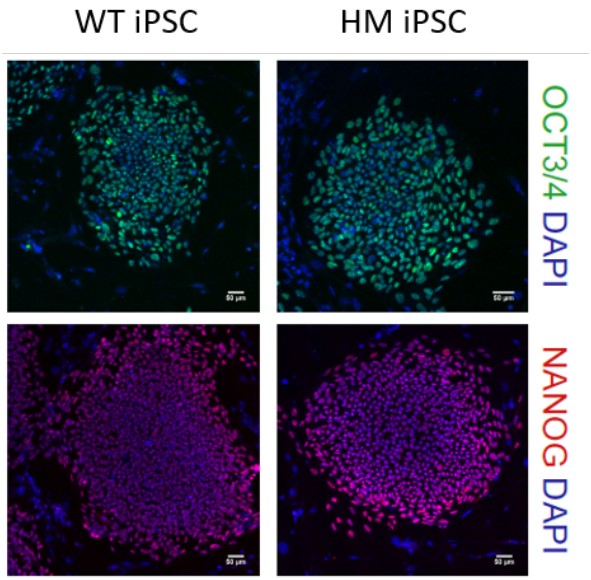

Figure 5.9. iPSC Characterization. iPSCs showed expected OCT3/4, SSEA-4, NANOG and TRA-1-81 expression.

5.2.2. NLRP7 Deficiency Boosts Trophoblast Differentiation from iPSCs in Response to BAP Conditions

Despite the controversy that extra embryonic tissues cannot be derived from human embryonic stem cells, increasing studies have exhibited the capacity of BMP4 to induce trophoblast differentiation from hESCs. Amita *et al.* have shown that BMP4 when combined with 2 inhibitors (A83-01, PD173074) is able to stimulate trophoblast differentiation. For the derivation of trophoblast cells, we seeded iPSCs onto matrigel and cultured with mouse fibroblast conditioned medium (MEF-CM) supplemented with 10ng/mL FGF2 (+FGF) for 24 hours (Day -2). Then, the medium was changed to mouse fibroblast conditioned medium (MEF-CM) with 4 ng/mL of FGF2 (Pre-differentiated) (Day -1). On the following day, the cells were cultured with DMEMF12/KOSR containing bone morphogenic protein 4 (BMP4), plus inhibitors of ACTIVIN signaling (A83-01) and FGF2 signaling (PD173074) up to 4 days (BAP) and the medium was replenished daily (Figure 5.14). On the second day of BAP exposure, WT cells were distinguishable by their flattened morphology from undifferentiated

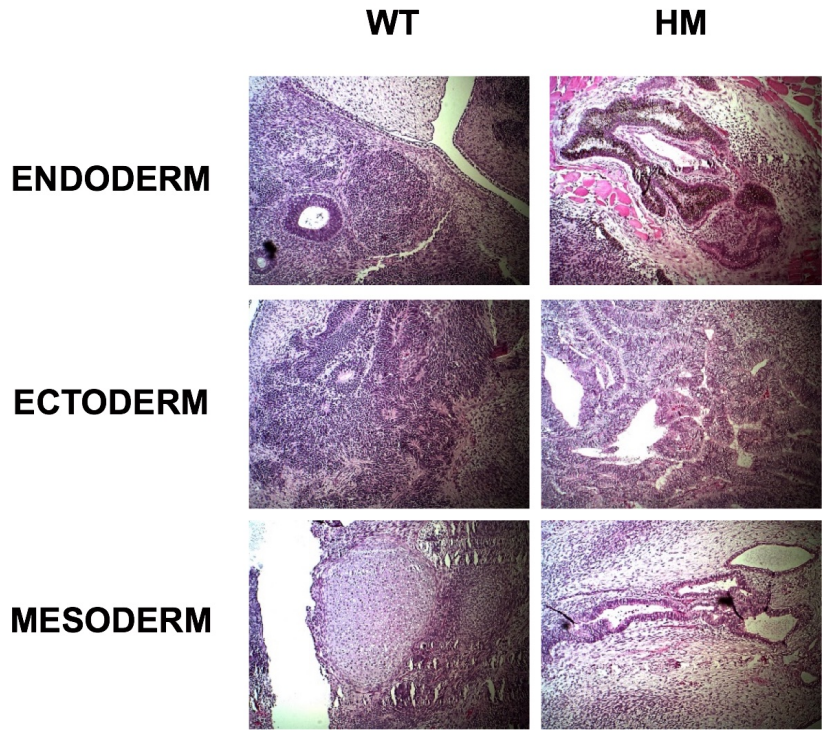

Figure 5.10. iPSC Characterization by Teratoma Formtion Assay. Both iPSCs gave rise to three embryonic germ layers; endoderm, ectoderm, mesoderm.

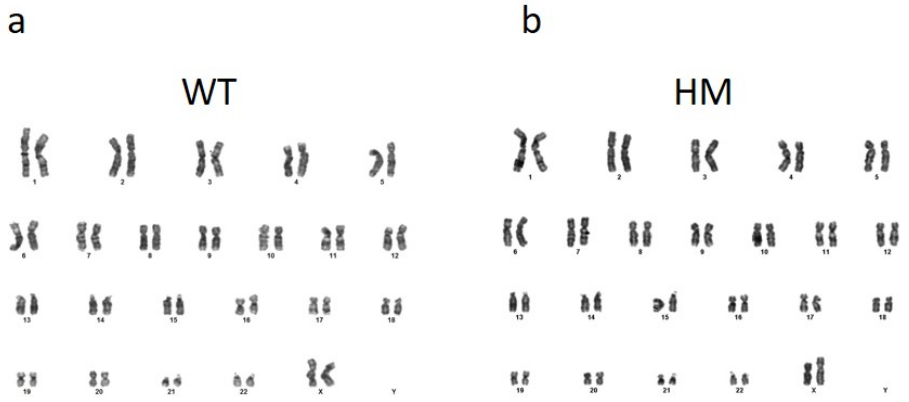

Figure 5.11. iPSC Characterization. Karyotyping analysis of a) WT iPSCs b) HM iPSCs. Both groups showed normal karyotype.

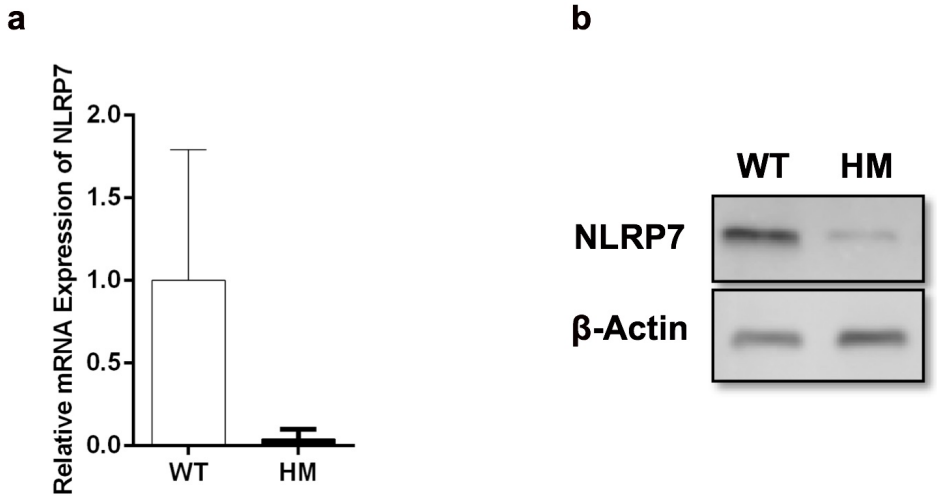

Figure 5.12. NLRP7 Expression in WT and HM iPSCs. a) mRNA transcript levels were determined by RT-qPCR, b) protein levels of NLRP7 were shown by Western blotting.

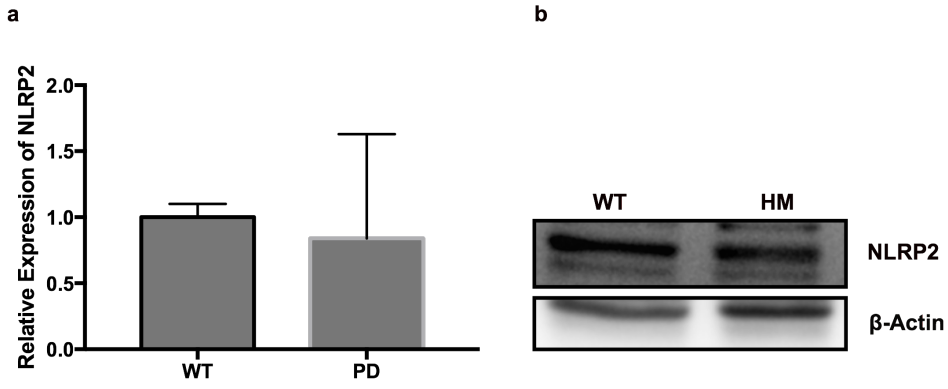

Figure 5.13. Normal levels of NLRP2 Expression in WT and HM iPSCs. a) mRNA transcript levels were determined by RT-qPCR, b) protein levels of NLRP2 were shown by Western blotting.

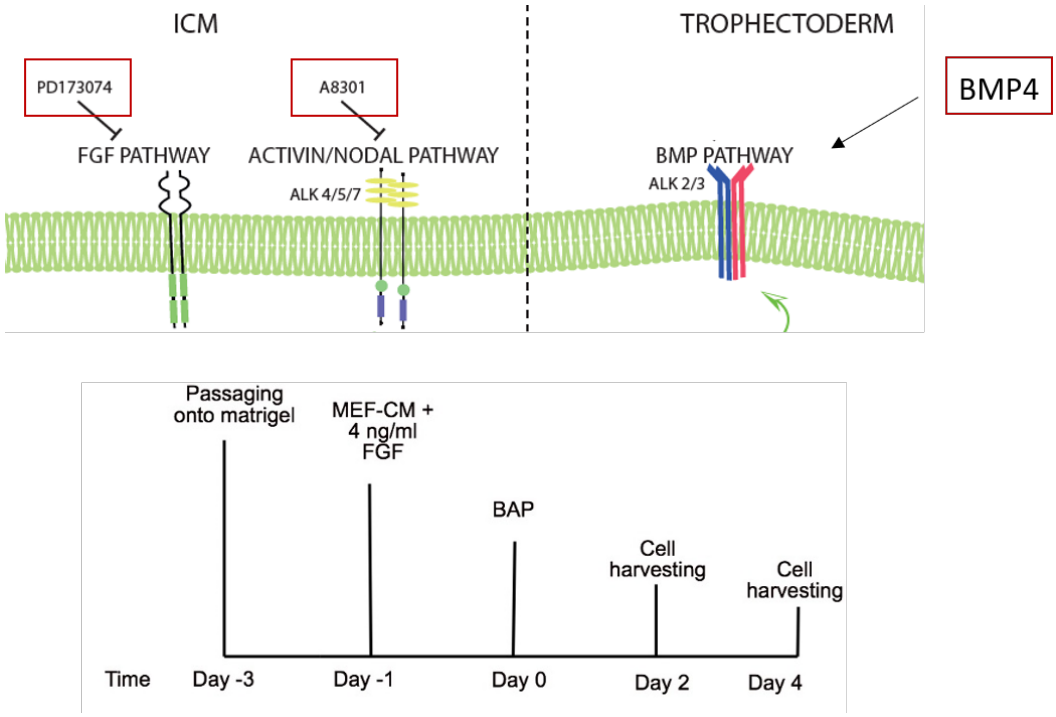

Figure 5.14. Diagram of the trophoblast differentiation procedure.

(control) counterparts which were continued to be cultured with MEF-CM containing FGF2 (10ng/mL). Intriguingly, patient derived (HM) cells lost their circular morphology peculiar to iPSCs only after 24 hours of BAP treatment indicating that HM cells gave faster response to BAP treatment than WT cells (Figure 5.15).

To assess the efficacy of BAP exposure for the differentiation of iPSCs towards trophoblasts, we conducted a comprehensive gene expression analysis of trophoblast linage markers including *CDX2*,*CGB*,*INSL4*, *deltaNp63*, *PGF*, and *PSG4*. mRNA levels of those markers were dramatically upregulated by BAP exposure, whereas pluripotency markers, *NANOG* and *POU5F1*, decreased significantly in both treatment groups. *CDX2* and *deltaNp63* have been reported to be early trophoblast markers and predominantly expressed in cytotrophoblast cells which are the progenitors of trophoblast subtypes in placenta. Increasing pattern in gene expression was followed by late trophoblast markers (*CGB*, *INSL4*, *PGF*, *PSG4*) at day 4 (Figure 5.16). BAP treatment primarily increased the expression of *CDX2* (∼30 fold) and *deltaNp63* (∼95 fold) in

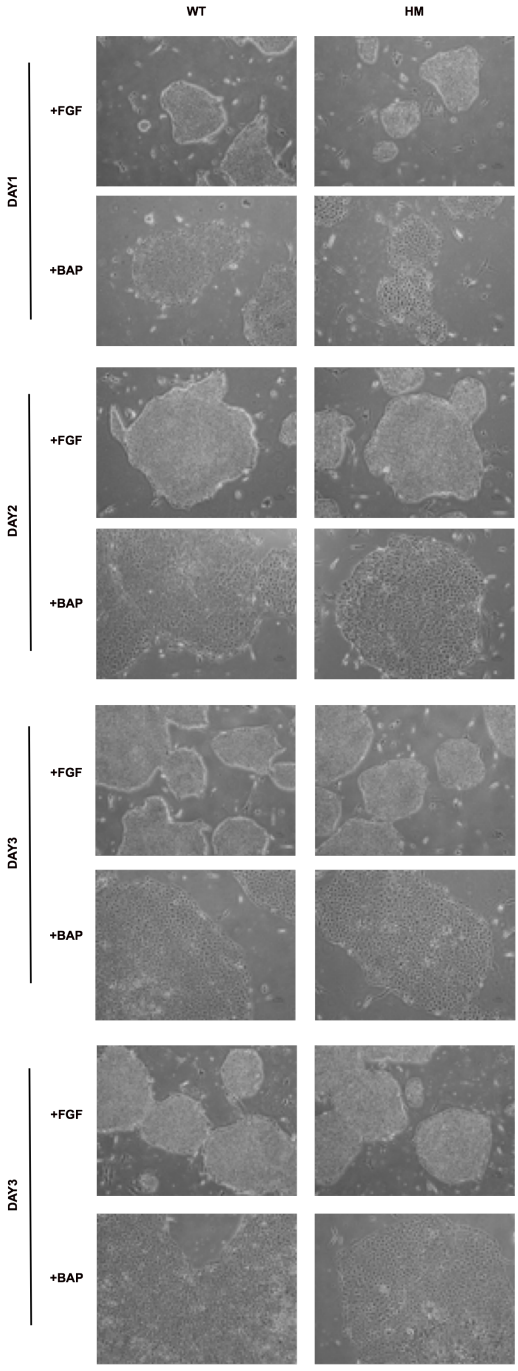

Figure 5.15. Changes in colony morphologies upon BAP exposure. Colony morphologies were shown under BAP exposure at day 1,2,3,4. Accelerated differentiation was evident in HM group even on day 1.

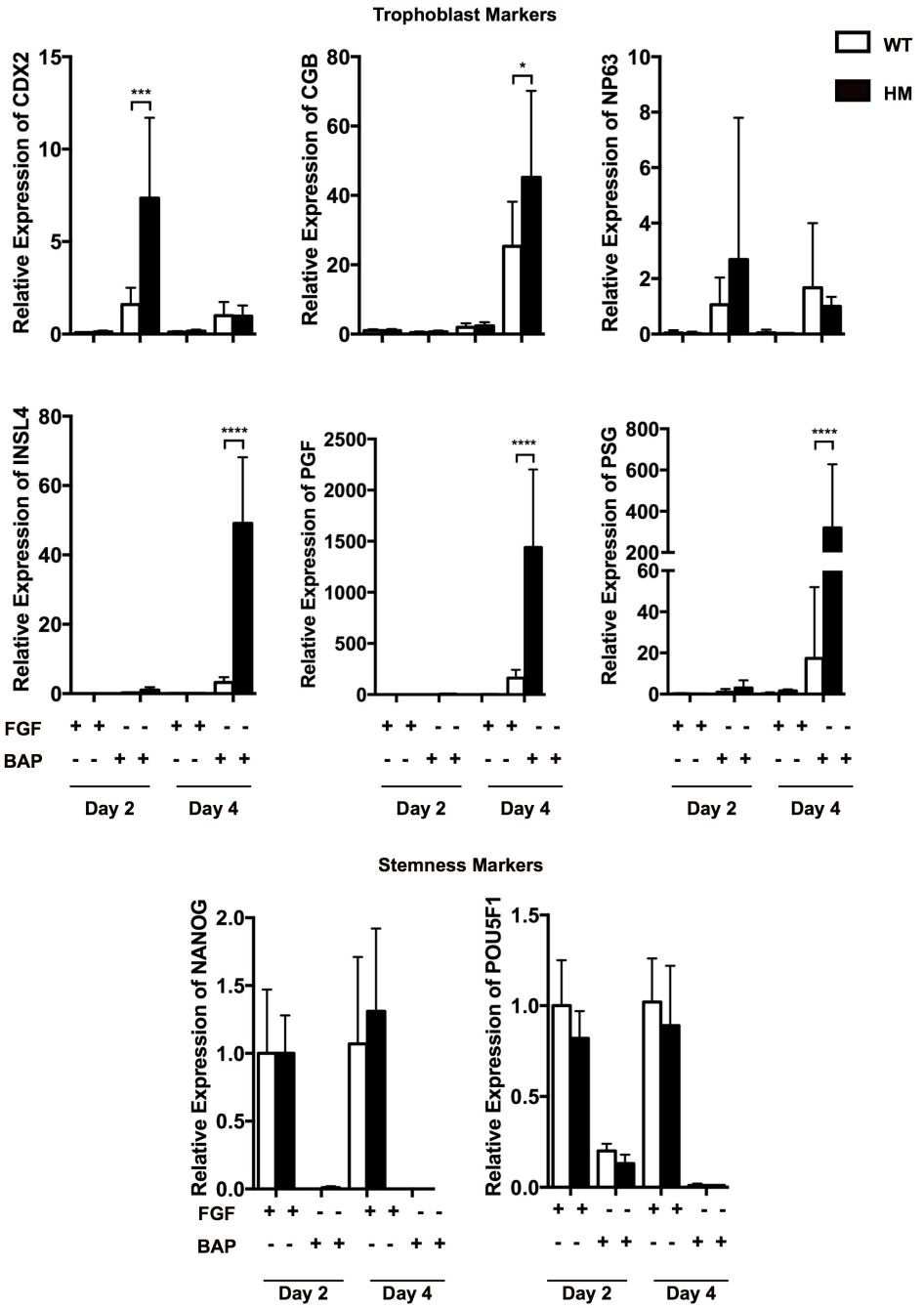

Figure 5.16. Trophoblast specific gene expressions were upregulated in HM group upon BAP exposure. Changes in gene expression of trophoblast and stem cell markers in response to BAP treatment were analyzed by RT-qPCR. Relative mRNA levels were normalized to *GAPDH* housekeeping gene.

WT cells at day 2. Among the examined markers, *CGB*, *INSL4*, *PGF*, *PSG4* have been reported as late markers of trophoblast differentiation and the expression of those markers considerably rose at day 4 in both BAP treated groups. On the other hand, we detected significantly higher mRNA levels of all trophoblast markers in HM cells than that of WT cells. The most drastic alterations in fold changes were observed for *CDX2*, *PGF*, *PSG* and *INSL4* in which 10 fold or more mRNA transcripts were identified in HM cells by comparison with WT cells upon BAP exposure. Conversely, *POU5F1* expression that encodes *OCT4*, were started to decrease after 2 days of BAP exposure and *NANOG* expression was almost undetectable even at day 2.

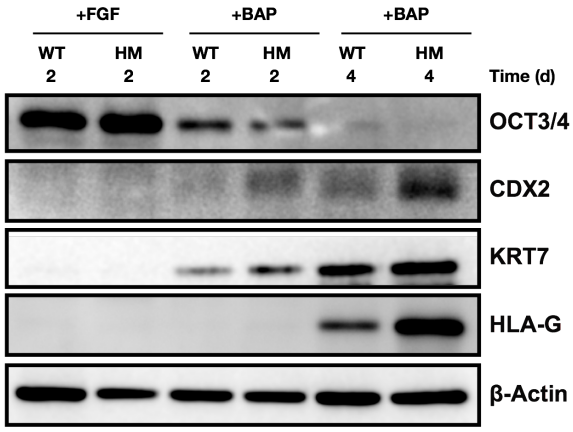

Figure 5.17. The expressions of trophoblast specific proteins were elevated in BAP treated HM cells. Western blotting were performed for trophoblast markers; CDX2, HLA-G, KRT7 and stem cell marker; Oct3/4. β-ACTIN was used as loading control.

After the verification that BAP treatment was able to up-regulate the expression of trophoblast associated genes as reported previously, we further investigated the tendency of HM iPSCs to differentiate towards trophoblasts via Western blotting. In accordance with gene expression results, OCT3/4 protein expressions were not detectable after 4 days of BAP treatment, whereas the cells from both groups started to express CDX2 (cytotrophoblast marker), KRT7 (pan-trophoblast marker) and HLA-G proteins in a time dependent manner (Figure 5.17). Elevated expression of trophoblast markers in HM group were also verified and demonstrated in a protein level by western blotting.

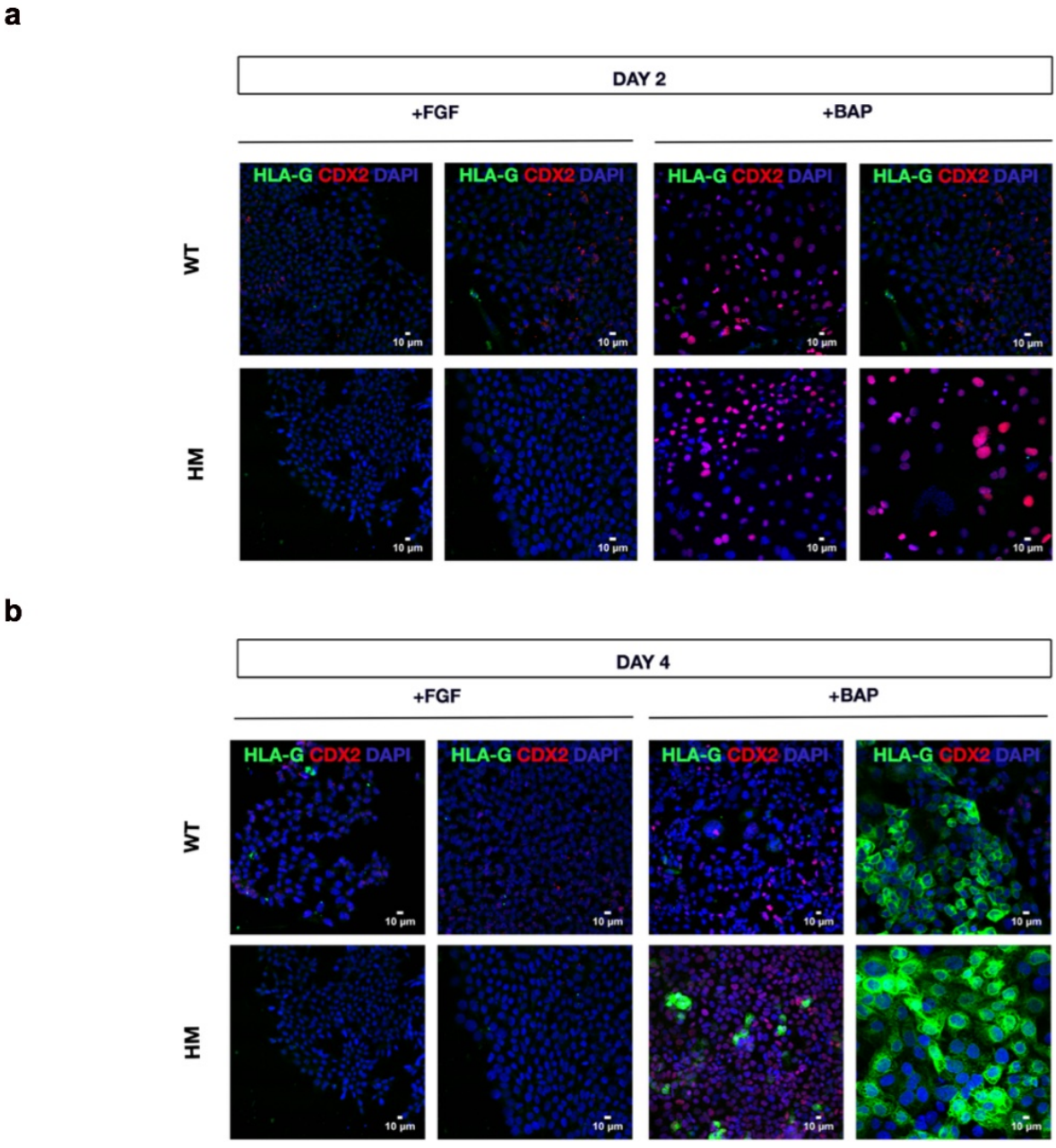

Figure 5.18. BAP treated cells became positive for CDX2 and HLA-G. a) BAP exposure converted cells to CDX2 (red) positive and HLA-G (green) negative phenotype at day 2. b) Cells gained both CDX2 and HLA-G expression upon BAP exposure at day 4.

Additionally, BAP treated cells were immunostained for CDX2, HLA-G, KRT7 and OCT4. BAP treated cells started to be positive for CDX2 at day 2 whereas at the same time cells were negative for HLA-G. HM cells appeared to gain more CDX2 positive phenotype than WT cells (Figure 5.18). On the other hand, HLA-G positive areas were visible mostly where CDX2 were not stained at day 4. Staining for HLA-G was considerably stronger and more uniform in HM cells. As, HLA-G is a differentiated trophoblast marker, these HLA-G positive areas inferred progressive differentiation of the cells through trophoblasts.

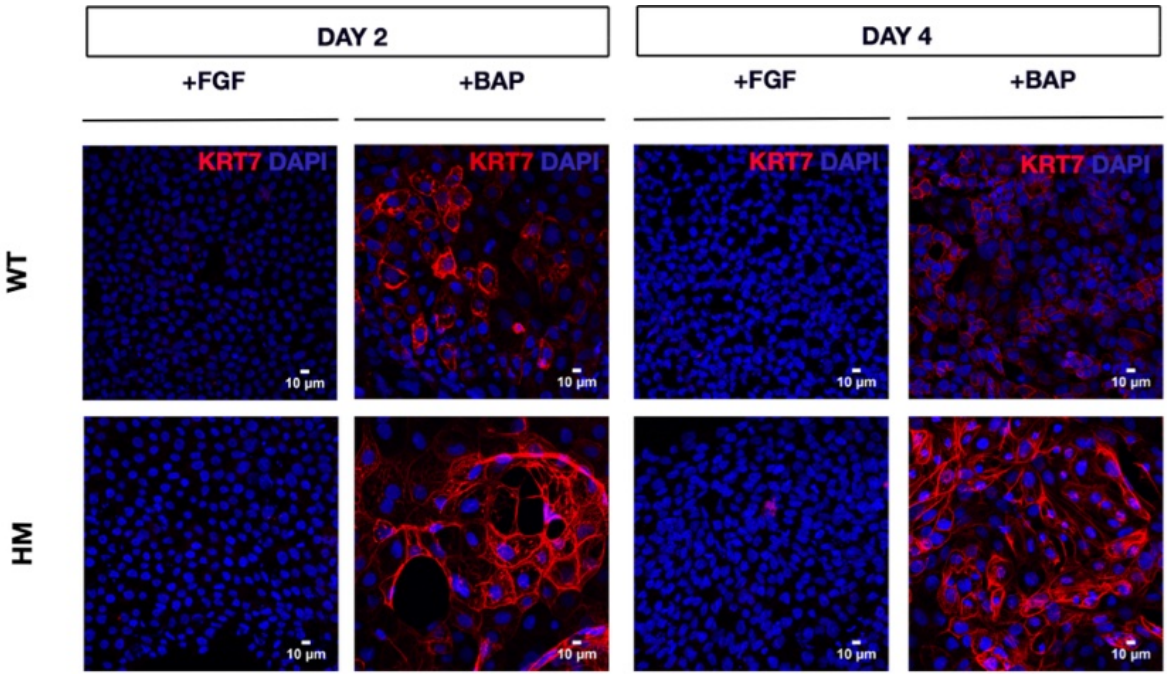

Figure 5.19. BAP treated cells became positive for KRT7. Cells gained KRT7 (red) expression upon BAP exposure.

KRT7 expression were detectable at day 2. Individual and dispersed cells became positive for KRT7 in WT cells while KRT7 positive enlarged cell patches emerged in HM group (Figure 5.19). Although, most of the cells gained KRT7 positive phenotype in both groups at day 4, HM cells stained dramatically stronger than WT cells.

As the cells lost their pluripotency during BAP treatment, strong OCT4 staining in FGF treated control cells declined proportionally upon BAP exposure (Figure 5.20).

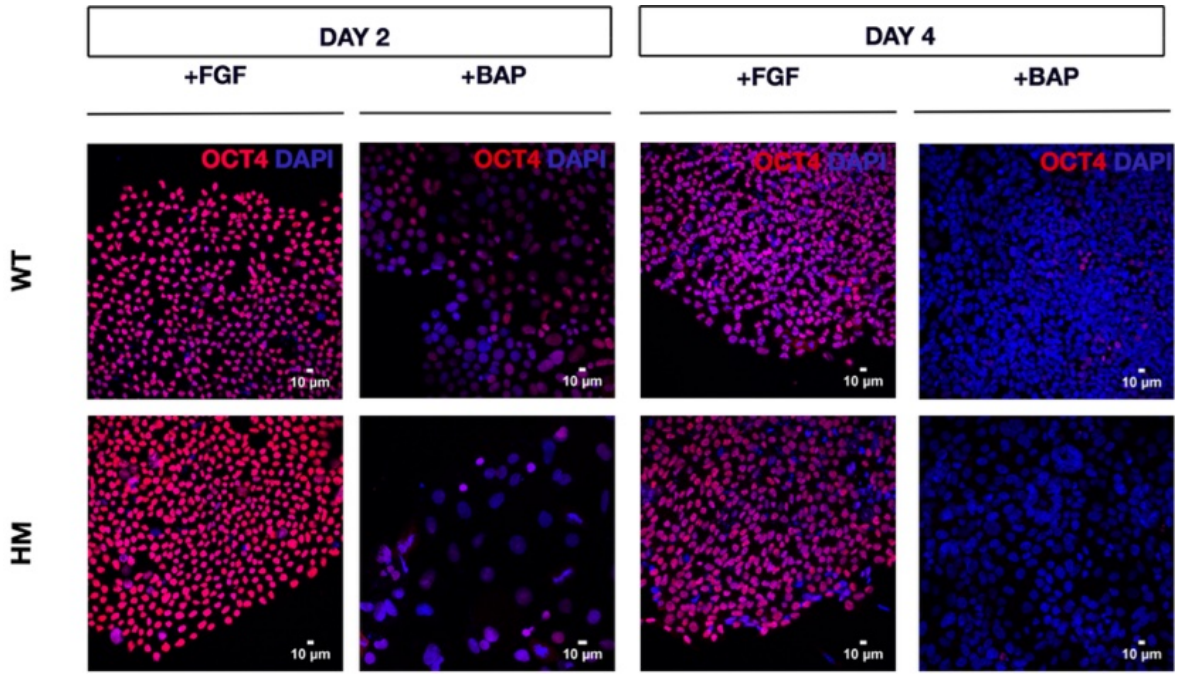

Figure 5.20. BAP treated cells lost OCT4 staining in BAP conditions.

Most of the cells of HM group lost OCT4 expression even at day 2 which was a evidence of rapid differentiation observed in HM cells. Mouse IgG were immunostained as a negative control (Figure 5.21).

Immunostaining studies also revealed the differences in the size of cells, which was also observed in bright field images as shown in Figure 5.15. HM cells became enlarged and more uniform when compared to WT cells in response to BAP treatment. As increases in cell sizes exhibit initial evidence of trophoblastic differentiation, we measured the sizes of DAPI stained-cell nuclei. In correlation with the microscopic observations, HM cells displayed significantly larger nuclei than that of WT cells (Figure 5.22).

Placental growth factor (PGF) is a placental hormone produced predominantly by trophoblasts during pregnancy. As an evidence for trophoblast differentiation, we compared the levels of PGF secretion by BAP treated cells. HM cells produced high levels (-6000 pg/mL) of PGF at day 4 whereas PGF secretion of their WT counterparts were 600 pg/mL (Figure 5.23).

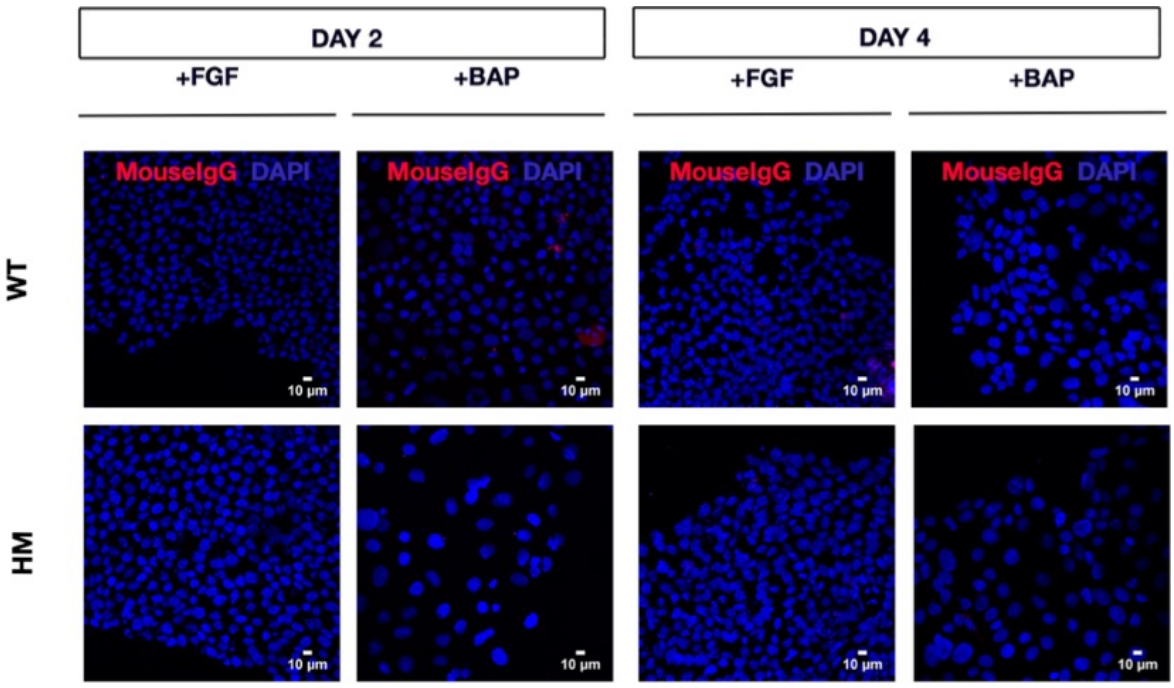

Figure 5.21. Mouse IgG was immunostained as a negative control.

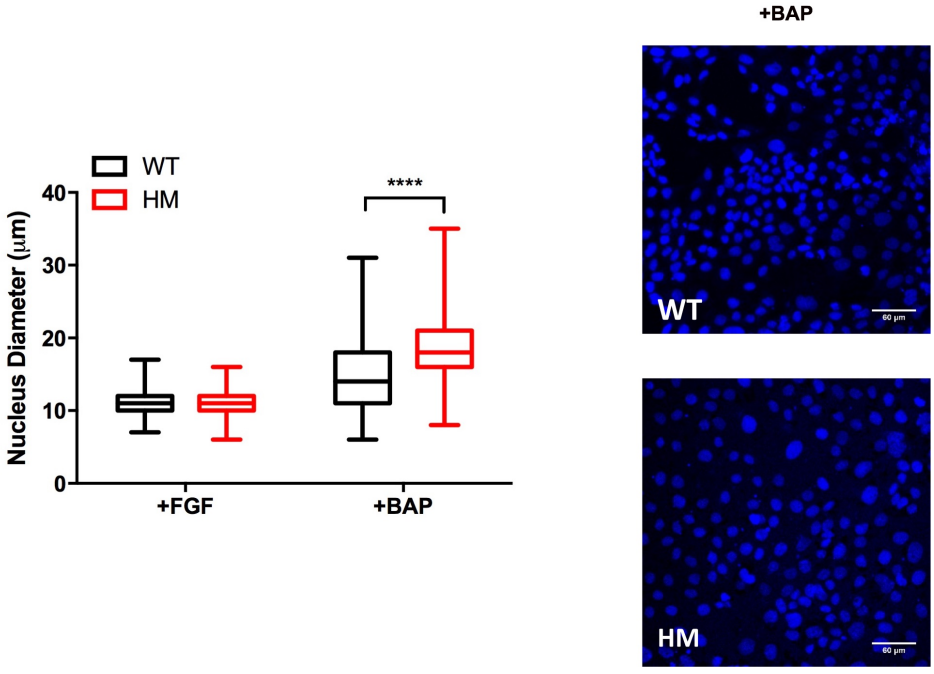

Figure 5.22. BAP exposure increased the size of the nucleus. Nucleus sizes of DAPI stained cells were measured by ImageJ. n=100

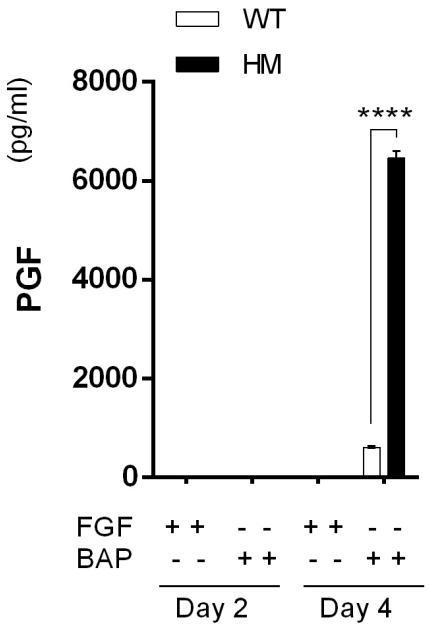

Figure 5.23. PGF production of BAP treated cells. Daily PGF production were assessed by ELISA. PGF secretion increased 10 fold more in HM cells relative to WT cells. ****$p<0.0001$

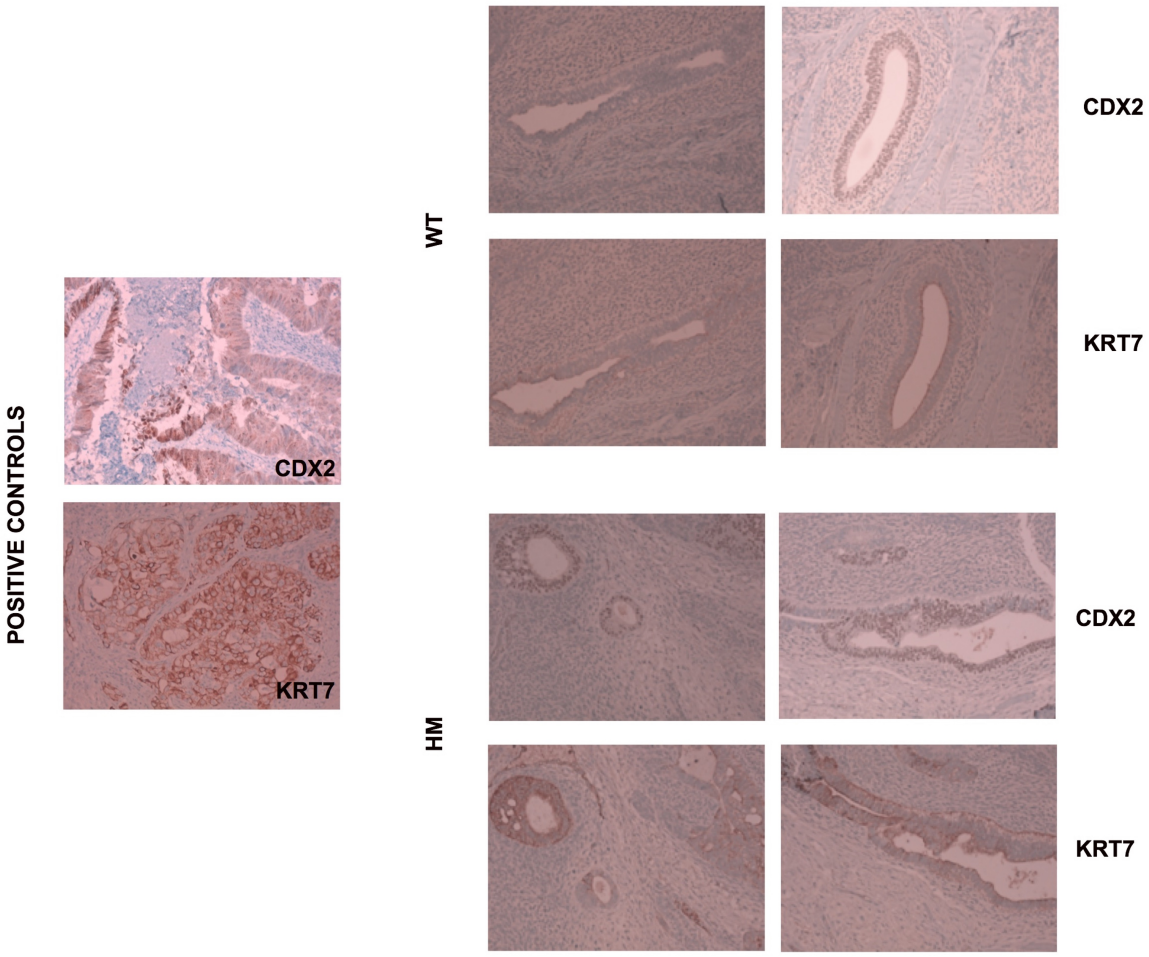

Figure 5.24. Teratoma IHC. Teratoma sections were stained for CDX2 and KRT7.

Although contingency to form trophoblast cells in teratomas produced from human embryonic stem cells is a rare situation, there are several studies reported to observe trophoblast cells in teratomas formed by hESCs. From this phenomenon, we examined the presence of trophoblast-like cells within teratoma sections to assess predisposition of HM derived iPSCs towards trophoblastic differentiation *in vivo*. For this purpose, immunohistochemistry with CDX2, KRT7 was performed from teratoma sections in Koc University Hospital. Accordingly, we observed areas where CDX2 and KRT7 were positive in HM cells implying those cells resembled to trophoblast cells. However, such overlap in staining was not observed for WT cells. Although, there were positive areas for CDX2 in WT group, KRT7 staining were not strong as in HM group. (Figure 5.24). Unfortunetly, HM iPSCs used for teratoma IHC were diagnosed to have trisomy 12. Therefore, this set of experiment should be recapitulated.

Taken together, these data suggest that patient derived cells carrying NLRP7/2 heterozygous deletion (HM) had accelerated trophoblast differentiation in response to BAP conditions. Considering the pathology of hydatidiform mole, HM trophoblasts reflected quite similar phenotype *in vitro* in terms of elevated trophoblast differentiation as is also observed in HM.

5.2.3. BMP4 is Dispensable to Derive Tophoblasts from HM Derived iPSCs

As we revealed above, the insufficient expression of NLRP7 resulted in excessive trophoblast differentiation in HM cells. We next hypothesized that NLRP7 may regulate trophoblast differentiation through BMP-4 pathway. To investigate this hypothesis, endogenous BMP4 expression was assessed during BAP mediated differentiation. FGF2 removal and BAP addiction caused 2.13 fold increase in WT cells compared to FGF treated cells of WT (Figure 5.25a). Though, the total mRNA levels were almost same for both groups upon BAP treatment, in HM group, BAP exposure increased BMP4 mRNA levels to 6.13 fold of observed in FGF treated HM group. This may indicate hyper-trophoblast differentiation observed in HM cells was associated with BMP4 pathway (Figure 5.25a).

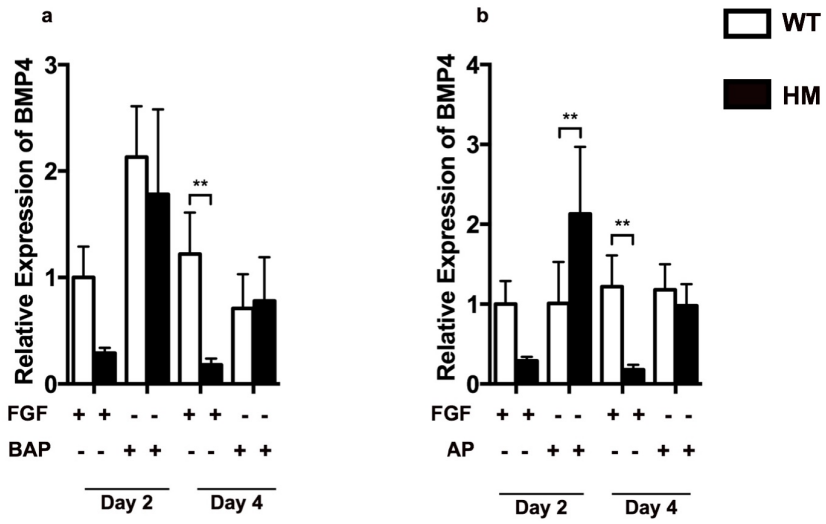

Figure 5.25. *BMP4* expressions were upregulated in HM group upon BAP and AP exposure. Changes in gene expression of *BMP4* in response to BAP (a) and AP (b) treatment were analyzed by RT-qPCR. Relative mRNA levels were normalized to *GAPDH* housekeeping gene.

This result led us to stimulate differentiation through trophoblasts in the absence of *BMP4* (AP condition) to test whether NLRP7 deficiency was able to enhance the differentiation even in AP conditions. We first determined mRNA levels of *BMP4* during AP exposure to compare with BAP conditions. *BMP4* mRNA expression did not get induced in WT cells cultured under AP conditions, while its expression was increased to 7.34 fold of observed in FGF-exposed HM cells under the same conditions at day 2 (Figure 5.25b). Thereafter, gene expression analyses were performed for trophoblast markers to assess the potency of HM cells to differentiate into trophoblasts in the absence of exogenous BMP4. Conspicuously, qPCR results revealed that transcripts of *CDX2* (more than 20 fold), *deltaNp63* (more than 12 fold) at day 2 and *PGF* (38 fold), *INSL4* (all mRNA transcripts were undetermined except for AP treated HM group), *PSG* (29 fold) at day 4 were highly enriched in HM cells compared to WT cells (Figure 5.26). These results mirrored the phenotype observed for BAP exposure with an accompanied lower mRNA transcripts of trophoblast specific markers. However, *CGB* expressions slightly differed between WT and HM groups (3 fold). The expres-

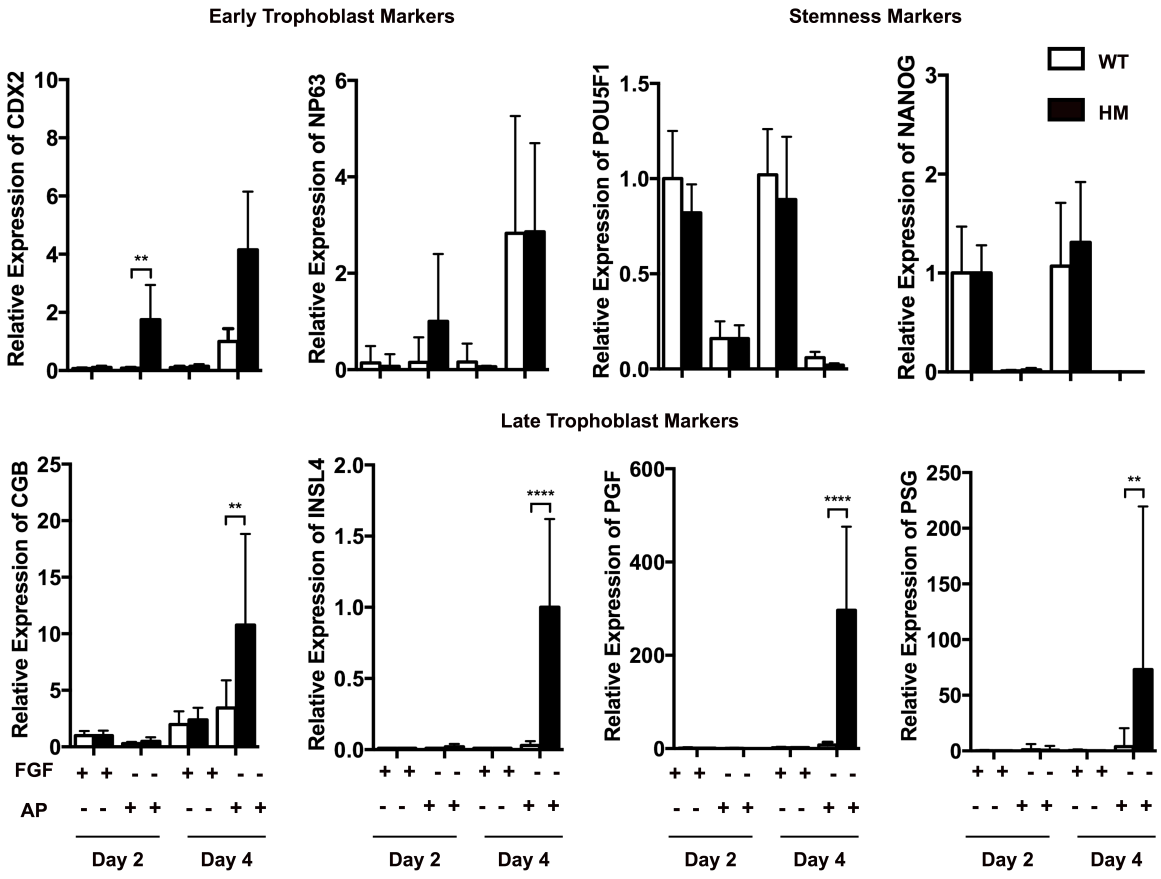

Figure 5.26. Trophoblast specific gene expressions were upregulated in HM group upon AP exposure. Changes in gene expression of trophoblast and stem cell markers in response to AP treatment were analyzed by RT-qPCR. Relative mRNA levels were normalized to *GAPDH* housekeeping gene.

sion of stemness markers also decreased upon AP exposure as expected. *POU5F1* expression was more down-regulated in HM group, possibly due to expedited differentiation. Based on gene expression results of both BAP and AP conditions, NLRP7 seemed to regulate early transcription factors (*CDX2*, *deltaNp63*) leading trophoblast lineage commitment and further this regulation resulted an increase in expressions of *PGF*, *PSG* and *INSL4* at later time points (Figure 5.26).

Trophoblast specific protein expression profile was in correlation with the gene expression analysis. AP treated HM cells expressed CDX2, KRT7 and HLA-G at day 4 whereas slight protein levels of trophoblast markers were determined in WT cells (Figure 5.27). OCT4 protein levels decreased dramatically at day 4 in HM cells under AP conditions showing that the cells lost pluripotency properties prior to WT cells.

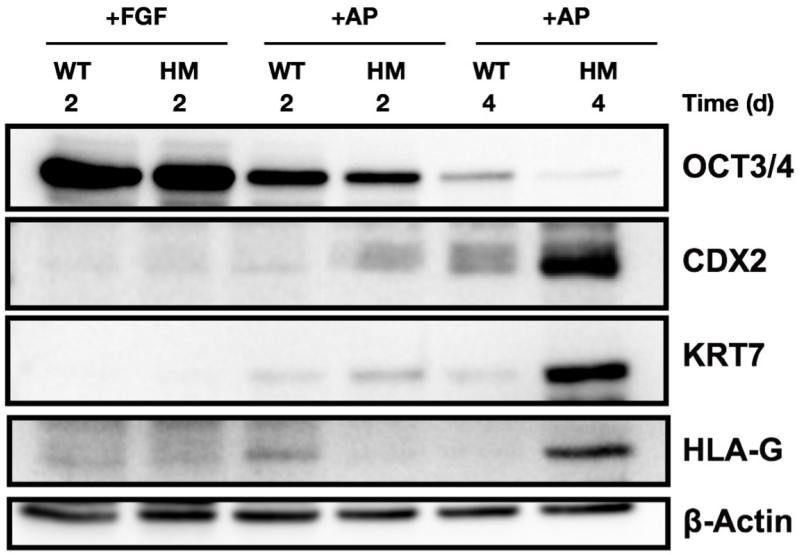

Figure 5.27. The expressions of trophoblast specific proteins were elevated in AP treated HM cells. Western blotting were performed for trophoblast markers; CDX2, HLA-G, KRT7 and stem cell marker; Oct3/4. β-ACTIN was used as loading control.

We next immunostained the cells with CDX2, HLA-G, KRT7 and OCT4. CDX2 positive cells were evident in HM group at day 2 and HLA-G positive cells emerged at day 4 upon AP treatment (Figure 5.28). Although, they were few in number, HM cells appeared to be positive for KRT7 from day 2 and they were strongly stained for

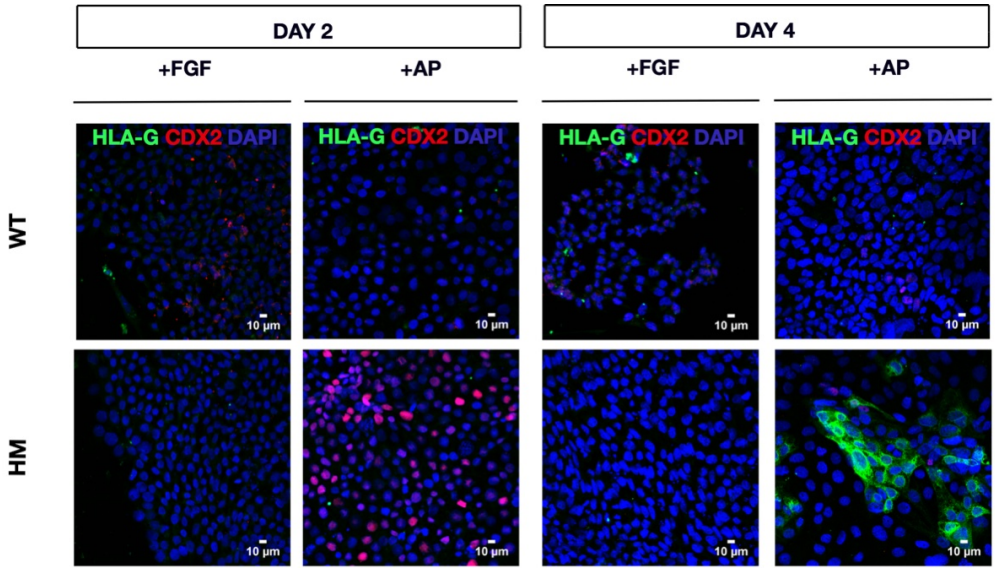

Figure 5.28. AP treated cells became positive for CDX2 and HLA-G in HM group. AP exposure converted cells to CDX2 (red) positive at day 2 and HLA-G (green) positive phenotype at day 4 in HM group.

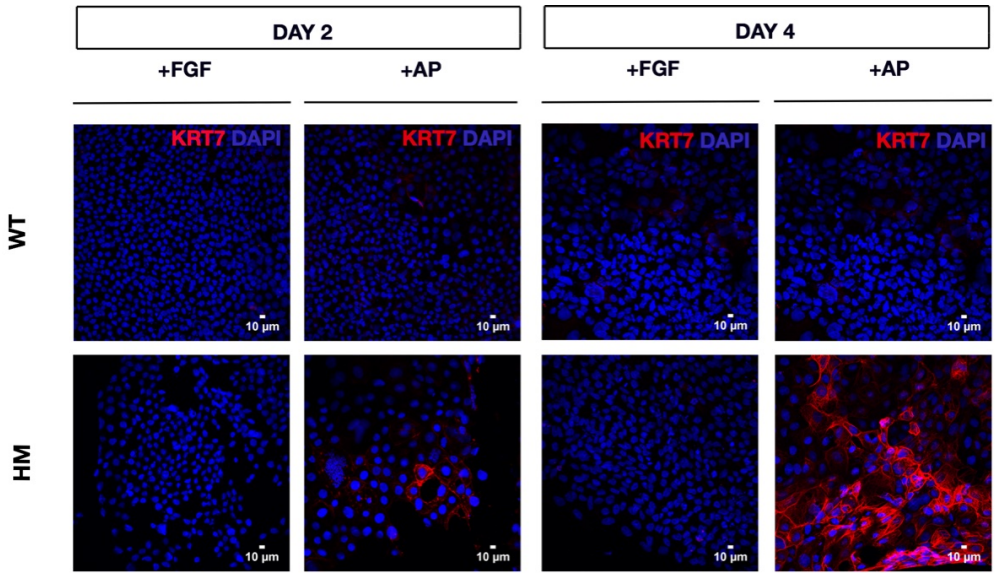

Figure 5.29. AP treated cells became positive for KRT7 in HM group. HM cells gained KRT7 (red) expression upon AP exposure.

KRT7 at day 4 (Figure 5.29). Such staining with trophoblast markers was not observed for WT cells. OCT4 staining weakened gradually by AP exposure for both groups as expected (Figure 5.30).

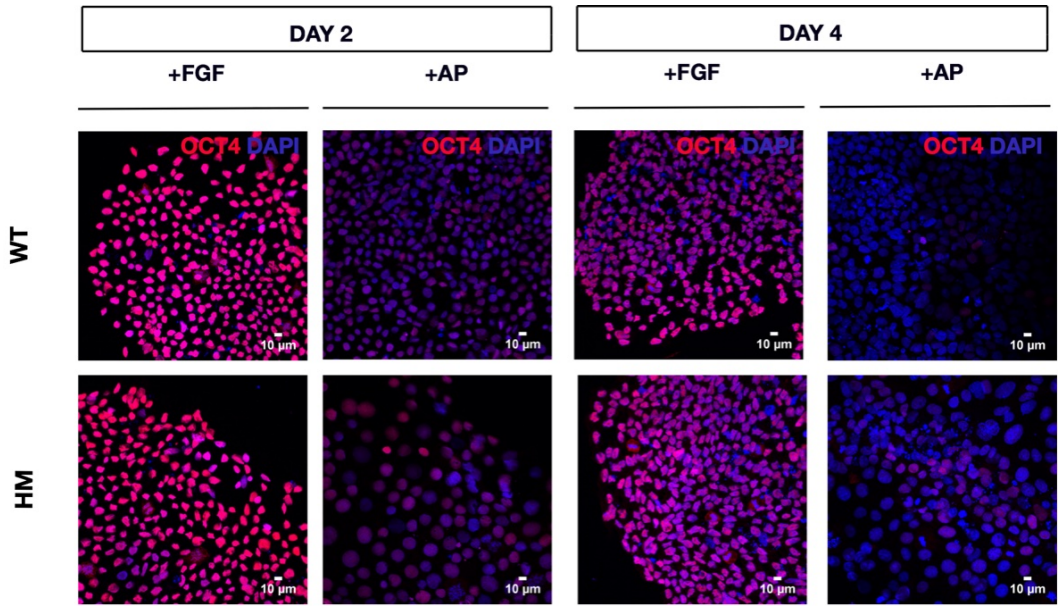

Figure 5.30. OCT4 staining declined in AP treated cells. WT and HM groups weakly stained with OCT4 upon AP exposure.

Trophoblastic feature of AP treated cells were further examined by detection of PGF secretion. HM cells secrete detectable levels of PGF at day 4 in response to AP, yet PGF secretion of WT cells were under threshold values (Figure 5.32). NLRP7 deficiency appeared to initiate trophoblast differentiation even in the absence of BMP4 but most probably it caused delayed differentiation with regard to BAP treatment, as PGF secretion was about 300 pg/mL in HM cells exposed to AP, whereas the same cells when treated with BAP secreted 6455 pg/mL of PGF (Figure 5.30).

These results were similar with that of BAP treatment, HM cells presented more trophoblast-specific phenotype than WT group even though the differentiation medium lack of BMP-4.

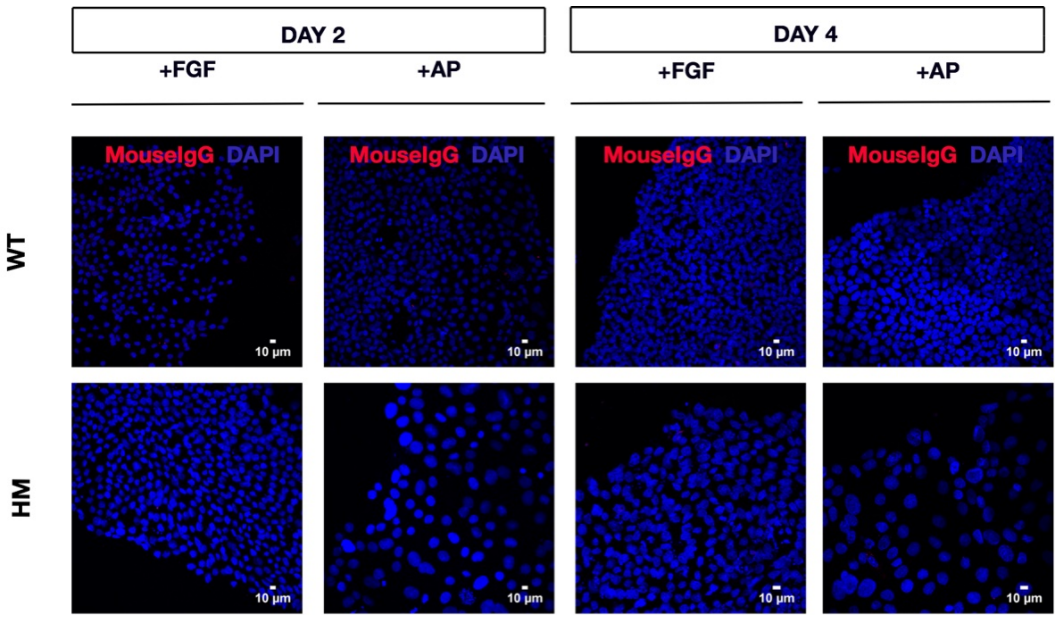

Figure 5.31. Mouse IgG was immunostained as a negative control.

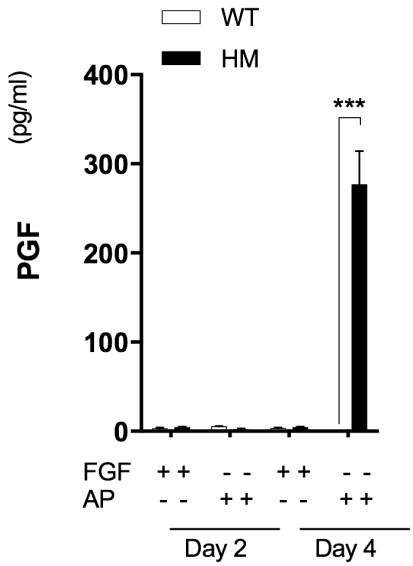

Figure 5.32. AP treated HM cells produced PGF. Daily PGF productions were assessed by ELISA. PGF accumulated in the medium of HM cells cultured with AP condition by day 4 whilst PGF secretion was below detectable threshold for WT cells. ***$p<0.001$.

5.2.4. Inhibition of BMP Pathway Recovers Redundant Trophoblast Differentiation of Patient Specific iPSCs

Subsequent experiments were conducted to further assert association of NLRP7 with BMP4 pathway during trophoblast differentiation by using LDN193189, an inhibitor of BMP receptor isotypes ALK2 and ALK3. To evaluate if LDN193189 was able to attenuate trophoblast differentiation, AP medium were supplemented with LDN193189 (100 nM). Treatment with BMP pathway inhibitor resulted in reduction of BMP4 expression by half in WT cells at day 2, while BMP4 expression levels were not affected by LDN193189 in HM cells (Figure 5.33). One possible explanation could be that NLRP7 deficiency constitutively activated endogenous BMP4 mRNA expression. No difference was observed for day 4 samples compared to their LDN193189 untreated samples. Strikingly, BMP pathway inhibition resulted in a dramatic decline on *NLRP7* mRNA levels (16.4 fold) of WT cells at day 4. BMP4 and NLRP7 expression patterns appeared to have the same expression pattern in WT cells and both of the genes were down-regulated in the presence of LDN193189. From this point, we may hypothesized that NLRP7 and BMP4 are expressed in a coordinated manner and they negatively regulate each other.

Thereafter, we examined the expression of trophoblast markers in response to LDN193189. All of the trophoblast markers assessed were down-regulated dramatically in each group when exposed to LDN193189 albeit the difference in CDX2 ($\sim$3 fold change) and *nP63* ($\sim$5 fold change) expressions on day 4 between groups (Figure 5.34). In HM cells, although endogenous *BMP4* levels were high, BMP4 could not activate its receptors in an autocrine manner and so trophoblast-specific gene expression due to inhibition of its receptors via LDN193189.

In addition to inhibition of trophoblast mRNA expression, BMP pathway inhibitor hindered elevated protein expression of CDX2, KRT7 and HLA-G in HM group for all time points (Figure 5.35). On the other hand, LDN193189 exposure regained OCT4 protein expression at day 4 in HM groups. Interestingly, cells ex-

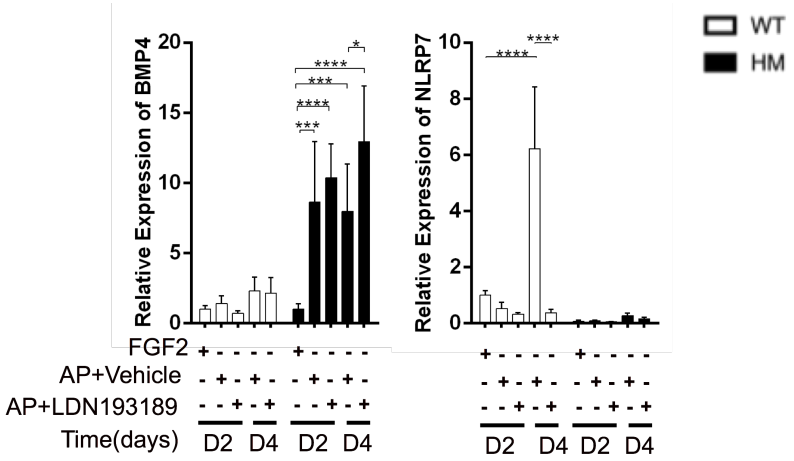

Figure 5.33. BMP pathway inhibition altered *BMP4* and *NLRP7* gene expressions. Changes in gene expression of *BMP4* and *NLRP7* in response to LDN193189 treatment were analyzed by RT-qPCR. Relative mRNA levels were normalized to HPRT housekeeping gene.

pressed more OCT4 than WT cells under LDN193189 conditions for both days 2 and 4. In LDN193189 treated WT cells OCT4 expression was reduced in comparison to that of AP treated cells. For HM cells, OCT4 expression pattern was opposite as its expression increased upon LDN193189 treatment. The same reverse expression pattern was also detected with regard to *OCT4* in gene expression analysis as shown in Figure 5.34. Overall, these results provided another evidence that losing stemness characteristics and rapid differentiation process through trophoblasts in HM cells were associated with the BMP pathway.

These findings may present a possible therapeutic strategy to cure improper pregnancy due to hyper proliferation/differentiation of trophoblasts observed in HM patients.

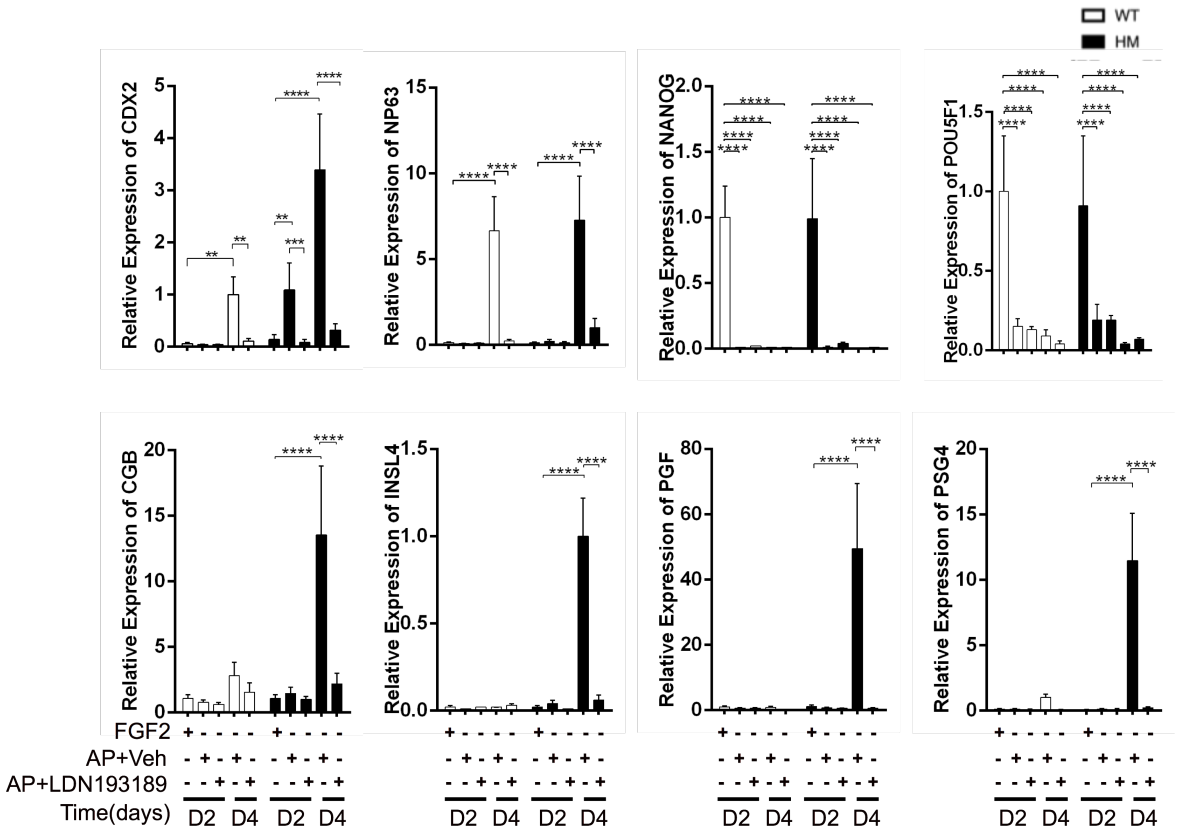

Figure 5.34. BMP pathway inhibition diminished elevated trophoblast specific gene expression in AP treated HM cells. Changes in gene expression of trophoblast and stem cell markers in response to LDN193189 treatment were analyzed by RT-qPCR. Relative mRNA levels were normalized to *HPRT* housekeeping gene.

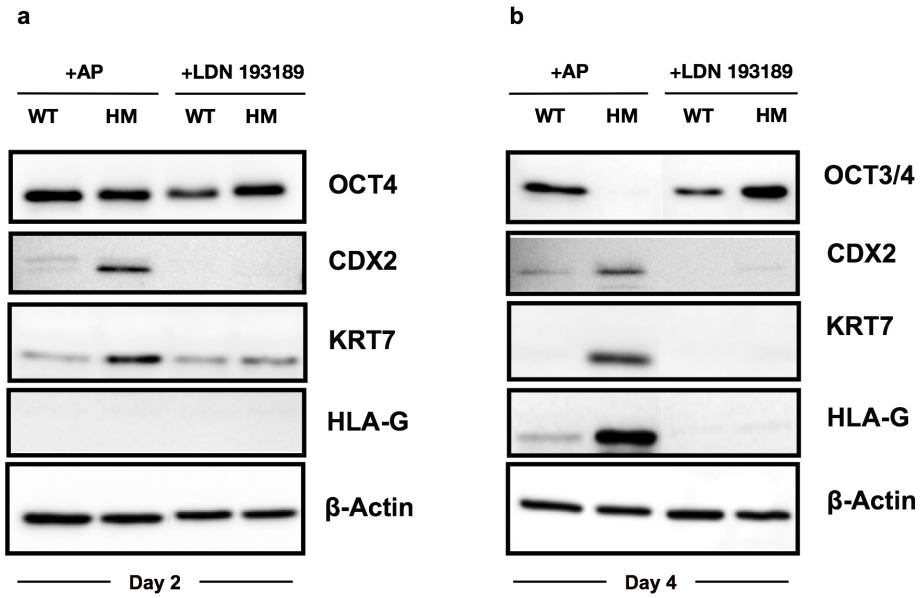

Figure 5.35. BMP pathway inhibition reverted augmented trophoblast protein expression in AP treated HM cells. Western blotting were performed for trophoblast markers; CDX2, HLA-G, KRT7 and stem cell marker; OCT3/4. β-ACTIN was used as loading control.

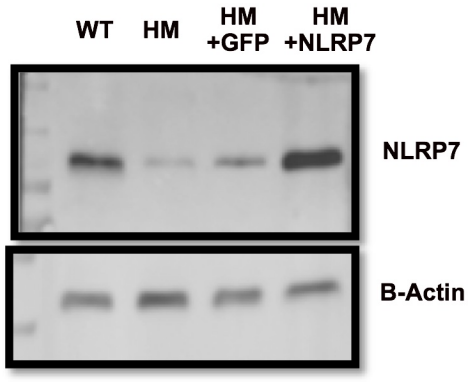

Figure 5.36. NLRP7 recovery in HM cells.HM cells were infected with pLEX307-NLRP7 or pLEX307-GFP containing lentiviruses. NLRP7 protein levels were shown by Western blotting.

5.2.5. Reintroduction of NLRP7 Rescues Excessive Differentiation Toward Trophoblasts

After demonstrating the increased potential for trophoblast differentiation in HM cells, we next asked whether re-introduction of NLRP7 could recover that phenotype. To test this hypothesis, NLRP7 was stably over-expressed in NLRP7 deficient cells (HM+NLRP7) and GFP transduced cells were used as a control (HM+GFP). Stable GFP expressing HM cells were imaged with fluorescence microscopy. NLRP7 reconstitution was confirmed via Western blotting (Figure 5.36). Thereafter, we proceeded to BAP treatment to initiate trophoblast differentiation.

Introducing NLRP7 to HM group (HM+NLRP7) engendered reduction of the majority of trophoblast gene expression relative to HM+GFP group. Among them, most striking differences were detected for *CDX2*, *deltaNp63*, *PGF*, and *INSL4* for each time point where expression was detected (more than 2 fold reduction in expression values for each time point) in consequence of NLRP7 reconstitution (Figure 5.37). On the other hand, NLRP7 introduction did not effect *GABRP*, *TFAP2C*, *KRT7* and *HLA-G*. The expression of stemness markers, *POU5F1* and *NANOG*, were down-regulated upon BAP exposure as expected (Figure 5.38). Similar results were obtained for protein expressions such that KRT7 and HLA-G levels were not rescued upon NLRP7 introduction under BAP conditions (Figure 5.39). Most interestingly, NLRP7 recovery restored OCT4 levels, dramatically on day 4 under BAP conditions. However, such rescue on protein levels could not observed for CDX2 (Figure 5.40)

The effect of NLRP7 recovery on trophoblast differentiation in HM cells were also investigated under AP conditions. In correlation with BAP results, most dramatic attenuations in gene expressions were observed for *CDX2*, *deltaNp63*, *PGF*, and *INSL4*. On the other hand, *CGB* and *HLA-G* mRNA expressions were slightly reduced under AP conditions (Figure 5.41). Interestingly, in the presence of 4 ng/ml FGF, NLRP7 recovery augmented *POU5F1* expression (Figure 5.42). Protein levels of HLA-G and KRT7 did not change dramatically upon AP exposure (Figure 5.43).

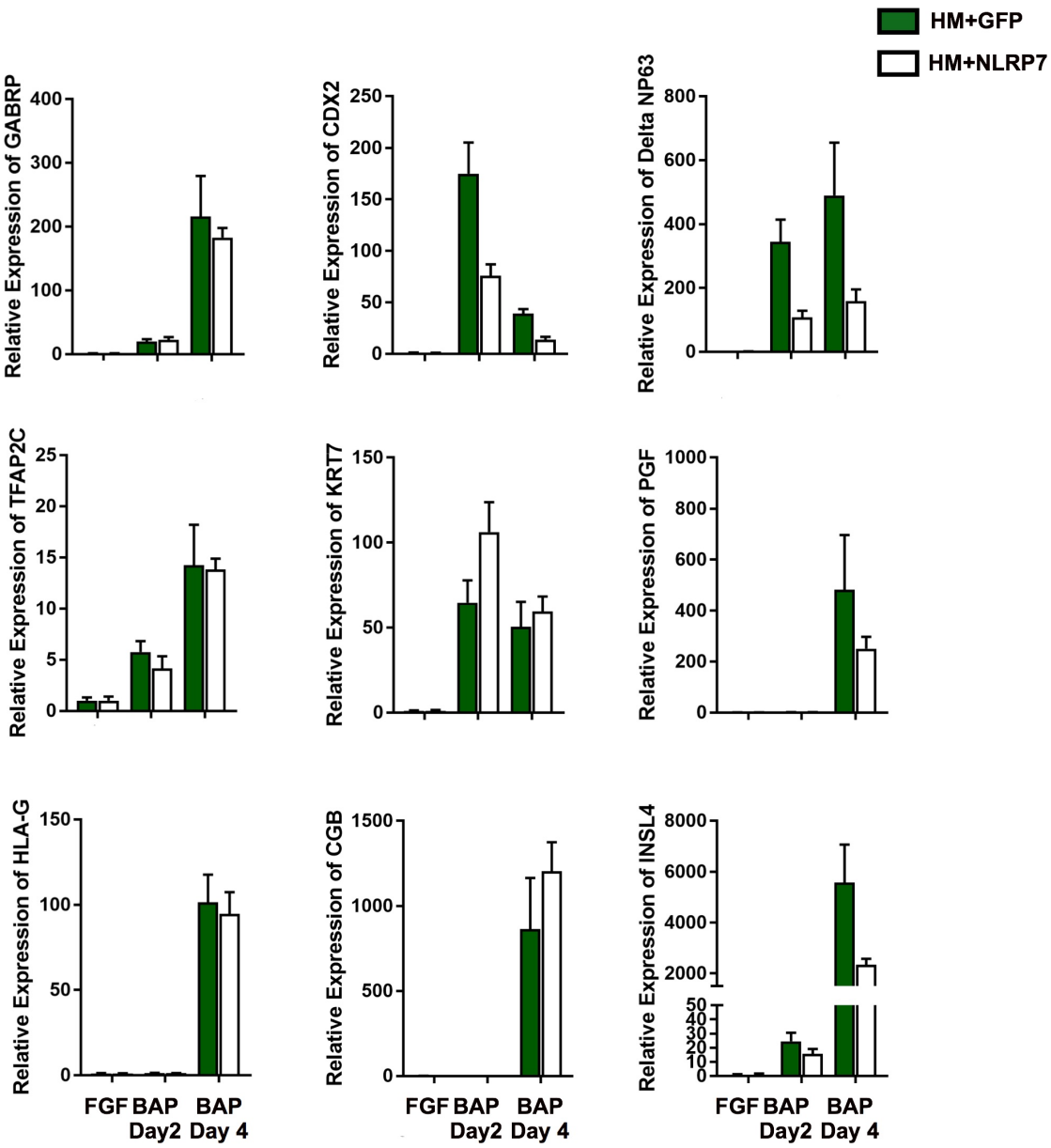

Figure 5.37. *CDX2, NP63, PGF* and *INSL4* gene expressions were attenuated in HM+NLRP7 group upon BAP exposure. Changes in gene expression of trophoblast markers in response to BAP treatment were analyzed by RT-qPCR. Relative mRNA levels were normalized to *HPRT* housekeeping gene.

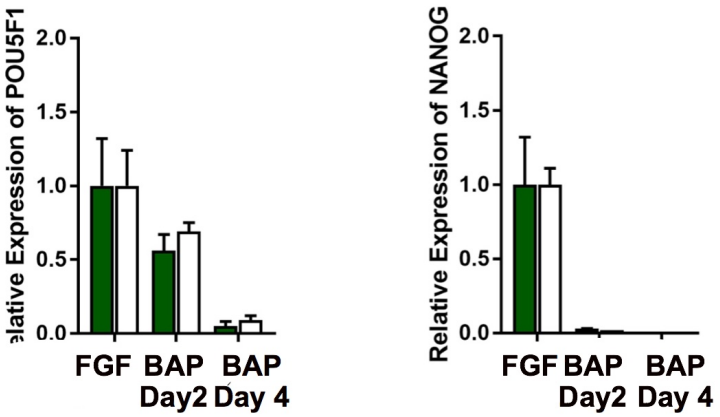

Figure 5.38. Stem cell specific gene expressions were downregulated in both groups upon BAP exposure. Changes in gene expression of stem cell markers in response to BAP treatment were analyzed by RT-qPCR. Relative mRNA levels were normalized to HPRT housekeeping gene.

Intrinsically, it was not surprising that no differences in KRT7 and HLAG levels were observed in HM+NLRP7 cells, as the same situation was evident in gene expression analysis. Similar to BAP conditions, recovery of NLRP7 restored OCT4 expression under AP conditttions. On the other hand, CDX2 expression showed increasing pattern in HM+GFP cells, while HM+NLRP7 cells showed decreasing pattern (Figure 5.44). Expressions of the genes such as, *INSL4* and *PGF*, which are greatly affected in HM and HM+NLRP7 groups, should be examined to observe the effect of NLRP7 introduction. Also, longer time points should be assessed to observe efficient recovery.

Flow cytometry analysis displayed that most of the cells became positive for KRT7 by day 4 while only FGF treated cells were negative for KRT7. When NLRP7 reintroduced to cells, both the percentage of the KRT7 positive cells and mean fluorescent intensity (MFI) of KRT7 were decreased in WT and HM+NLRP7 groups relative to HM cells (Figure 5.45). However, flow cytometry results did not correlate with gene expression analysis, as *KRT7* mRNA levels were not affected by NLRP7 recovery.

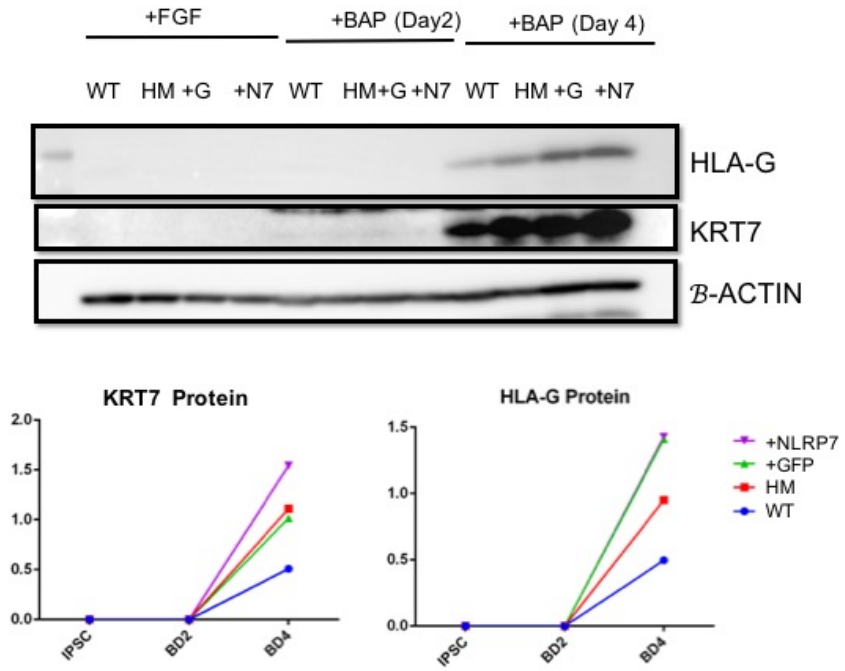

Figure 5.39. KRT7 and HLA-G protein levels were not rescued in HM+NLRP7 group upon BAP exposure. β-ACTIN was used as loading control.

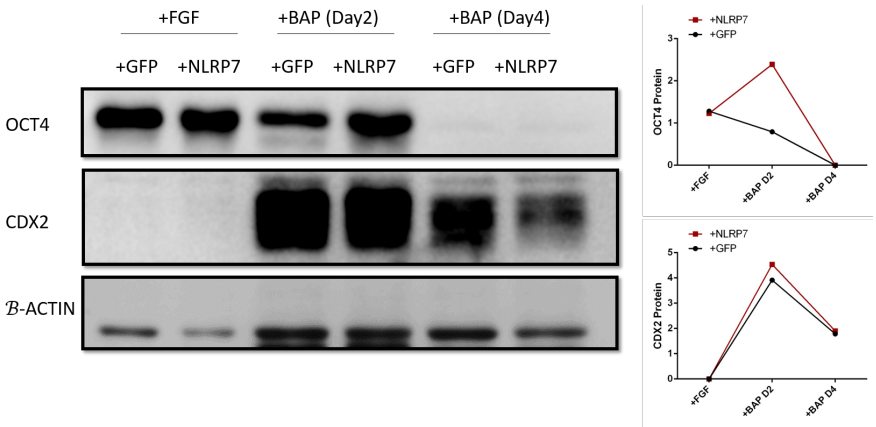

Figure 5.40. OCT4 levels were rescued in HM+NLRP7 group upon BAP exposure. β-ACTIN was used as loading control.

The results of recovery experiments along with that of HM group implied that lack of NLRP7 inclined iPSCs towards trophoblast linage by dominantly affecting the expressions of CDX2, NP63, PGF and INSL4. Although, from these results, it was evident that the absence of NLRP7 expedited the differentiation of iPSCs into trophoblast cells under BAP and AP conditions and NLRP7 re-introduction was able to decelerate this differentiation process. Karyotyping revealed that those cells used in recovery experiments had trisomy 12. Showing abnormal karyotype, especially for chromosome 12 is a common situation for hESC cultured *in vitro* [66]. So, we still might claim that the phenotype observed for recovery experiments is because of NLRP7 introduction rather than trisomy 12, as both of the groups derived from the same progenitor cells and shared the same karyotype (trisomy 12).

5.2.6. NLRP7 Deficiency Alters the Expression of YY1 Target Genes in Response to BAP Conditions

Mahadevan *et al.* showed that NLRP7 regulates trophoblast differentiation and interacts with YY1 which is an ubiquitous transcription factor and involved in diverse biological processes. For example, mouse embryos carrying homozygous mutated YY1 allele did not survive beyond the blastula stage [67]. Furthermore, it is well known that YY1 transcription factor regulates the BMP pathway, which is a crucial growth factor group for trophoblast differentiation, by inhibiting the DNA binding ability of SMAD transcription factors [68]. Therefore, SMADs cannot bind to BMP promoter and induce its expression. Considering the relationship between YY1, BMPs and trophoblast differentiation pathway, NLRP7 may coordinate to trophoblast differentiation by regulating BMP4 levels in relation with YY1. So, we decided to investigate the expressions of YY1 and BMP-4 in iPSCs and differentiated trophoblast cells. In addition to BMP-4 as a YY1‘s target gene, we studied several other YY1 target genes from the literature, *ID1*, *LIF*, *c-FOS*, *ZFP42*, which may take roles in trophoblast differentiation [69–73]. We designed qPCR primers for these genes. After PCR optimization experiments were performed for *YY1* (regulates BMP-4 pathway), *BMP-4* (induces the differentiation of human ES cells to trophoblast), ID1 (Inhibitor Of DNA Binding 1, major downstream

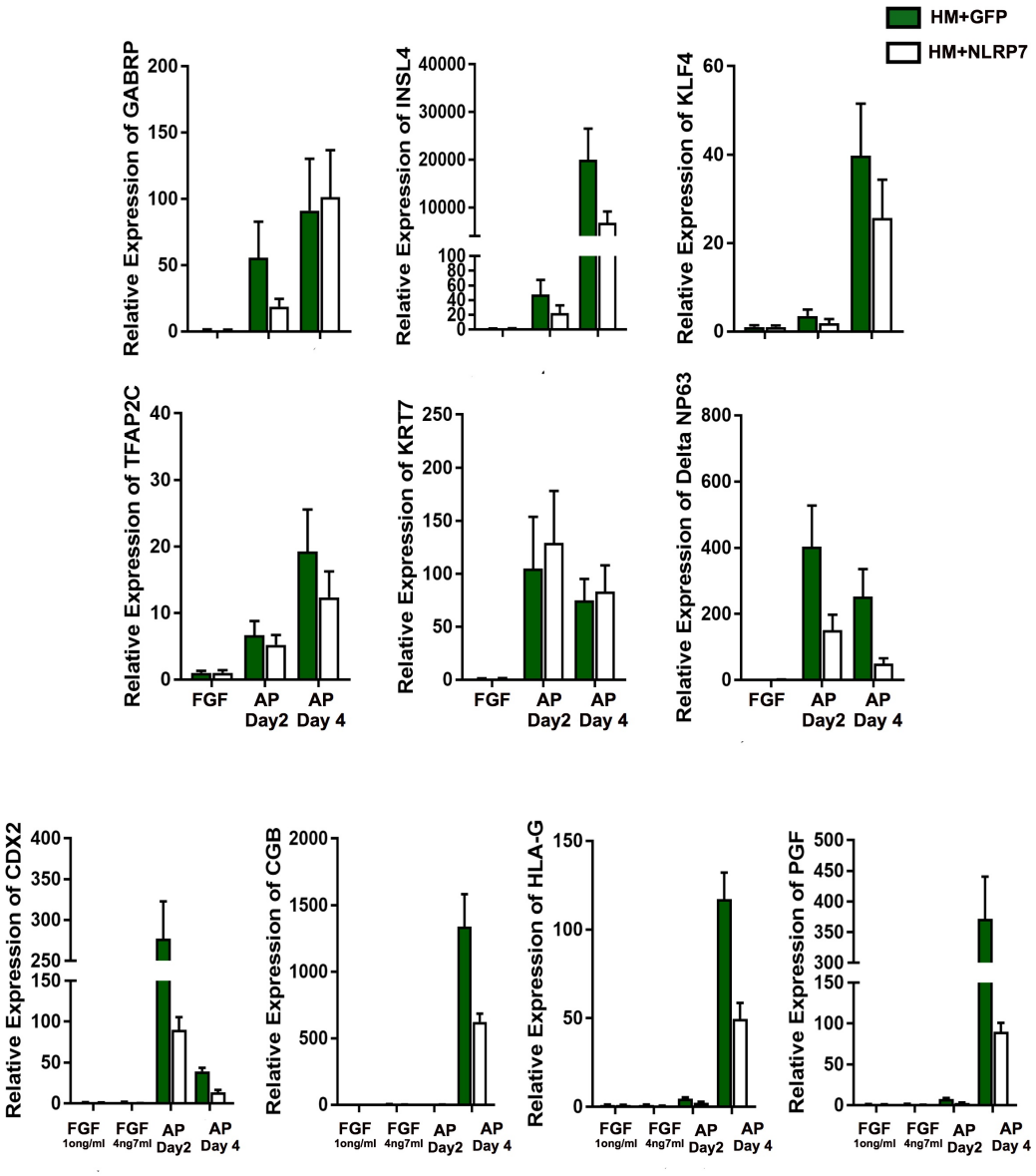

Figure 5.41. The majority of trophoblast specific gene expression was attenuated in HM+NLRP7 group upon AP exposure. Changes in gene expression of trophoblast markers in response to AP treatment were analyzed by RT-qPCR. Relative mRNA levels were normalized to HPRT housekeeping gene.

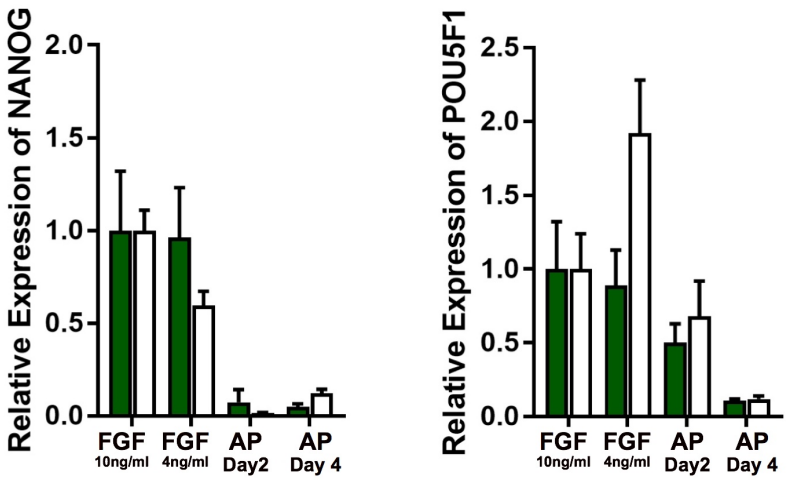

Figure 5.42. Stem cell specific gene expressions were downregulated in both groups upon BAP exposure. Changes in gene expression of stem cell markers in response to BAP treatment were analyzed by RT-qPCR. Relative mRNA levels were normalized to HPRT housekeeping gene.

transcriptional targets of BMP signaling), *LIF* (ES cell self-renewal and pluripotency, trophoblast migration), *c-FOS* (proto-oncogene, possible role in trophoblast migration and invasion.), *ZFP42* (Involved in the reprogramming of X-chromosome inactivation during the acquisition of pluripotency, interacts with YY1) and *NLRP2*, qPCR was performed with same RNA samples used in trophoblast marker qPCR. Interestingly, *BMP-4* and *YY1* mRNA levels increased in HM BAP group compared to WT groups upon differentiation (Figure 5.46). Although, we supplemented the cells with the same amounts of exogenous BMP-4 during BAP treatment, differentiated HM BAP group expressed more *BMP4* and *YY1* mRNAs whereas before BAP treatment, HM iPSCs expressed less *BMP4* than WT iPSCs. On the contrary, WT iPSCs expressed less *YY1* than HM iPSCs. As a result, NLRP7 appeared to operate the expression of many genes that mainly take role in BMP pathway and trophoblast differentiation. However, in order to clarify the action mechanism of NLRP7, more comprehensive studies should be established such as; RNA-seq and methylation profiling. Also, it should be considered that using inhibitors, in this case AP, may masked the effect of NLRP7 in particular

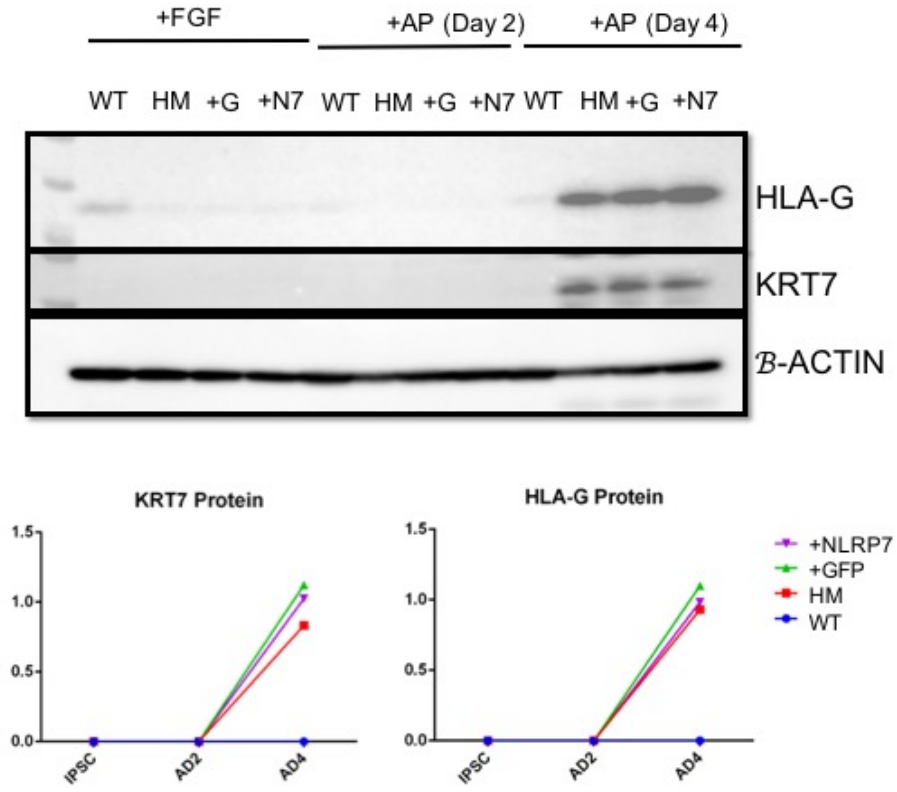

Figure 5.43. KRT7 and HLA-G protein levels were not recovered in HM+NLRP7 group upon BAP exposure. β-ACTIN was used as loading control.

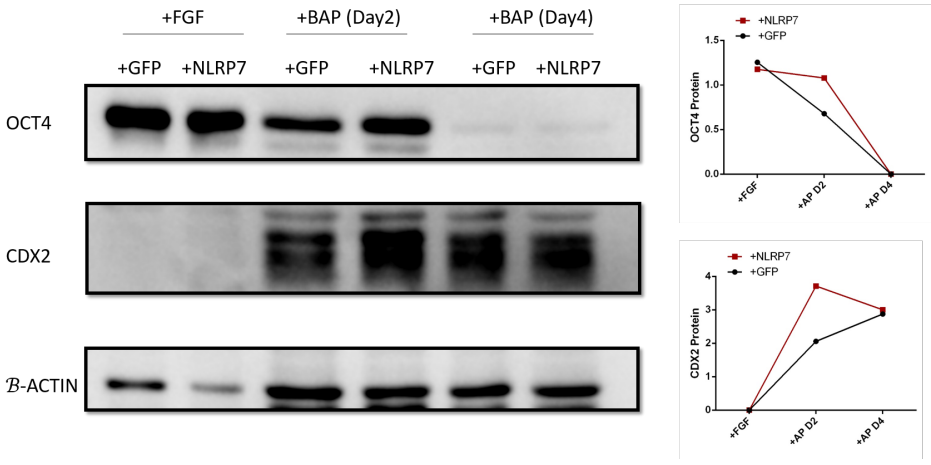

Figure 5.44. OCT4 protein levels were recovered in HM+NLRP7 group upon BAP exposure. β-ACTIN was used as loading control.

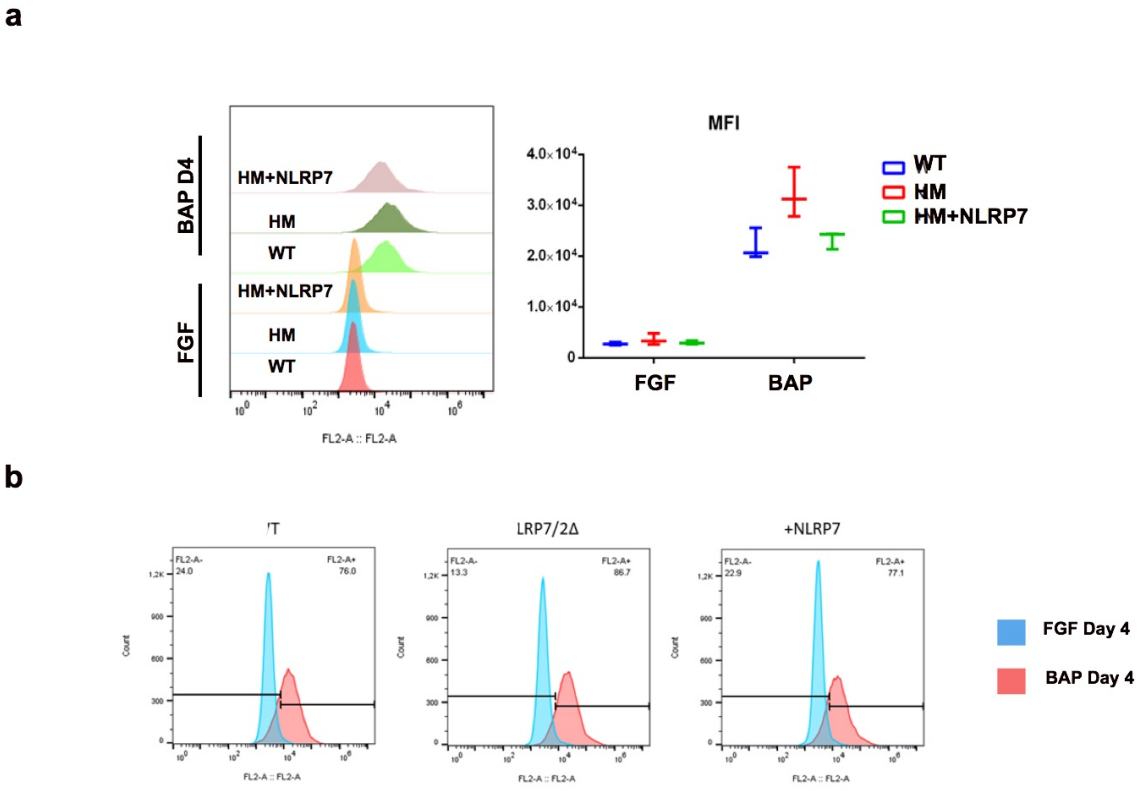

Figure 5.45. Flow cytometry analysis of KRT7 expression upon BAP treatment. a) Histogram and Mean Fluorescence Intensity of KRT7 b) Representative histograms of KRT7. The numbers represent the percentage of cells within each quadrant.

pathways.

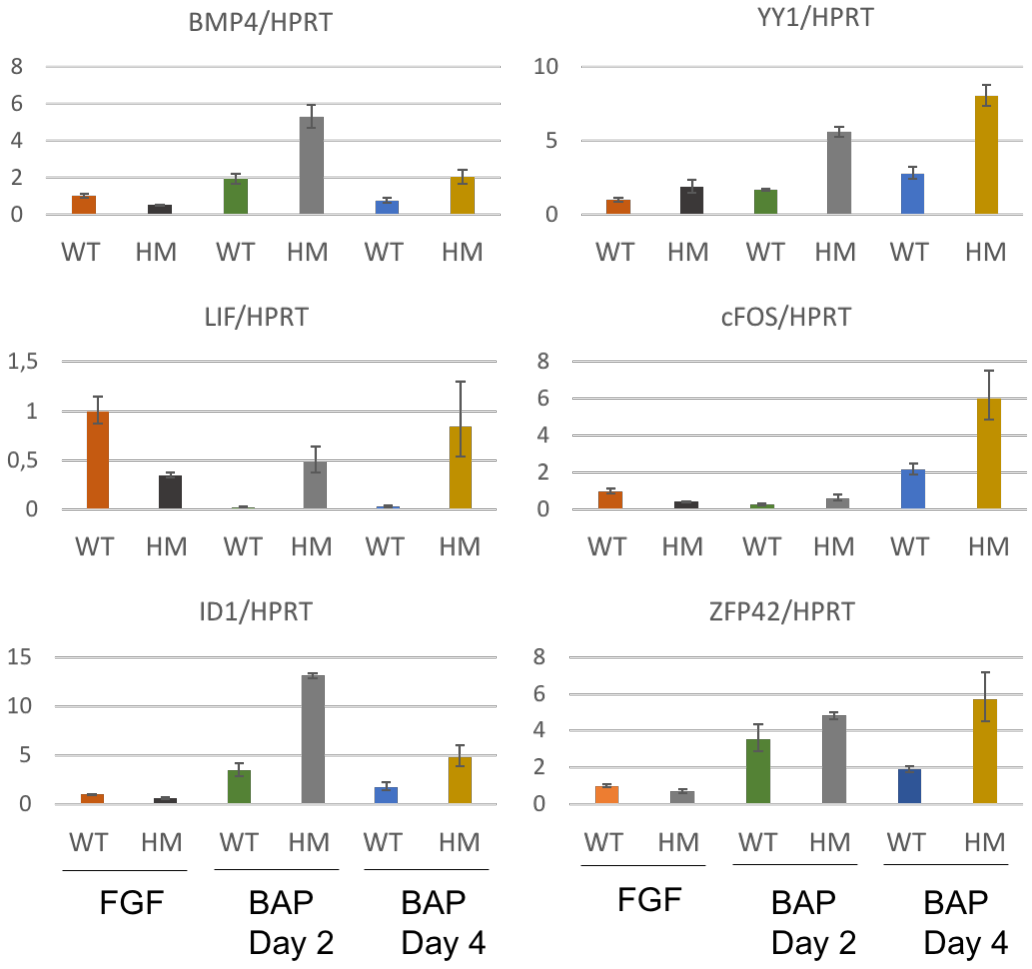

Figure 5.46. RT-qPCR assessments of YY1 and its target genes. Relative mRNA levels were normalized to HPRT housekeeping gene. HM groups expressed more BMP4, YY1, C-fos, LIF, ZFP42 and ID1 mRNA than WT group after BAP treatment. n=1

5.3. Identification of NLRP7's Function in Inflammatory Pathways

5.3.1. Polyclonal Antibody Production Against Human NLRP7

At the time we started this project, there was no commercially available NLRP7 antibody. Therefore, we aimed to produce NLRP7 antibody to use for further experi-

ments.

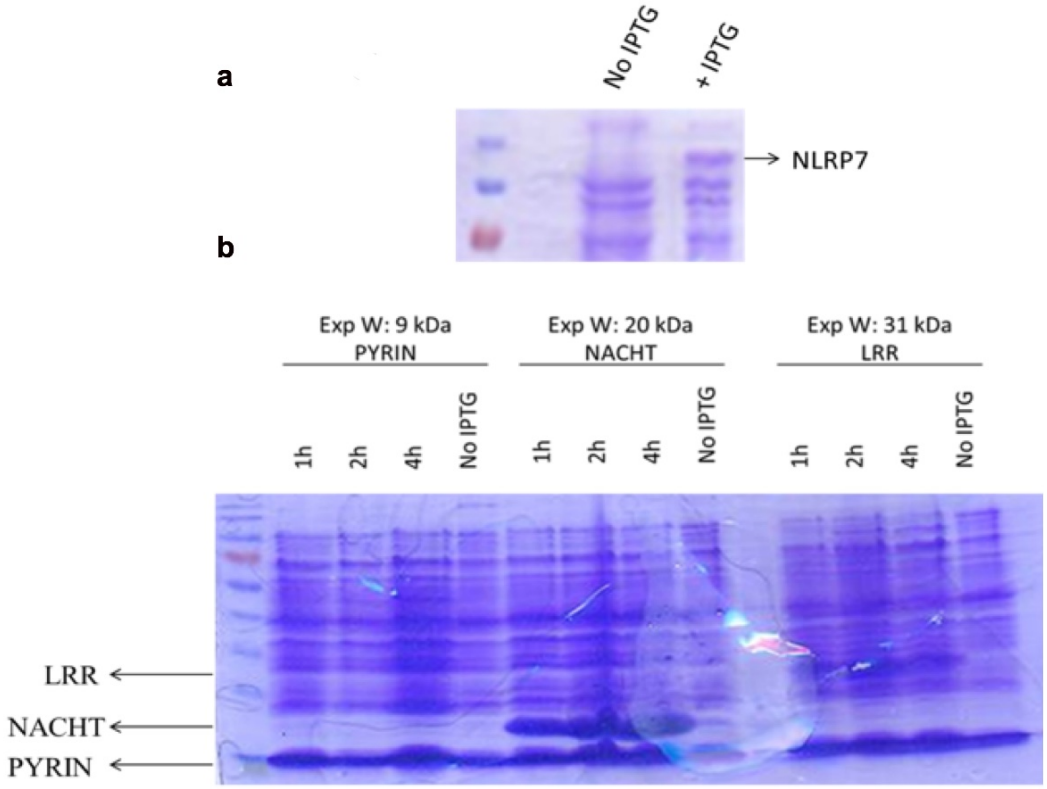

Figure 5.47. Protein expression after IPTG induction of E.coli Rosetta strain. a)His-NLRP7 b) His-Pyrin, His-Nacht, His-LRR.

5.3.1.1. IPTG Induction and Protein Purification of NLRP7. In order to produce His-tagged NLRP7, bacterial expression vector pet30a-NLRP7 was used and IPTG induction was performed. We could not achieve induction at 37°C due to that NLRP7 was located in inclusion bodies, whereas Pyrin, Nacht and LRR domains were able to induced at 37°C. The bacterial culture (*E.coli* Rosetta strain) for full length NLRP7 was incubated at 22°C for 8 hours. After that, induction efficiency was examined by Coomasie blue staining. As a result, successful induction was made and shown in Figure 5.47. Full length NLRP7 induced bacteria were lysed by using sonication and Triton-X. However, full length NLRP7 and LLR domain wcould not be purified using nickel chromatography columns, therefore they were isolated from SDS-PAGE gel slices. Isolated NLRP7 and LLR were verified by Coomasie Blue staining. Although

there were several bands other than NLRP7, it was purified enough to proceed to injection steps to Wistar albino rabbits and BalB/c mice whereas LRR purification was not successful. On the other hand, domains of NLRP7 induced bacteria were lysed with 0.1M KHPO4, 8M Urea (pH:8) to be further purified with nickel columns. Purified proteins were shown with Coomassie Blue staining (Figure 5.48).

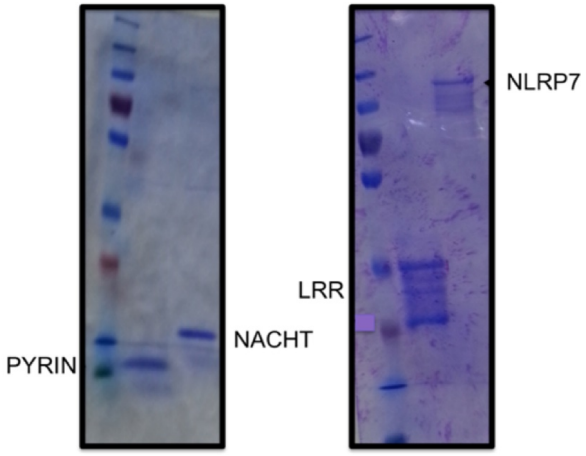

Figure 5.48. Pyrin and NACHT were purified via nickel columns. His-NLRP7 and His-LRR were isolated from SDS-PAGE gel.

5.3.1.2. Rabbit Immunization aganist NLRP7 and NLRP7 $^{\text{Pyrin}}$. In order to produce polyclonal antibody against NLRP7, 50μg purified His-NLRP7 protein was used to immunize a Wistar-Albino rabbit. 2 other Wistar-Albino rabbit were immunized with NLRP7 $^{\text{Pyrin}}$. After 3 sub-cutaneous injections, sera were collected. The response of the sera was verified via ELISA and Western blotting. To assess the presence of NLRP7 and Pyrin specific antibodies in serum, ELISA was performed by coating plates with 50 ng of proteins used for immunizations. All of the sera gave response to their target protein when compared with PBS (Figure 5.49a). To ensure that the antibody was not specific for His tag, different tagged NLRP7 proteins were tested. Western blotting displayed that polyclonal antibody for NLRP7 protein and NLRP7 $^{\text{Pyrin}}$ was produced, successfully (Figure 5.49b). However, among them full length NLRP7 serum gave the highest response. Therefore, the serum produced against full length NLRP7 was used for further studies.

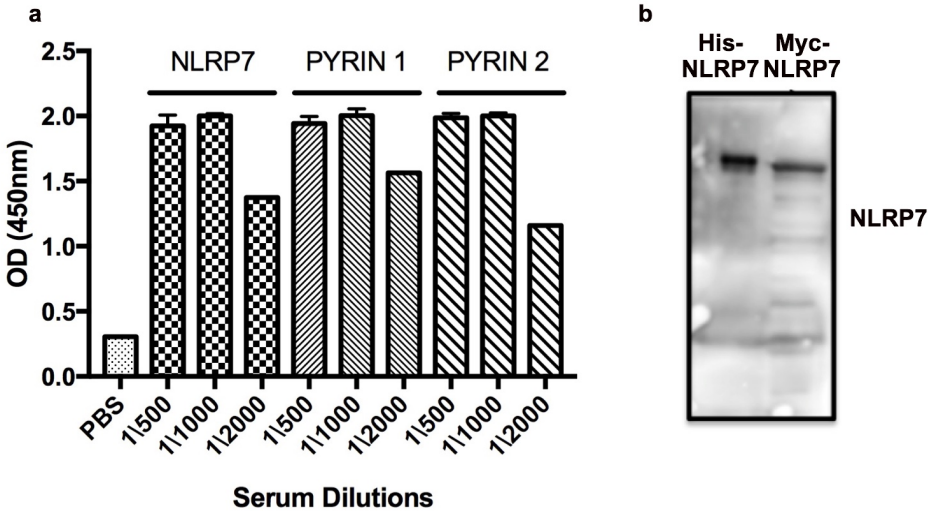

Figure 5.49. Verification of human NLRP7 polyclonal antibody production. a) Serum titration of tree immunized Wistar Albino rabbits by ELISA. b)Purified His-NLRP7 and pCDNA3-Myc-NLRP7 transfected HEK293 cell lysates were tested via western blotting with full length NLRP7 serum (1:1000).

5.3.2. Generation of Monoclonal Antibody aganist Human NLRP7

In addition to polyclonal antibody production, we tried to produce monoclonal anti NLRP7 antibody. As explained above, BALB/c mice were immunized with full length NLRP7 (50ug). After 3 immunizations, successful antibody response was tested by Western blotting (Figure 5.50). To produce monoclonal antibody, classical hybridoma technique, in which an antibody-producing B cell is fused with a F0 myeloma (B cell cancer) cell, was used. After fusion, antibody response was tested by ELISA. Although the hybridoma fusion was successful and several colonies were positive against NLRP7 protein, the cells did not survive due to problems caused by the incubator. As, monoclonal NLRP7 antibody became commercially available at that time, studies of monoclonal antibody production were discontinued.

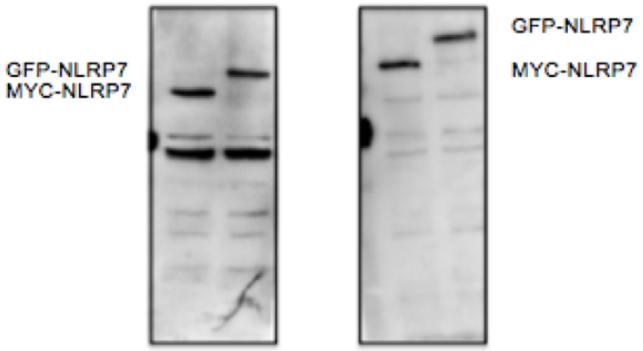

Figure 5.50. Verification of human NLRP7 immunization for monoclonal antibody production. pEGFP-C3-NLRP7 and pCDNA3-Myc-NLRP7 transfected HEK293 cell lysates were tested via western blotting with sera of 2 mice separately (1:1000).

5.3.3. Generation of Stably NLRP7 Expressing THP-1 Cells

5.3.3.1. Generation of pENTR1A-NLRP7 and pLEX307-NLRP7. To generate stable NLRP7 expressing cell lines, NLRP7 gene was cloned into lentiviral vector. To do so, NLRP7 was cloned into pENTR1A no ccDB (W48-1) gateway entry vector to transfer NLRP7 into pLEX-307. In addition to NLRP7, its Pyrin, Nacht and LRR domains were cloned pENTR1A no ccDB (W48-1). First, NLRP7 and its domains were amplified separately by PCR from pET30a-NLRP7 vector by using SalI and NotI restriction sites added primers. Digested PCR products were ligated into SalI and NotI double digested pENTR1A no ccDB (W48-1) vector and positive colonies were verified by colony PCR and sequencing (Figure 5.51). Then, no SNP or frameshift containing PENTR1A/NLRP7 vector used to transfer NLRP7 into pLEX-307 vector by LR reaction. Positive colonies detected by colony PCR were sequenced to verify absence of SNP or frame shift (Figure 5.52).

5.3.3.2. THP-1 Transduction with pLEX307-NLRP7. To generate stably over expressing NLRP7 THP-1 cell line, pLEX-307/NLRP7 vector containing virus particles was

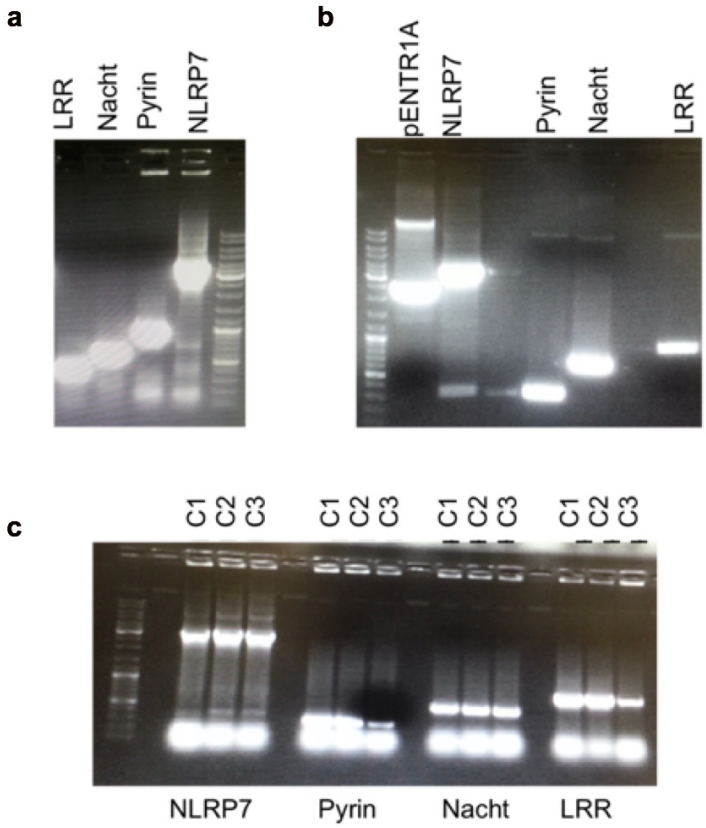

Figure 5.51. Cloning of NLRP7 into pENTR1A no ccDB (w48-1) vector. a) PCR results of NLRP7 and its domains Pyrin, Nacht, LRR from pcDNA3-Flag-NLRP7 vector. b) Digestion with SalI and NotI restriction enzymes c) Colony PCR results. All the colonies gave the expected band.

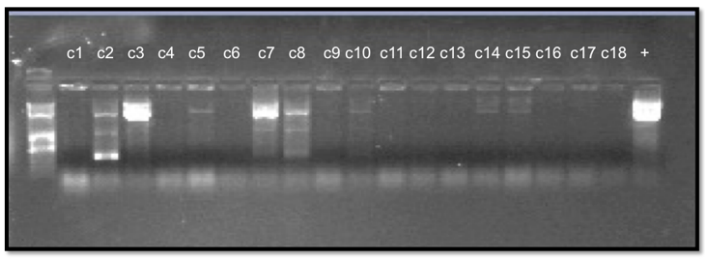

Figure 5.52. Cloning of NLRP7 into pLEX-307 by Gateway cloning system. Colony PCR reults. pET30a-NLRP7 vector was used as a positive control.

introduced to human monocytic cell line THP1 via lentiviral transduction. After puromycin selection, NLRP7 over expression was visualized by Western blotting (Figure 5.53).

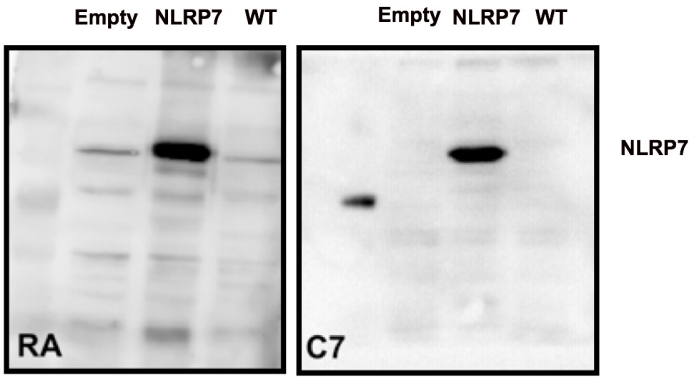

Figure 5.53. The Stable NLRP7 overexpression in THP-1 cells (THP1-NLRP7^{OE}). Cell lysates of THP-1 cells transduced with an empty vector (THP1-Empty), NLRP7-containing vector (THP1-NLRP7^{OE}) and non-transduced THP-1 cells (WT) were analysed by Western blotting with (a) home made polyclonal NLRP7 antibody (1:1000) and (b) commercial monoclonal NLRP7 antibody (sc-377190) (1:1000).

5.3.4. Generation of NLRP7 Knock-down THP-1 Cells via CRISPR/CAS9 Technology

During this phD thesis, several strategies to knock-down NLRP7 gene in THP-1 cells were endeavored. First, three shRNA sequence targeting NLRP7 separately were cloned into KH-1 vector. Then, LentiCRISPRv2, one vector based CRISPR system, were used. 25 different NLRP7 targeting sequences were designed via CRISPR target design tool and cloning of these sequences to LentiCRISPRv2 were performed by Seda Yasa, a former lab member. Although knock-down of NLRP7 was demonstrated just after transduction or selection by both using KH-1 vectors or LentiCRISPRv2, knock-down could be maintained only for one or two weeks. Therefore, we decided to purchase commercial NLRP7-shRNA plasmid from SantaCruz Biotechnology. However, consistent with previous results, stable knock-down of NLRP7 was unsuccessful. Based on this observation; NLRP7 expression was regained at later time points, even

NLRP7 expression was reduced at early time points, we hypothesized that knock-down of NLRP7 affects proliferation or survival of THP-1 cells, therefore the cells that do not express NLRP7 are removed from the population and only NLRP7 expressing cells survive in the population. The notion that stable NLRP7 knock-down/knock-out cells cannot be propagated led us to use inducible systems. For this strategy, Doxyxcycline (Dox) inducible two vector based CRISPR system was used. First, Dox inducible-cas9 containing lentiviruses were produced in HEK293FT cells via calcium phosphate transfection. The cells were transduced with cas9 containing lentiviruses and selected with puromycin until all the untransduced cells died. The second step of the procedure was to produce lentiviruses containing pLKO5.sgRNA.EFS.GFP vector. In order to express sgRNAs, three sgRNA oligos that have the highest targeting scores previously designed via CRISPR target design tool were annealed and cloned into BsmBI digested pLKO5.sgRNA.EFS.GFP vector. After verification via sequencing, pLKO5.sgRNA.EFS.GFP containing lentiviruses were produced in HEK293FT cells.

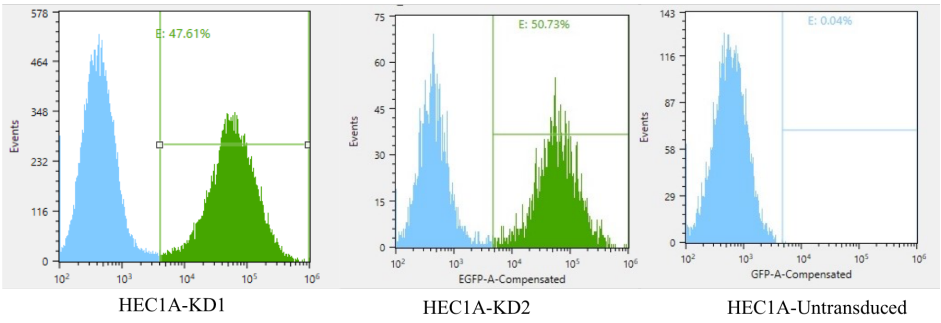

Figure 5.54. Lentiviral transduction efficiency of Hec1a Cells. The percentage of GFP expressing sg-NLRP7-1 (KD1) and sg-NLRP7-2 (KD2) cells was determined via Flow cytometry.

Our previous transduction experiments showed that the transduction efficiency of THP1 cells is low as it is a monocytic cell line. Therefore, we first tested the targeting efficiency of sgRNAs in Hec1a cell line in which endogenous NLRP7 expression is high. By this way, the most efficient sgRNAs were aimed to be determined for further usage in THP1 cells. Hec1a-cas9 cells were infected with sg-NLRP7-1 (KD1) and sg-NLRP7-2 (KD2). Non-targeting sgRNA vector eas used as a control. Transduction efficiency was

determined via flow cytometry (Figure 5.54). Then, the cells were treated with Dox to express cas9. qPCR results demonstrated that NLRP7 mRNA levels were reduced upon induction with doxyxcycline (Figure 5.55). When compared with NLRP7 expression in WT Hec1a cells to that of sgNLRP7 transduced cells, WT cells had more NLRP7 mRNA. Transduction itself seemed to have effect on NLRP7 expression. Yet, NLRP7 expression attenuated in Dox treated cells. This result was further verified by western blotting. KD2 and KD3 sgRNAs appeared to reduce NLRP7 protein levels upon Dox treatment (Figure 5.56).

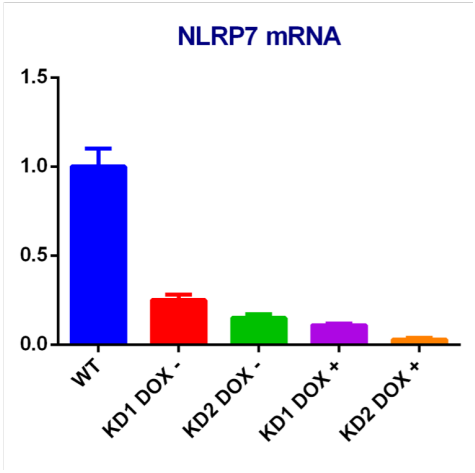

Figure 5.55. Knock-down of NLRP7 in Hec1a cells. RT-qPCR was performed to detect NLRP7 mRNA levels in KD1 and KD2 cells with or without Dox treatment.

As knock-down studies were promising for KD-2 and KD-3 in Hec1a cell lines, we proceeded to knock-down NLRP7 in THP-1 cells. THP1-Cas9 stable cells were infected with pLKO5.sgRNA.EFS.GFP viruses and 3 days later, GFP expressing cells were sorted via SONY Cell Sorter. Unfortunately, those sorted cells did not survive even cas9 expression was not induced by dox treatment. This result was possibly due to leakage effect caused by presence of tetracycline derivatives in FBS which result in induction of cas9 promoter. Therefore, we skipped cell sorting and decided to use pooled cells transduced with KD-2 sg-NLRP7 and for each experiment new transduction was performed and the cells were used within a week. Transduction efficiency were visualized by fluorescence microscopy (Figure 5.57). Cells were treated with Dox for

24 hours prior to western blot analysis. NLRP7 protein levels reduced in KD-1 and KD-2 cells in comparison to THP1-cas9 cells albeit the low expression of NLRP7 in control cells (Figure 5.58).

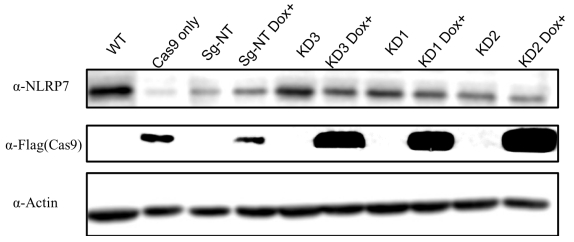

Figure 5.56. Knock-down of NLRP7 in Hec1a cells. Western blotting was performed to detect NLRP7 protein levels in KD1, KD2 and KD3 cells with or without Dox treatment.

5.3.5. *Pseudomonas Aeruginosa* Infection Activates NLRP7 Inflammasome

At the time we started to investigate the involvement of NLRP7 in inflammasome formation, it was unknown whether NLRP7 forms an inflammasome or which pathogens it senses. From our group, Duygu Bas in her master thesis documented that over-expressed NLRP7 caused IL-1β maturation along with over-expression of ASC and Caspase-1. Also, she demonstrated that NLRP7 interacted with ASC and Caspase-1 in an over-expression system performed in HEK293FT cells. Those results revealed that NLRP7 is a pro-inflammatory cytokine and most probably participates in inflammasome assembly. Considering these results, the potential activators of NLRP7 inflammasome were screened by treating cells with many known inflammasome stimulators, such as; LPS, ATP, MSU, R837. None of these activators caused significant difference on endogenous NLRP7 protein levels. Additionally, heat-killed *Staphylococcus aureus, Listeria monocytogenes, Enterococcus faecalis and Pseudomonas Aeruginosa* treatments were performed in THP1 cells to examine the changes in NLRP7 protein levels. Among those infections, *P.Aeruginosa* appeared to have an effect on NLRP7 expression. In order to further investigate the possible involvement of NLRP7

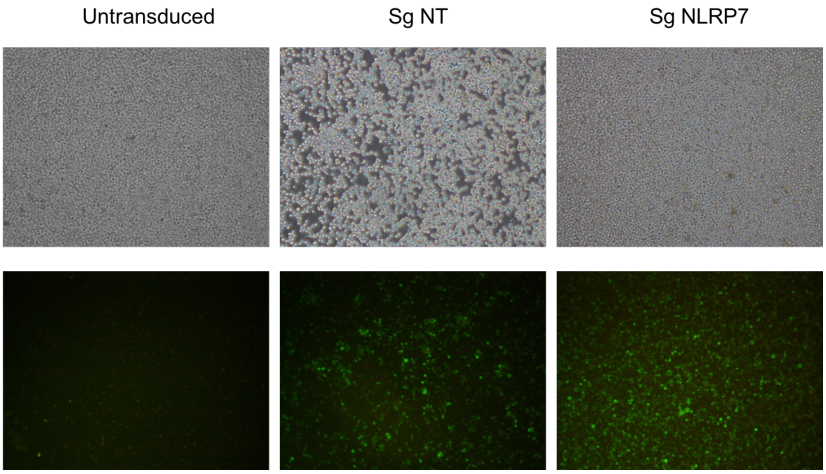

Figure 5.57. Transfection efficiency of pLKO5.sgRNA.EFS.GFP virus production. HEK293FT cells were trasfected with pCMV-VSV-G, PSPAX2, sg-non-targeting (sgNT), or sgNLRP7. Representative images were given.

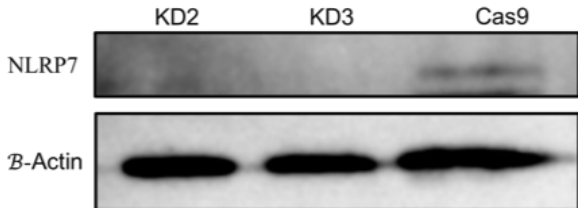

Figure 5.58. Knockdown of NLRP7 in THP1 cells. NLRP7 protein levels were determined via western blotting upon Dox treatment).

in inflammatory response against *P.Aeruginosa* infections, live infection (MOI:10) was performed in THP1-NLRP7^{OE} for 2 hours following to PMA differentiation and then medium replenished with gentamycin containing medium to remove remaining bacteria for 30 minutes. Sixteen hours later medium was collected for analysis of IL-1β secretion which is a readout of inflammasome formation. ELISA results clearly demonstrated the elevated secretion of 1β in THP1-NLRP7^{OE} compared to THP1-Empty cells upon *P.Aeruginosa* infection (Figure 5.59).

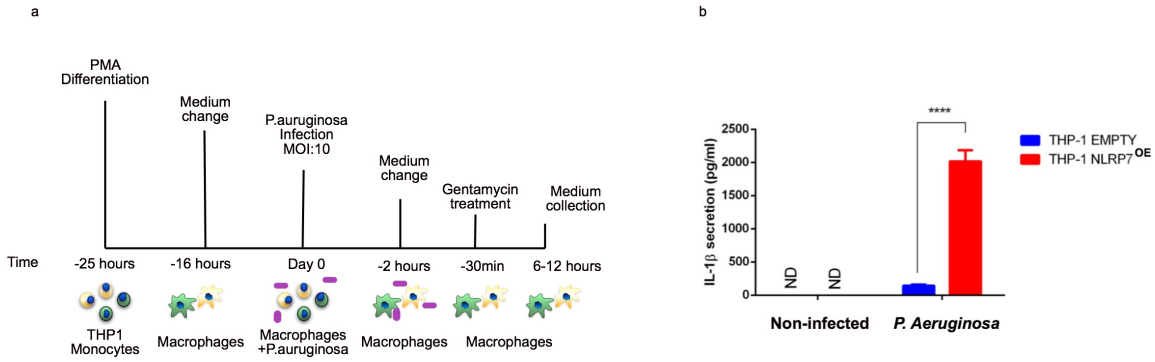

Figure 5.59. Transfection efficiency of pLKO5.sgRNA.EFS.GFP. THP1-cas9 cells were transduced with sgNT or sgNLRP7 lentiviral particles.

Contribution of NRLP7 to the innate immune response against *P.Aeruginosa* infection was also tested in knock-down system. NRLP7 knock-down cells were generated as explained in 5.3.4 section via lentiviral transduction of sgRNAs. After 2 days of infection cells were treated with Dox (0.5μM) overnight. On the third day, THP-1 KD2 cells were infected with *P.Aeruginosa* for two hours without prior PMA treatment. Then, medium was replenished with gentamycin containing medium. The supernatants of the cells were collected at 6 and 12 hours post Gentamycin treatment. Western blot analysis revealed that not only secretion of IL-1β but also protein levels were diminished in sgNLRP7 cells (Figure 5.60 and Figure 5.61). p10 subunit of caspase1 levels can be detected at early time points in cell lysates after inflammasome activation, whereas it is secreted at later time points. Increased p10 levels in sgNLRP7 cells indicated improper caspase-1 activation or secretion (Figure 5.61). As a result,

NLRP7 is an another PRR, sensing *P.Aeruginosa*.

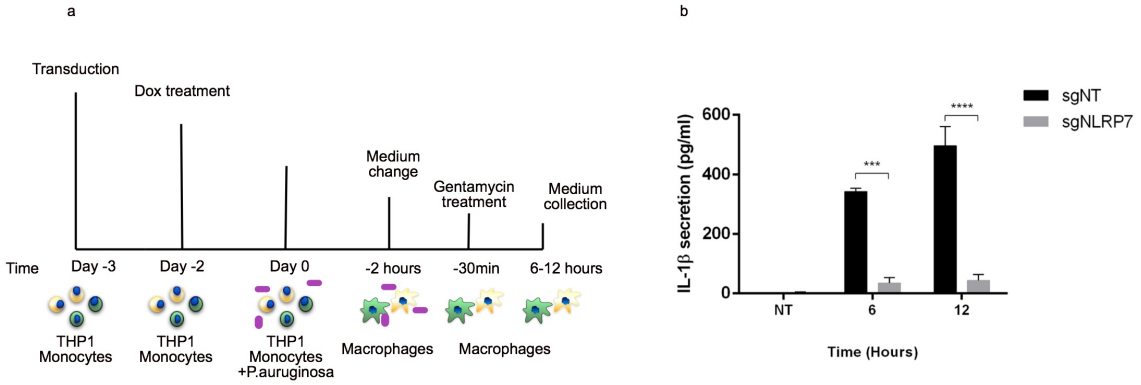

Figure 5.60. NLRP7 is required for *P.Aeruginosa* driven IL-1β secretion. Knockdown of NLRP7 dampened IL-1β secretion in response to *P.Aeruginosa* infection. a) experimental procedure b) IL-1β ELISA results.

5.3.6. Cytokine Profiling of THP1- NLRP7^{OE} Cells

So far, several studies examined the effects of NLRP7 on IL-1β secretion. Besides, it was previously shown by our group that NLRP7 is a pro-inflammatory protein and increased IL-β secretion in overexpression system in HEK293FT cells. In order to further characterize if there is any change on cytokine secretion profile in stable-NLRP7 expressing THP1 cells, dot blot membrane based Human Inflammation Antibody Array was purchased. Forty different inflammatory cytokines can be analyzed with this array system. PMA differentiated THP1-NLRP7^{OE} and THP1-Empty cells were infected with *Pseudomonas Aeruginosa* (MOI:10) for 2 hours. Conditioned media (CM) was harvested at 16 hours post infection. Then, CM was implemented to array membranes according to manufacturer's protocol and chemiluminescence signals were visualized by Stella imaging system (Figure 5.62). For analysis of the array data, positive control spots were used to normalize spot densities. Positive control spots are provided with biotin-conjugated IgG and there are 6 positive spots on each membrane. Each cytokine's signal was normalized by dividing them to average of positive signals. Then, fold change in cytokine secretions was calculated by dividing

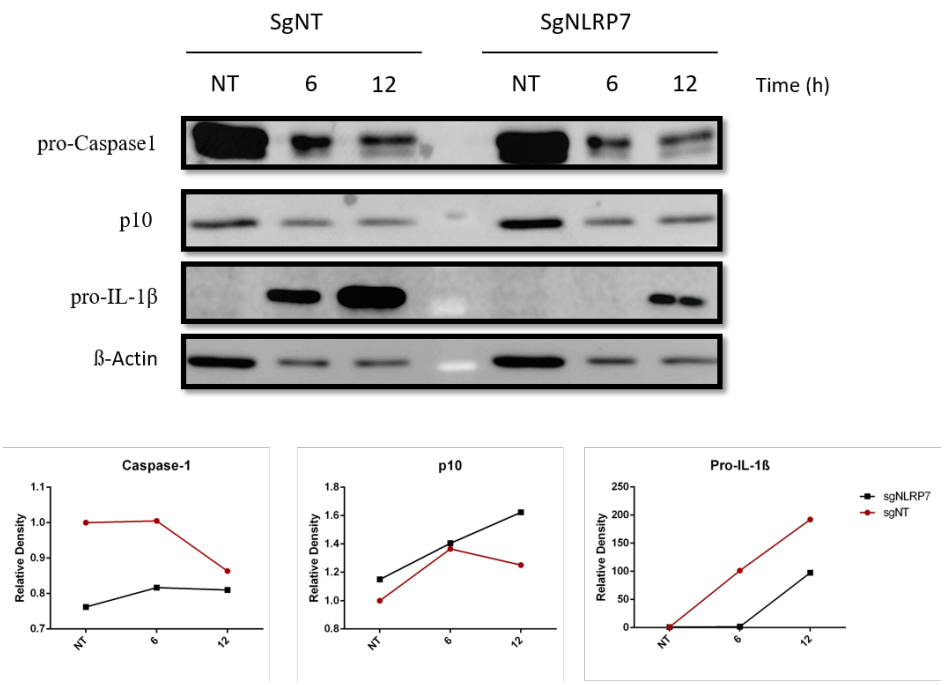

Figure 5.61. NLRP7 is required for *P.Aeruginosa* driven IL-1β cleavage.

normalized cytokine signals of THP1-NLRP7^{OE} to THP1-Empty ones. As a result, IL-6 (downstream target of IL-1β), IL-8 (chemotactic for basophils, T-cells and especially neutrophils), RANTES (attraction and activation of leukocytes), TNF, GM-CSF (activation of monocytes/macrophage), i-309 (chemotactic for monocytes), EOTAXIN (eosinophil-specific chemoattractant), IL-13 (up-regulates CD23 and MHC class II expression, down-regulates macrophage activity), levels increased in THP1-NLRP7^{OE} cells (Figure 5.63). All of these cytokines upregulated in THP1-NLRP7^{OE} cells upon *P.Aeruginosa* infection were pro-inflammatory cytokines except for IL-13 whose secretion was considerably low in comparison to pro-inflammatory cytokines. Among the analyzed, pro-inflammatory cytokines, IL-6 and i-309 (CCL-1) levels increased dramatically. Besides, a substantial difference was not observed for IL-β levels between groups. As IL-6 is a downstream target of IL-β, heightened IL-6 levels may implicate that IL-1β levels already increased before 16 hours and then activated its downstream effectors, so we were able to see elevated levels of IL-6.

a

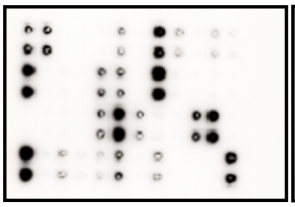

b

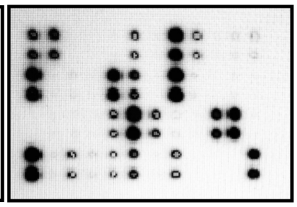

c

	A	B	C	D	E	F	G	H	I	J	K	L
1	Pos	Pos	Neg	Neg	EOTAXIN	EOTAXIN-2	GCSF	GM-CSF	ICAM-1	IFN-γ	I-309	IL-1α
2	Pos	Pos	Neg	Neg	EOTAXIN	EOTAXIN-2	GCSF	GM-CSF	ICAM-1	IFN-γ	I-309	IL-1α
3	IL-1b	IL-2	IL-3	IL-4	IL-6	IL-6sR	IL-7	IL-8	IL-10	IL-11	IL-12 p40	IL-12 p70
4	IL-1b	IL-2	IL-3	IL-4	IL-6	IL-6sR	IL-7	IL-8	IL-10	IL-11	IL-12 p40	IL-12 p70
5	IL-13	IL-15	IL-16	IL-17	IP-10	MCP-1	MCP-2	M-CSF	MIG	MIP-1α	MIP-1β	MIP-1δ
6	IL-13	IL-15	IL-16	IL-17	IP-10	MCP-1	MCP-2	M-CSF	MIG	MIP-1α	MIP-1β	MIP-1δ
7	RANTES	TGF-β1	TNF-α	TNF-β	s TNF RI	s TNF RII	PDGF-BB	TIMP-2	BLANK	BLANK	Neg	Pos
8	RANTES	TGF-β1	TNF-α	TNF-β	s TNF RI	s TNF RII	PDGF-BB	TIMP-2	BLANK	BLANK	Neg	Pos

Figure 5.62. Cytokine profiling of THP1-NLRP7^{OE} cells. Supernatants of THP1-NLRP7^{OE} (a) and THP1-Empty (b) cells were subjected to membrane based cytokine array after 16 hours of *P.aeruginosa* infection. Normalization of dot blots were done by ImageJ software. c) Array map

5.4. Investigation of the Oncogenic Role of NLRP7

Elevated NLRP7 expression was reported in endometrium cancer tissues and testicular seminomas [**?**, 19]. Also, mutations of NLRP7 cause hyper proliferation of trophoblast cells in hydatidiform mole which have a risk to transform into highly malignant trophoblastic tumor, choricarcinoma. From the literature knowledge, NLRP7 appears to be involved in oncogenesis especially in germ line tumors. In this section, the ability of NLRP7 to promote tumor formation was examined and possible interaction partners of NLRP7 were identified in the human endometrium cancer cell line (Hec1a).

5.4.1. Genereation of Stably Expressing Hec1-a and Swan-71 Cell Line

To investigate the possible oncogenic role of NLRP7, stable-NLRP7 expressing human endometrium cancer cell line and human trophoblast cell line (Swan-71) were

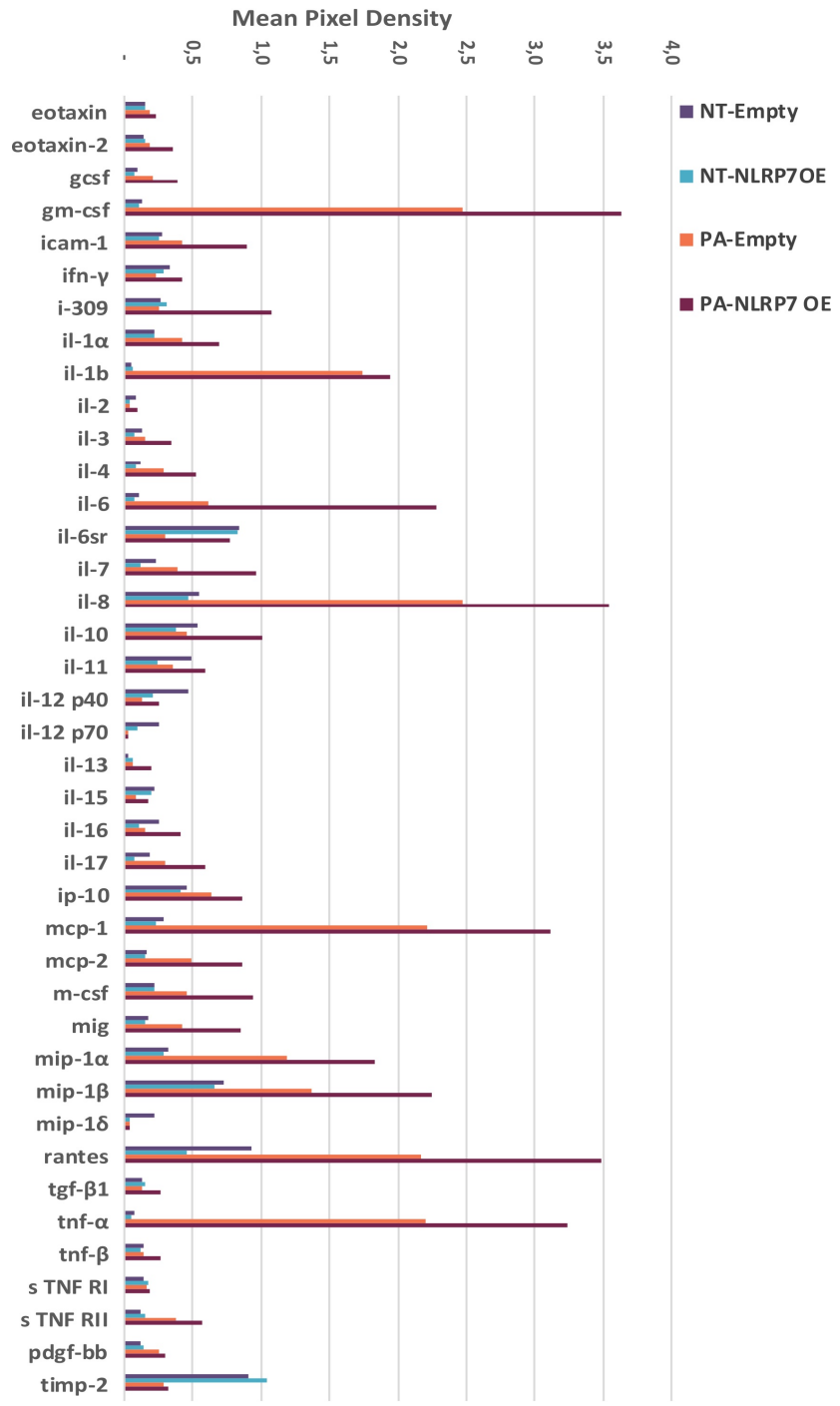

Figure 5.63. Cytokine profiling of THP1-NLRP7^{OE} cells. Supernatants of THP1-NLRP7^{OE} and THP1-Empty cells were subjected to membrane based cytokine array after 16 hours of *P.aeruginosa* infection. Normalization of dot blots were done by ImageJ software.

generated by using lentiviral viruses for further experiments. Lentiviruses were produced in HEK293FT cells via calcium phosphate transfection by using pLEX-307-NLRP7 plasmid. As the plasmid contains puromycin resistance gene, cells were selected by treatment with puromycin (1mg/ml) and NLRP7 expression was verified via Western blot analysis (Figure 5.64).

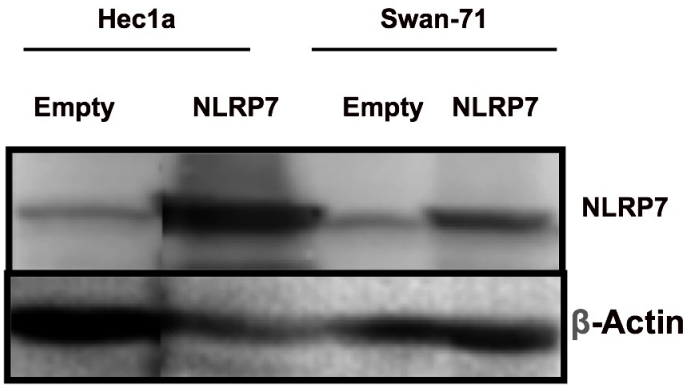

Figure 5.64. The Stable NLRP7 overexpressing Hec1a and Swan-71 cells. Lysates of control Swan71 and Hec1a cells transduced with an empty vector (empty) and a NLRP7 vector (NLRP7) were analyzed by Western blotting with home made polyclonal NLRP7 antibody (RA) (1:1000).

5.4.2. Tumor Load Studies

To investigate the possible oncogenic roles of NLRP7, stable-NLRP7 expressing human endometrium cancer cell line was generated as described above. Tumor formation abilities of Hec1a and Hec1a-NLRP7 cells were first analyzed *in vivo* in SCID mice. SCID mice (2-month-old), were given a 0.5 mL subcutaneous injection of 5×10^6 to each costa and flank of mice (Figure 5.65). Hec1-a, or Hec1a-NLRP7 cells prepared separately in PBS (200uL). Two mice were sacrificed 6 week after injection to measure tumor weights. NLRP7 overexpression promoted tumor formation (Figure 5.66). Then the experiment was reproduced with Hec1a-Empty and Hec1a-NLRP7 cells. Four weeks after injection, three mice were sacrificed and tumor weights were measured (Figure 5.67). Moreover, ten mg of tumor tissues were lysed to verify NLRP7 expression in tumor tissues. Western blot analysis showed that tumors collected from

Hec1a-NLRP7 injected sites express NLRP7 whereas that much NLRP7 expression was not detected for Hec1a-Empty injected tumors with an exception of one sample. That NLRP7 expressing tumor tissue also displayed increased tumor formation among other tumors within the control group which may be a result of a confusion with the samples. Consequently, NLRP7 seemed to enhance tumor formation in SCID mice in both 4 weeks and 6 weeks. When compared to first tumor load experiment, NLRP7 seemed to be more effective at later time points (at 6 week). Besides, experimental group should be extended for statistical analysis.

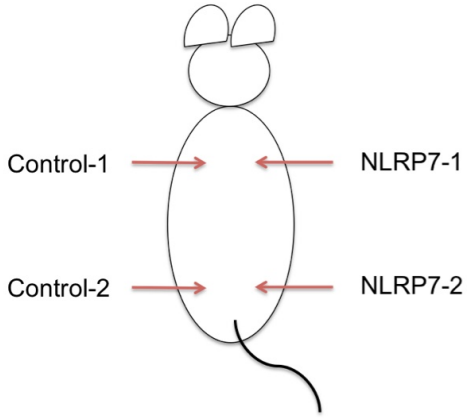

Figure 5.65. Tumor injection sites of mice. Flank and costa tumors were established in SCID mice.

5.4.3. Identification of Novel Potential Interaction Partners of NLRP7

Based on the literature data that NLRP7 is over-expressed in endometrium cancer tissues and tumor formation assays mentioned above provided supportive information. We aimed to identify the endogenous interaction partners of NLRP7 in different cell lines. To this end, endogenous immunoprecipitation (IP) studies were performed in Hec1a, THP-1, Tera-2 (Testicular seminoma) and Swan-71 cell lines. Although the IP results of Western blot analysis were successful, the same efficiency could not achieved for Coomassie blue stainings. It can be explained, as without stimulation, NLRP7 expression in these cell lines was not high enough to detect in SDS gel. Therefore, further studies were performed on overexpression conditions. For this purpose, IP studies on

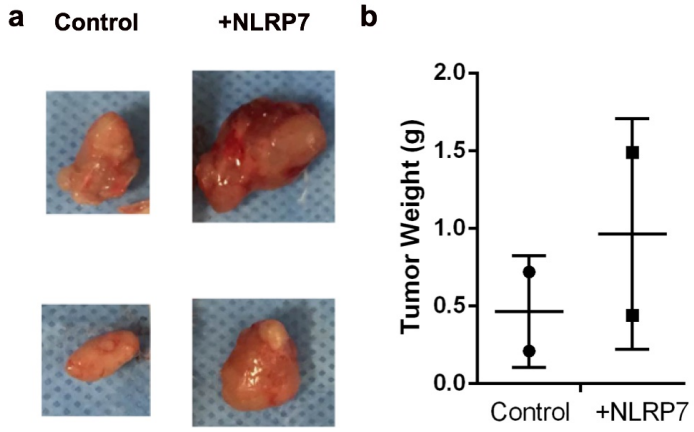

Figure 5.66. NLRP7 enhances tumor formation. Flank and costa tumors were established in SCID mice (n=2). Tumor tissues were collected after 6 weeks of injection. Representative tumors were shown in (a) and tumor tissue weights were measured (b).

over-expression conditions were performed in human endometrium cell line (Hec1a). pcDNA3-Flag-NLRP7 plasmid was used to overexpress NLRP7 in Hec1a cell lines. Pull down of NLRP7 were performed with monoclonal NLRP7 antibody and verified via Coomasie blue staining. In the negative control group (mouse IgG), NLRP7 band was not observed as expected and samples were found to be proper for mass spectrometry (MS) analysis according to EMBL proteomics core facility where the samples were analyzed (Figure 5.68). In MS results, NLRP7 was clearly enriched (27 fold) in the sample group compared to control (IgG) group. After confirming that IP procedure was optimized and working successfully, second biological replica was sent for MS analysis. Obtained results were analyzed via iBAQ (Intensity Based Absolute Quantification) to calculate the relative abundance of the proteins in log2 scale in sample group compared to control group by EMBL proteomics core facility. Proteins enriched in the sample group are more than 5 fold and also the proteins showed similar patterns in terms of fold change differences for both of the biological replica which were considered and listed in Table 5.1. MS result of first sample was implemented into Ingenuity pathway analysis (IPA) tool (data not shown). According to this analysis, potential interaction partners of NLRP7 belong to the cellular proliferation, cell death related pathways and

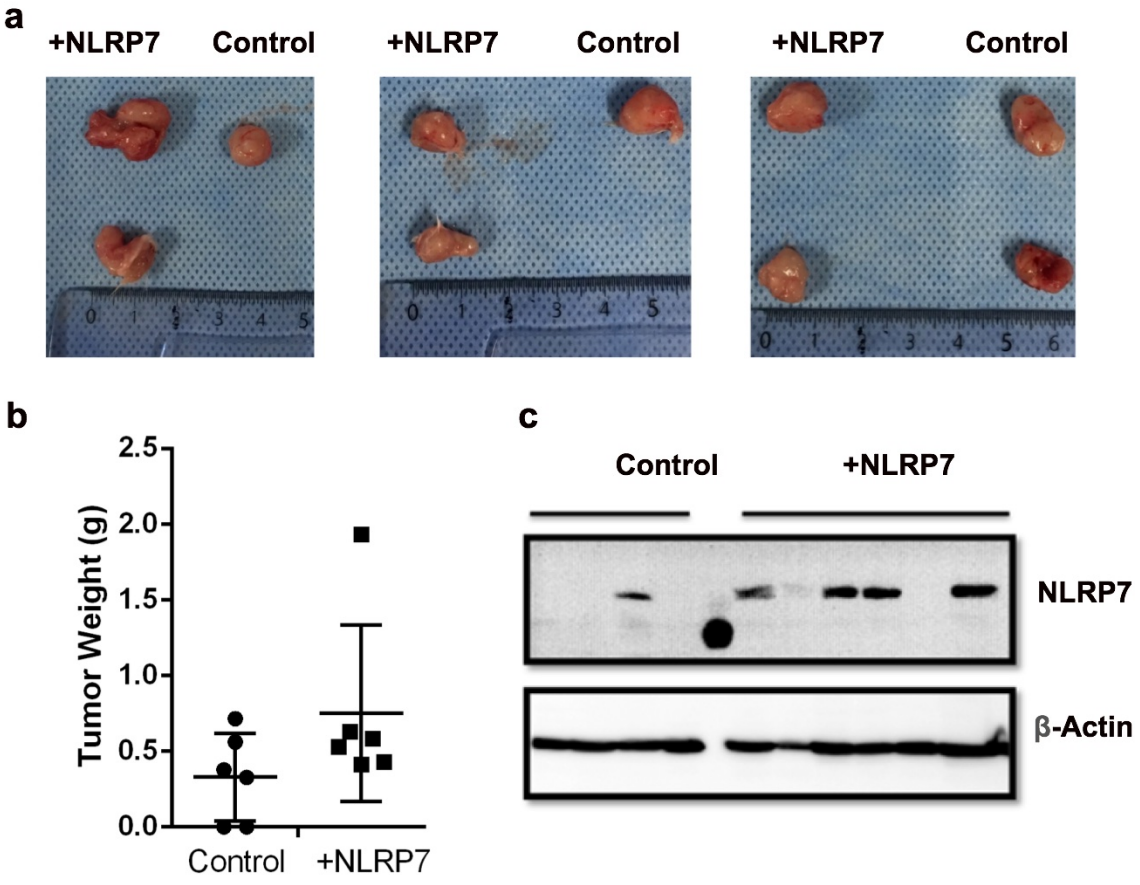

Figure 5.67. NLRP7 enhances tumor formation. Flank and costa tumors were established in SCID mice (n=3). Tumor tissues were collected after 4 weeks of injection. Representative tumors were shown in (a) and tumor tissue weights in (b). NLRP7 expression was verified for tumor tissues via western blotting (c).

top regulatory pathways, which is an algorithm showing the relationship between possible upstream regulators of interested gene with downstream diseases, were identified as ERK, FOS, TP63 proteins and estrogen receptors which mostly involve in microtubule dynamics. Same proteins were also analyzed by Reactome browser. Biological pathways, where potential interaction partners of NLRP7 participate in, were listed in Figure 5.69. When these pathways were examined in detail, most of the obtained proteins from mass spectrometry data were associated with innate immunity, cancer and transcriptional regulation of pluripotent stem cells. Also, potential NLRP7 interacting proteins identified after MS analyses were shown to be involved in YAP1-TEAD4, NODAL, FGF, TFAP2A, SMAD pathways according to Reactome pathway browser. As a result, we successfully immunoprecipated NLRP7 and its interaction partners. Three candidates will be further verified via CO-IP studies.

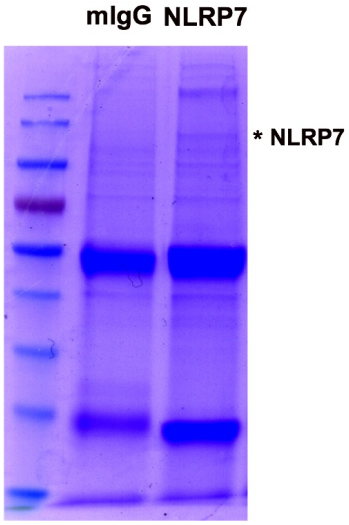

Figure 5.68. Immunoprecipitation of NLRP7 in Hec1a cells. IP results were shown by SDS-PAGE. mouse IgG represents the negative group and NLRP7 represents the experimental group that monoclonal NLRP7 antibody was used.

Table 5.1: Potential interaction partners of NLRP7

Protein names	**Gene names**	**Log2_rel_fc_ NLRP7/Con trol rep1**	**Log2_rel_fc_ NLRP7/Con trol rep2**
Protein spinster homolog 1	SPNS1	11,4	10,5
Vacuole membrane protein 1	VMP1	14,2	14,5
Arf-GAP with SH3 domain,	ASAP2	11,2	11,3
Thiamine transporter 1	SLC19A2	11,8	12,9
Pre-mRNA-splicing factor SPF27	BCAS2	11,3	13,9
Ras-related protein Ral-B	RALB	11,8	11,0
Methyltransferase-like protein 7B	METTL7B	9,6	10,8
Condensin complex subunit 2	NCAPH	9,3	9,9
Isocitrate dehydrogenase [NAD] subunit gamma, mitochondrial	IDH3G	8,9	9,2
Exocyst complex component 6	EXOC6	7,0	7,3
DNA-binding protein SMUBP-2	IGHMBP2	10,1	10,0
Neurofibromin; Neurofibromin truncated	NF1	6,3	6,9
Liprin-beta-1	PPFIBP1	8,5	9,3
WD repeat-containing protein 61, N-terminally processed	WDR61	10,5	10,4
Fanconi anemia group D2 protein	FANCD2	8,0	8,6
NCOAT;Protein O-GlcNAcase; Histone acetyltransferase	MGEA5	9,2	9,9
Proteasome-associated protein ECM29 homolog	KIAA0368; ECM29	6,7	6,0
Glutaminyl-peptide cyclotransferase-like protein	QPCTL	9,8	12,0

Table 5.1. Possible interaction partners of NLRP7 (cont.).

Eukaryotic translation initiation factor 3 subunit K	EIF3K	9,8	9,4
Splicing factor, arginine/ serine-rich 15; Protein SCAF8	SCAF4;SCAF8	6,7	8,1
Collagen alpha-1(I) chain	COL1A1	8,8	9,2
Ornithine aminotransferase	OAT	8,6	10,5
Ras-related protein Rab-5A	RAB5A	10,4	8,8
Short/branched chain specific acyl-CoA dehydrogenase, mitochondrial	ACADSB	10,0	9,1
Ribosomal RNA processing protein 1 homolog B	RRP1B	10,1	9,0
Probable E3 ubiquitin-protein ligase HERC1	HERC1	6,0	8,6
General transcription factor 3C polypeptide 5	GTF3C5	8,5	7,4
Rho guanine nucleotide exchange factor 2	ARHGEF2	7,7	10,8
BRCA1-associated ATM activator 1	BRAT1	8,7	8,2
Protein MON2 homolog	MON2	6,1	8,9
Transcriptional repressor p66-alpha	GATAD2A	8,2	9,1
Hermansky-Pudlak syndrome 6 protein	HPS6	7,1	7,7
Zinc finger protein 511	ZNF511	9,4	8,5
RNA polymerase-associated protein LEO1	LEO1	6,7	8,7

Table 5.1. Possible interaction partners of NLRP7 (cont.).

Serine/threonine-protein phosphatase PGAM5, mitochondrial	PGAM5	8,6	12,7
Exocyst complex component 2	EXOC2	7,4	6,4
Partner of Y14 and mago	WIBG	8,2	13,6
GrpE protein homolog 1, mitochondrial	GRPEL1	11,1	7,0
Kinesin-like protein KIF13B	KIF13B	6,9	5,6
L-aminoadipate-semialdehyde dehydrogenase-phosphopantetheinyl transferase	AASDHPPT	9,7	7,7
Poly [ADP-ribose] polymerase 4	PARP4	7,8	5,7

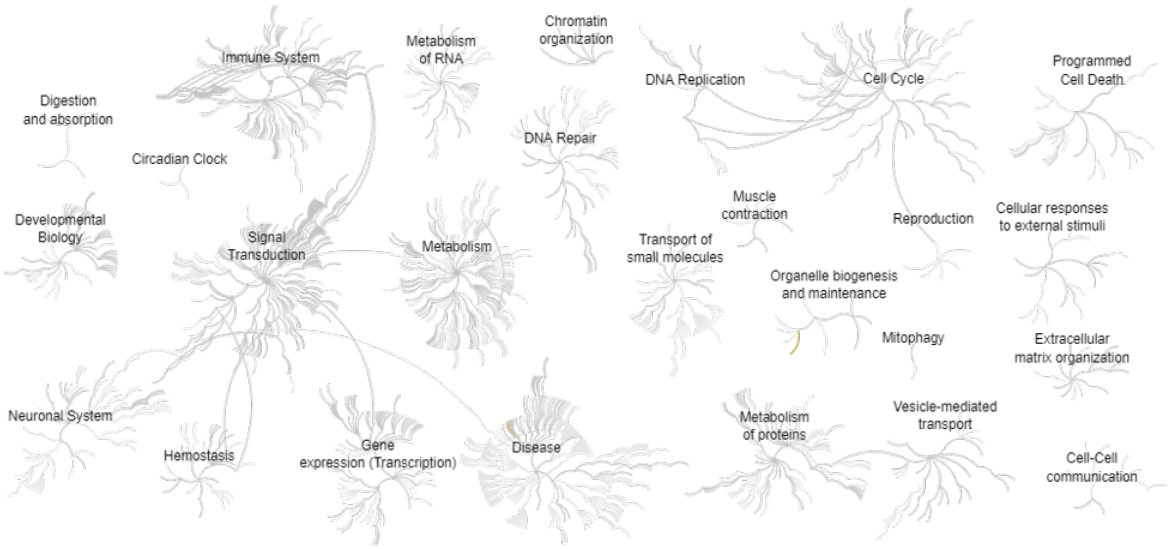

Figure 5.69. A genome-wide overview of pathway analysis in which possible NLRP7 interaction partners take role. Highly enriched proteins listed in Table 1 in NLRP7 pull-down group were implemented to Reactome pathway anaysis browser.

6. DISCUSSION AND CONCLUSIONS

6.1. NLRP7 in Embryogenesis

NLRP7 is a relatively understood member of NLR family with possible involvement in early embryogenesis, inflammation induction and putative proto-oncogenic proporties. In this thesis, we aimed to elucidate the molecular mechanisms upstream of NLRP7, as well as downstream targets and partners, that may be relevant to these diverse biological functions.

As mentioned before, NLRP7 mutations causes FRHM. However, neither which conditions/factors lead HM nor contribution of NLRP7 to disease pathology is still unknown. A mystery persist about the molecular mechanism behind FRHM. Possibly because of the absence of NLRP7 gene in rodent genome and inaccessibility of early human embryo tissues due to ethical considerations. iPSCs disease modeling technology thus presents a great opportunity to research HM molecular pathogenesis.

Within the scope of this Ph.D thesis, patient specific iPSC based HM model was established for the first time in literature. iPSCs were generated from fibroblasts of a patient with a prior diagnosis of three HMs. The patient was also reported to carry a large deletion (60kb) in chromosome 19 which encompasses NLRP7 and its adjacent gene, NLRP2 in a heterozygous stage. Also, cells from a healthy person were included as a control. iPSCs were generated via episomal iPSC reprogramming strategy which is a virus-free, transgene-free system that does not disrupt host genome. Obtained iPSCs colonies displayed a morphology peculiar to iPSC (Figure 5.7). EBNA PCR from the genomic DNA of three iPSC colonies showed that iPSCs were negative for EBNA sequence verifying the vectors that contain EBV nuclear antigen-1 (EBNA-1), did not integrate into the host genome (Figure 5.8). Immunostaining technique verified that the cells were positive for human embryonic stem cell markers, OCT3/4 and SSEA-4 (Figure 5.9). Teratoma formation assay also confirmed that the cells were able to give

rise to 3 embryonic germ lines *in vivo* (Figure 5.10). Karyotyping revealed normal chromosomes (Figure 5.11).

Subsequent to iPSC characterization, the effect of NLRP7 and NLRP2 heterozygous partial deletion on their mRNA and protein levels were ascertained via RT-qPCR and Western blot analysis. According to these results, although NLRP7 deletion reported to be heterozygous, both mRNA and protein levels were barely detected in HM iPSCs.Thus, the cells from HM patient could be accespted as knock-out for NLRP7. However, significant difference in NLRP2 regarding to mRNA and protein levels could not be detected in HM iPSCs in comparison to WT iPSCs. As mentioned above, this patient was reported to carry both NLRP2 and NLRP7 partial deletion in a heterozygous state by Ulker *et al.*, in 2013 [64]. They showed that 60kb deletion encloses from 5'UTR to exon 8 of *NLRP7* and 5'UTR to intron 11 of *NLRP2*. Later on, the same patient was subjected to genomic analysis by another group in 2016 [74]. The group claimed that NLRP7 deletion extended from exon 1 to intron 5 rather then from 5'UTR to intron 8 of NLRP7 as suggested by Ulker *et al.* Moreover, they did not mention about NLRP2 deletion. It is possible that they could not detect a deletion on *NLRP2* gene. We also could not show any defect on NLRP2 expression whilst NLRP7 mRNA and protein levels vastly diminished (Figure 5.12 and Figure 5.13). One possible explanation for normal NLRP2 protein and mRNA levels in HM patient iPSCs may be because of the differences in regulation of NLRP2 and NLRP7 genes. Also, undetermined SNP in the healthy allele of NLRP7 may cause slight expression of NLRP7.

Ensuing studies were conducted to derive trophoblast cells from iPSCs. Although, several groups attempted to generate trophoblast cells in the literature mainly by using recombinant BMP-4, there is no well-accepted or well-characterized method for trophoblast differentiation [**?**, 55, 75]. In addition, some groups claim that extra embryonic cells cannot be derived from embryonic cells as the trophoblast cells and ICM cells are separated from each other before embryo develops .

Recently, two publications from R. Michael Roberts' laboratory reported that differentiation of stem cells towards trophoblast cells can be acquired by introduction of transient BMP4 exposure and inhibition of ACTIVIN/FGF2 pathway [57]. In this procedure, BMP4 leads to trophoblast differentiation whereas, ACTIVIN/FGF2 inhibitors suppress pluripotency as ACTIVIN/FGF2 pathways required for pluripotency maintenance of stem cells. We followed this procedure and used recombinant BMP4, inhibitors of ACTIVIN (A83-01) and FGF2 (PD173074) pathways to generate trophoblasts with a different exposure time to BAP. We cultured cells continuously under combination of BMP-4, A83-01 and PD173074 (BAP) during the experiment rather than exposing cells to BAP for only 24 hours as Ying *et al* performed [58]. Later on, same group published another article where they also used continuous BAP treatment to derive trophoblast cells from human embryonic stem cell line [59]. In correlation with their results, BAP treatment significantly stimulated trophoblast specific gene expression (*CDX2,CGB,NP63,INSL4,PGF* and *PSG*) whereas the expression of stem cell markers decreased in both groups (Figure 5.16).

The main motivation behind HM disease modeling was to investigate the possible function of NLRP7 during first cell fate decision, since we hypothesized that NLRP7 deficiency (HM) promotes trophoblast differentiation. As shown in Figure 5.13 HM cells gave faster response to BAP treatment and they started to lose certain iPSCs morphology, become monolayered and flattened. By day 2, the majority of the cells were differentiated in HM group, while WT cells retained iPSC specific morphology at the center of the colonies. Alterations in cell morphology progressed during differentiation process. Then, the cells were analyzed by RT-qPCR whether they exhibited gene expression pattern pertaining to trophoblasts features. It was quite evident that mRNA levels of *CDX2* (4.6 fold) and *NP63* (2,5 fold), early markers of trophoblast differentiation, increased significantly at 2^{nd} day of differentiation in comparison to WT counterparts. On the fourth day of BAP exposure, *INSL4* (15.2 fold), *CGB* (1.78 fold), *PGF* (8.8 fold) and *PSG4* (18.4 fold), which are late trophoblast markers, were excessively expressed by HM cells in comparison to WT cells. On the other hand, expressions of pluripotency markers, *POU5F1* and *NANOG*, were down-regulated with

each day of BAP exposure. NLRP7 deficiency of HM cells provoked trophoblast associated protein expression, namely CDX2, KRT7 and HLA-G. OCT4 protein levels were decreased upon BAP exposure, parallel to gene expression analysis (Figure 5.17). Appearance of relatively more CDX2 positive areas at day 2 was a further evidence of accelerated differentiation through trophoblasts. At day 4, cells belonging to both groups gained HLA-G expression which is also a late trophoblast marker again substantially more HLA-G positive regions were observed in HM cells. However none of the groups were completely positive for HLA-G and presence of CDX2 positive areas (Figure 5.18) implied heterogeneous population in terms of the differentiation stage through trophoblast. The cells were negative for HLA-G where CDX2 expression was determined. Gradual acquisition of CDX2 followed by HLA-G expression also proved the success of trophoblast differentiation procedure (Figure 5.18). Similar to these findings KRT7 positive regions were more abundant in HM cells for all time points (Figure 5.19). Immunostaining experiments have brought another intriguing observation that the cells of HM group represented bigger nucleus which may also associated to trophoblast differentiation as trophoblast cells were relatively large. Blind measurements of nucleus diameters showed significantly larger nucleus size in HM cells when treated with BAP (Figure 5.22). Lastly, vast secretion of PGF in HM cells further verified that those cells represented excessively trophoblast-phenotype (Figure 5.23).

These results of expedited trophoblast differentiation observed in patient derived HM cells upon BAP exposure were correlated with the previous study where Mahedevan *et al.* showed that NLRP7 knock-down in H9 hESCs resulted in increased expression of trophoblast specific genes; *GCM1*, *INSL4* and *PAPPE* when H9 cell cultured with BMP4 [16]. Considering the pathology of Hydatidiform moles characterized as hyperplasia of trophoblast tissue, patient derived HM cells represented similar phenotype upon BAP exposure. These observations shed light on the contribution of NLRP7 on Hydatiform mole pathology. Moreover, these results presented conclusive evidence that BAP is able to convert iPSCs to trohoblast-like linage.

The ensuing question was what gives rise to augmented lineage differentiation of trophoblasts in HM cells? As BMP4 exposure leads cells to trophoblast linage fate, elevated endogenous BMP4 levels in HM group may alter overall BMP4 concentrations even we treat the cells with equal amounts of BMP4 during the differentiation procedure. To test this hypothesis, we analyzed *BMP4* mRNA levels and observed to be upregulated in HM group during BAP exposure (Figure 5.25). Based on these observations, the cells were treated with AP in the absence of BMP4. mRNA and protein levels of trophoblast markers were upregulated upon AP exposure in HM group. Emergence of CDX2 positive and latter HLA-G and KRT7 positive cells further supported the idea that HM cells were provoked to choose trophoblast linage despite the lack of BMP4 in the medium. Besides, it was explicit that BMP4 exposure expedited differentiation process as KRT7 positive cells were evident at day 2 when the cells treated with BAP whereas AP treatment generated KRT7 positive cells on day 4. Also, HLA-G positive areas in AP treated cells were comparably less in number then to that of BAP treatment on day 4. PGF secretion was only quantifiable in HM group under AP conditions (300 pg/mL) which also authenticated that differentiated cells resembled trophoblasts' phenotypes. Of note, NLRP7 deficiency most dramatically altered gene expressions of *CDX2*, *deltaNp63*, *PGF*, and *INSL4* implying that the observed phenotype stemmed from the differential expression pattern of these genes (Figure 5.16 and Figure 5.26).

Both BAP and AP conditions provided evidence about the tendency of HM cells towards trophoblast lineage differentiation. As shown in AP experiments, underlying mechanism of exaggerated trophoblast differentiation in HM cells may be associated with BMP4 pathway. To further assess the involvement of BMP pathway on trophoblast differentiation, driven by NLRP7 deficiency in HM cells, we used BMP pathway inhibitior, LDN193189, which targets BMP receptors; ALK1/2. Accordingly, LDN193189 was able to diminish trophoblast specific gene and protein expressions (Figure 5.34 and Figure 5.35). Interestingly, when the cells were treated with BMP inhibitor, HM cells gained more *OCT4* mRNA levels than WT cells for both time points that was implying the impotence and possibly dose dependent effects of BMP pathway during embryogenesis (Figure 5.34). Consequently, the factors driving hyper

trophoblast differentiation in HM cells could be halted by inhibition of BMP pathway. We have pinpointed in BMP4 as a critical regulator of early human cell fate decision, Furthermore, we provide evidence that NLRP7 may be upstream regulator of BMP4 pathway. Also, culturing the embryo with a certain concentration of LDN193189 during *in vitro* fertilization (IVF) may present a treatment strategy for those patients carrying NLRP7 deficiency and due cannot have a proper pregnancy.

In order to verify that NLRP7 deficiency was liable for the increased trophoblast differentiation of HM cells, NLRP7 was re-introduced to HM cells by lentiviral transduction (Figure 5.36). *CDX2*, *NP63*, *PGF* and *INSL4* gene expressions were decreased upon NLRP7 recovery (HM+NLRP7) in comparison to control group (HM+GFP) when the cells were exposed to BAP (Figure 5.37). On the other hand, recovery efficiency was more abundant under AP conditions, yet in addition to *CDX2*,*NP63*, *PGF* and *INSL4*, *HLA-G*, *CGB* were downregulated in HM+NLRP7 group (Figure 5.37). It was rational to observe more dramatic differences between groups under the presence of BMP4 (Figure 5.41). If we could perform experiments to detect the levels of the genes, which represented the bigger differences owing to fold change such as; CDX2, PGF, we could most probably observe bigger effects. Considering the literature, methylation patterns alter vastly in HM cells carrying NLRP7 deletions [13], also the data presented here that the expression patterns in several genes, such as *OCT4* and *CDX2* which are crucial in cell fate determination, change dramatically in NLRP7 deficient cells indicating that NLRP7 can also affect the reprogramming procedure. This hypothesis was also supported by three publications in which NLRP7 was found to be one of the mostly upregulated genes in embroyonic carcinomas, epiblasts, naive pluripotent stem cells, respectively [23, 76, 77]. Hence, re-introducing NLRP7 in patient fibroblasts rather than iPSCs would give more reliable results.

Mahedevan *et al.* reported that NLRP7 interacts with YY1 transcription factor in overexpression conditions and deteriorates methylation patterns in at germ-line differentially methylated regions (gDMRs) [16]. From this point and aforementioned results, we investigated the changes in expression levels of YY1 or BMP4 target genes.

YY1 has been reported as a repressor of BMP proteins. According to literature, we expected that increased YY1 levels should decrease BMP4 expression. However, even though *YY1* mRNA level was higher in differentiated HM group, BMP4 levels did not decline (Figure 5.46). This adverse expression pattern of HM and WT groups before and after BAP exposure made us think that NLRP7 may be essential for YY1 to exhibit its repressor function in BMP gene expression regulation. Thus, it is tempting to speculate that the cells carrying NLRP7 defects may not repress BMP4 expression through YY1 and excessive BMP4 levels may result in hyper trophoblast differentiation of stem cells during early embryogenesis. Moreover, ID1 was shown to be direct target of BMP4 [78] and expressed in undifferentiated trophoblast cells [79]. LIF was reported to induce proliferation and differentiation of trophoblast cells [80] and cFOS regulates trophoblast invasion [81]. ZFP42 is supposed to be ICM markers, but some studies showed that ZF42 can be found in trophoblast cells. To sum up, YY1 is a transcription factor which acts as a repressor or activator and it has been reported to interact with key regulatory proteins which determine its repressor or activator function. Since, NLRP7 defects cause variations in the expression of YY1 target genes has shown, we hypothesized that NLRP7 may be one of the key regulatory proteins that interact with YY1 hence may be controlling the expression of many genes that have taken role in trophoblast differentiation through YY1. On the other hand, NLRP7 may have a role in the pathways regulating BMP4 stability. As a result, NLRP7 appears to operate the expression of many genes that mainly take role in BMP pathway and trophoblast differentiation. However, in order to clarify the action mechanism of NLRP7, more comprehensive studies should be established such as; RNA-seq and methylation profiling. Also, it should be considered that using inhibitors, in this case AP, may mask the effect of NLRP7 in particular pathways.

Hereby, we can summarize the contribution of this section to literature; a) BAP treatment was unmistakably able to convert iPSCs towards trophoblast as it was proved by mimicking the phenotype of Hydatidiform mole in patient derived HM cells, b) NLRP7 knock-down was sufficient to convert cells to trophoblast lineage without additional requirement to activate trophoblast specific transcription factors, c) NLRP7

deficiency predisposed to trophoblast lineage commitment through BMP4 pathway by dominantly altering *CDX2*, *PGF*, *NP63* and *INSL4* expressions and so resulted in Hydatidiform mole. d) BMP pathway inhibition ameliorated redundant trophoblast differentiation arising out of NLR7 deficiency and may present novel therapeutic approaches for HM patients.

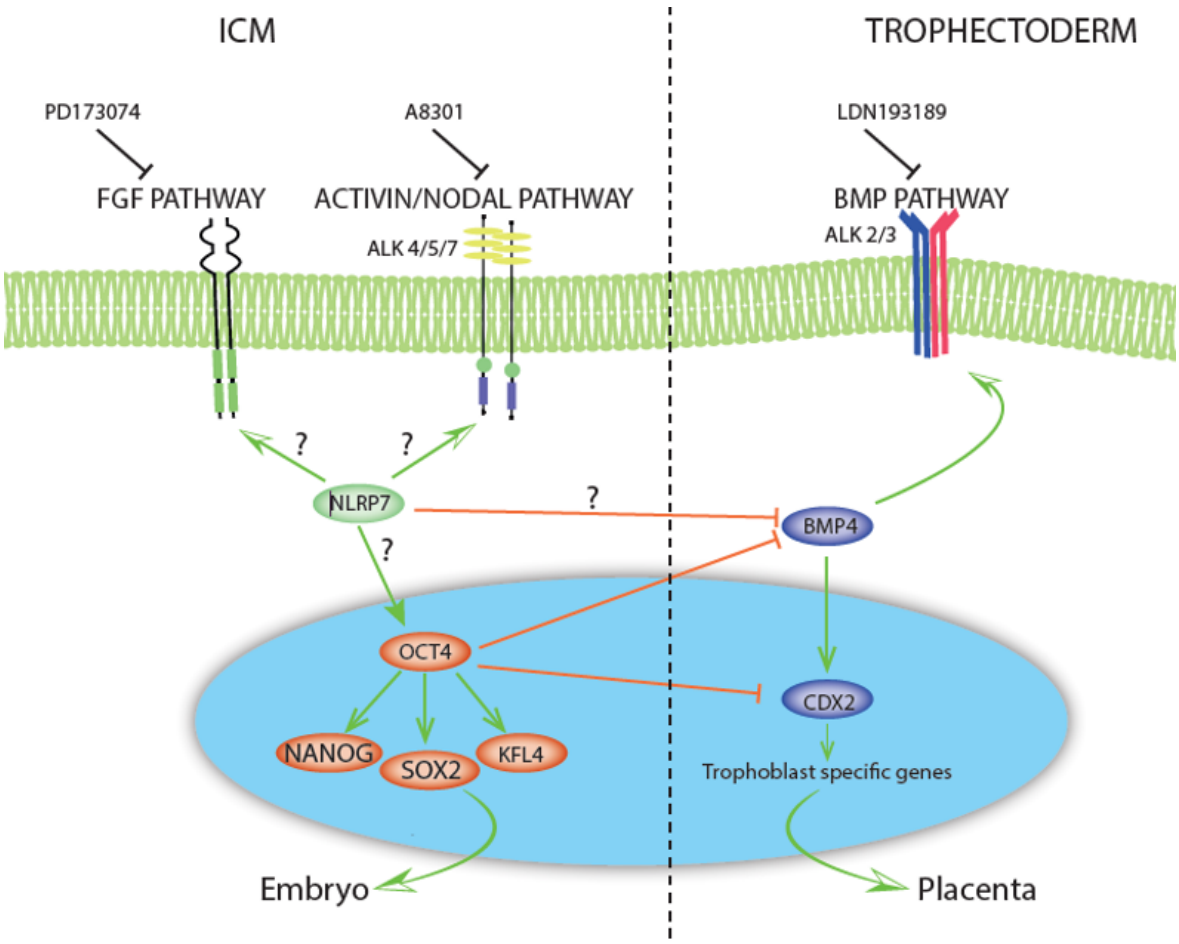

Figure 6.1. Proposed Model of First Cell Fate Decision Governed by NLPR7 .

6.2. NLRP7 in Inflammation

Nod Like Receptor Family which are cytoplasmic receptors and senses pathogen associated molecular patterns (PAMP) or danger associated molecular patterns (DAMP) to induce inflammation [82]. Upon stimulation with PAMPs or DAMPs, several NLRs

have been reported to form inflammasome complexes to mature pro-caspese-1 following with the cleavage and maturation of IL-1β by caspase-1. Canonical inflammasomes consist of particular NLR protein (a sensor), ASC protein (an adaptor) and pro-caspase-1 (effector). Among the 23 members of NLR family in humans, NLRP1(anthrax lethal toxin protease), NLRP3 (influenza A virus, *Candida albicans*, *Staphylococcus aureus*, NLRC4 (flagellin and type III secretion system containing bacteria), NLRC5 (*Esherishia coli*, *Shigella felxneri*, *staphylococcus aureus*), NLRP6 (enteric pathogens), NLRP9b (rota virus), NLRP12 (*Yersinia pestis*) have been reported to assemble inflammasome upon stimulation with certain pathogens by many groups [83].

NLRP7 is relatively less studied protein in inflammasome field and there are only two studies regarding to its role in inflammasome formation. In the first study, Khare *et al.* demonstrated that *Legionella pneumophilia*, *Acholeplasma laidlawii*, *Staphylococcus aureus* avtivated NLRP7 inflammasome which eventuated in IL-1β secretion [8]. Later, Zhou *et. al.* showed that NLRP7 contributed to inflammasome formation upon stimulation with Mycobacterium bovis Beijing Strain [11]. Also, Duygu Demiroz from our lab showed that NLRP7 is a pro inflammatory protein and it is able to interact with inflammasome componants, ASC, Caspase 1 and Caspase 5.

Flagellin of *P.aeruginosa* can trigger NLRC4 and NLRP3 inflammasomes [84] [85]. On the other hand, membrane vesicle of *P.aeruginosa* stimulates inflammasome formation via caspase-5 rather then caspase-1 [**?**]. Moreover, Pilin protein of *P.aeruginosa* was reported to activate inflammasome in NLRC4/NLRP3 independent manner [86]. These studies indicated that different proteins belonging to *P.aeruginosa* can trigger different inflammasome pathways. Here, we showed that NLRP7 overexpressing THP-1 cells secreted significantly more IL-1β, which is a readout of inflammasome formation, in response to *P.aeruginosa* infection (Figure 5.59). In concordance with this result, NLRP7 knock-down led to impaired IL-1β secretion in THP-1 cells upon infected with *P.aeruginosa* (Figure 5.60). In addition to reduction on IL-1β secretion, pro-IL-1β levels were decreased in NLRP7 knock-down cells in a time dependent manner (Figure 5.61). However, reduction in caspase-1 levels and its active form, p10

levels should be further assessed to clarify whether the decreased protein levels were because of their secretion to media or their expression was affected at transcriptional and/or translational level. Moreover, NLRP7 overexpression altered inflammatory cytokine secretion of THP-1 cells when infected with *P.aeruginosa*(Figure 5.62, Figure 5.63).

As a result , we claim that NLRP7 has a contribution to inflammasome formation which resulted in IL-1β secretion in THP-1 cells. Further experiments should be conducted to show whether NLRP7 inflammasome is ASC dependent or not. Possible interactions of NLRP7 with other inflammasome components, caspase-1 and ASC, should be investigated via Co-IP studies at the endogenous level upon *P.aeruginosa* infection. It is clear that muliple TLR and NLR proteins can be engaged by a single pathogen such as *P.aeruginosa* which carried multiple PAMPs.

6.3. NLRP7 in Oncogenesis

Until now, NLRP7 has been linked with testicular seminoma, endometrium cancer and embryonal carcinoma [19, 20]. Interestingly, NLRP7 has been found to be highly expressed in undifferentiated embryonal carcinomas along with POU5F1 that encodes OCT3/4, NANOG, DPPA-4 (developmental pluripotency-associated 4) and GAL (Galanin/GMAP Prepropeptide) [**?**]. Furthermore, complete hydatidiform moles are characterized as excessive trophoblast differentiation/proliferation [27], in which NLRP7 mutations have been found to be first causative gene, have a risk to transform into choriocarcinoma or invasive mole. Although, high NLRP7 expression in embryonal carcinoma and deficient expression of NLRP7 in hydatidiform mole cases seemed to be controversy, it can be hypothesized that NLRP7 may be associated with pluripotency and/or proliferation as its expression is upregulated in embryonal carcinoma together with POU5F1 and NANOG, and on the contrary its deficiency impedes embryo formation during gestation. Based on this knowledge, we hypothesized that increased NLRP7 expression may generate cancer stem cells in a tissue specific manner where NLRP7 is expressed. To test the contribution of NLRP7 in oncogenesis, tumor load

experiments were established for Hec1a cell line (human endometrium cancer cell line) *in vivo*. As a result, we showed that tumor formation was enhanced in NLRP7 stably overexpressing Hec1a cells, when they were injected to SCID mice. Despite inadequate number of experimental group (n=2 for 6weeks, n=6 for 4weeks), NLRP7 appeared to influence tumor formation later than 4 weeks. For each time point, stably NLRP7 overexpressing Hec1a cells generated bigger tumors in weight than corresponding control cells with one exception. This peculiar tumor of control group showed increased tumor weight along with NLRP7 expression as shown by Western blotting in Figure 5.67, indicating that most probably the tumor at the time of measurement or the cells at the time of injection were mixed up.

To further characterize the possible involvement of NLRP7 in oncogenesis, we aimed to find interaction partners of NLRP7 in Hec1a cells. For this purpose, ectopicly overexpressed NLRP7 were pulled down in Hec1a cells and analyzed by mass spectrometry. Accordingly, we find several proteins enriched in NLRP7 pull-down group in comparison mouse Ig-G control group. When we analyzed those proteins in functional annotation tools such as DAVID, Reactome and IPA, revealed that potential interaction partners of NLRP7 are linked with several pathways such as, innate immune pathway, cancer, transcriptional regulation of pluripotent stem cells. Also, potential NLRP7 interacting proteins were associated within YAP1-TEAD4, NODAL, FGF, TFAP2A, SMAD pathways according to Reactome pathway browser. For future work, after RNA-Seq analysis is performed from trophoblast cells of HM group, in combination with mass spectrometry results might give comprehensive aspect on how NLRP7 regulates different pathways.

Last but not least, we can conclude that NLRP7 has critical roles in early cell fate decision during human embryogenesis, regulation of innate immune signaling pathways via inflammasomes and by yet unclear effects may act as a proto-oncogene in endometrium.

REFERENCES

1. Leavy, O., "Turning on and off NLRP3", *Nature Reviews Immunology*, Vol. 13, No. 1, pp. 1–1, 1 2013.

2. Latz, E., T. S. Xiao and A. Stutz, "Activation and regulation of the inflammasomes", *Nature Reviews Immunology*, Vol. 13, No. 6, pp. 397–411, 6 2013.

3. Aachoui, Y., V. Sagulenko, E. A. Miao and K. J. Stacey, "Inflammasome-mediated pyroptotic and apoptotic cell death, and defense against infection", *Current Opinion in Microbiology*, Vol. 16, No. 3, pp. 319–326, 6 2013.

4. Lamkanfi, M. and V. Dixit, "Mechanisms and Functions of Inflammasomes", *Cell*, Vol. 157, No. 5, pp. 1013–1022, 5 2014.

5. Ting, J. P. Y., J. A. Duncan and Y. Lei, "How the Noninflammasome NLRs Function in the Innate Immune System", *Science*, Vol. 327, No. 5963, pp. 286–290, 1 2010.

6. Radian, A. D., L. de Almeida, A. Dorfleutner and C. Stehlik, "NLRP7 and related inflammasome activating pattern recognition receptors and their function in host defense and disease", *Microbes and Infection*, Vol. 15, No. 8-9, pp. 630–639, 2013.

7. Kinoshita, T., Y. Wang, M. Hasegawa, R. Imamura and T. Suda, "PYPAF3, a PYRIN-containing APAF-1-like protein, is a feedback regulator of caspase-1-dependent interleukin-1β secretion", *Journal of Biological Chemistry*, Vol. 280, No. 23, pp. 21720–21725, 2005.

8. Khare, S., A. Dorfleutner, N. B. Bryan, C. Yun, A. D. Radian, L. de Almeida, Y. Rojanasakul and C. Stehlik, "An NLRP7-Containing Inflammasome Mediates Recognition of Microbial Lipopeptides in Human Macrophages", *Immunity*, Vol. 36, No. 3, pp. 464–476, 2012.

9. Pinheiro, A. S., M. Proell, C. Eibl, R. Page, R. Schwarzenbacher and W. Peti, "Three-dimensional structure of the NLRP7 pyrin domain insight into pyrin-pyrin-mediated effector domain signaling in innate immunity", *Journal of Biological Chemistry*, Vol. 285, No. 35, pp. 27402–27410, 2010.

10. Messaed, C., E. Akoury, U. Djuric, J. Zeng, M. Saleh, L. Gilbert, M. Seoud, S. Qureshi and R. Slim, "NLRP7, a nucleotide oligomerization domain-like receptor protein, is required for normal cytokine secretion and co-localizes with golgi and the microtubule-organizing center", *Journal of Biological Chemistry*, Vol. 286, No. 50, pp. 43313–43323, 2011.

11. Zhou, Y., S. Z. A. Shah, L. Yang, Z. Zhang, X. Zhou and D. Zhao, "Virulent Mycobacterium bovis Beijing Strain Activates the NLRP7 Inflammasome in THP-1 Macrophages", *PLOS ONE*, Vol. 11, No. 4, p. e0152853, 4 2016.

12. Bednash J. S. et al., "Targeting the deubiquitinase STAMBP inhibits NALP7 inflammasome activity", *Nature Communications*, Vol. 8, p. 15203, 5 2017.

13. Slim, R. and E. P. Wallace, "NLRP7 and the Genetics of Hydatidiform Moles: Recent Advances and New Challenges", *Frontiers in Immunology*, Vol. 4, p. 242, 2013.

14. Milhavet, F., L. Cuisset, H. M. Hoffman, R. Slim, H. El-Shanti, I. Aksentijevich, S. Lesage, H. Waterham, C. Wise, C. Sarrauste de Menthiere and I. Touitou, "The infevers autoinflammatory mutation online registry: update with new genes and functions", *Human Mutation*, Vol. 29, No. 6, pp. 803–808, 6 2008.

15. Singer, H., A. Biswas, N. Zimmer, C. Messaed, J. Oldenburg, R. Slim and O. El-Maarri, "NLRP7 inter-domain interactions: The NACHT-associated domain is the physical mediator for oligomeric assembly", *Molecular Human Reproduction*, Vol. 20, No. 10, pp. 990–1001, 2014.

16. Mahadevan, S., S. Wen, Y. W. Wan, H. H. Peng, S. Otta, Z. Liu, M. Iacovino, E. M. Mahen, M. Kyba, B. Sadikovic and I. B. Van den Veyver, "NLRP7 affects trophoblast lineage differentiation, binds to overexpressed YY1 and alters cpg methylation", *Human Molecular Genetics*, Vol. 23, No. 3, pp. 706–716, 2014.

17. Akoury, E., L. Zhang, A. Ao and R. Slim, "NLRP7 and KHDC3L, the two maternal-effect proteins responsible for recurrent hydatidiform moles, co-localize to the oocyte cytoskeleton", *Human Reproduction*, Vol. 30, No. 1, pp. 159–169, 2015.

18. Singer, H., A. Biswas, N. Nuesgen, J. Oldenburg and O. El-Maarri, "NLRP7, Involved in Hydatidiform Molar Pregnancy (HYDM1), Interacts with the Transcriptional Repressor ZBTB16", *PLOS ONE*, Vol. 10, No. 6, p. e0130416, 6 2015.

19. Ohno, S., T. Kinoshita, Y. Ohno, T. Minamoto, N. Suzuki, M. Inoue and T. Suda, "Expression of NLRP7 (PYPAF3, NALP7) protein in endometrial cancer tissues", *Anticancer Research*, 2008.

20. Okada, K., E. Hirota, Y. Mizutani, T. Fujioka, T. Shuin, T. Miki, Y. Nakamura and T. Katagiri, "Oncogenic role of NALP7 in testicular seminomas", *Cancer Science*, Vol. 95, No. 12, pp. 949–954, 2004.

21. Huang, J.-Y., P.-H. Yu, Y.-C. Li and P.-L. Kuo, "NLRP7 contributes to in vitro decidualization of endometrial stromal cells.", *Reproductive biology and endocrinology*, Vol. 15, No. 1, p. 66, 8 2017.

22. Onoufriadis A. et al., "Exome Sequencing and Genotyping Identify a Rare Variant in NLRP7 Gene Associated With Ulcerative Colitis", *Journal of Crohn's and Colitis*, Vol. 12, No. 3, pp. 321–326, 2 2018.

23. Kilens S. et al., "Parallel derivation of isogenic human primed and naive induced pluripotent stem cells", *Nature Communications*, Vol. 9, No. 1, p. 360, 12 2018.

24. Li, R. and D. F. Albertini, "The road to maturation: somatic cell interaction and self-organization of the mammalian oocyte", *Nature Reviews Molecular Cell Biology*, Vol. 14, No. 3, pp. 141–152, 3 2013.

25. Nüsslein-Volhard, C. and E. Wieschaus, "Mutations affecting segment number and polarity in Drosophila.", *Nature*, Vol. 287, No. 5785, pp. 795–801, 10 1980.

26. Lu, X., Z. Gao, D. Qin and L. Li, "A Maternal Functional Module in the Mammalian Oocyte-To-Embryo Transition", *Trends in Molecular Medicine*, Vol. 23, No. 11, pp. 1014–1023, 2017.

27. Murdoch S. et al., "Mutations in NALP7 cause recurrent hydatidiform moles and reproductive wastage in humans", *Nature Genetics*, Vol. 38, No. 3, pp. 300–302, 3 2006.

28. Parry D. A. et al., "Mutations Causing Familial Biparental Hydatidiform Mole Implicate C6orf221 as a Possible Regulator of Genomic Imprinting in the Human Oocyte", *The American Journal of Human Genetics*, Vol. 89, No. 3, pp. 451–458, 9 2011.

29. Wu, X., "Maternal depletion of NLRP5 blocks early embryogenesis in rhesus macaque monkeys (Macaca mulatta)", *Human Reproduction*, Vol. 24, No. 2, pp. 415–424, 2 2009.

30. Docherty L. E. et al., "Mutations in NLRP5 are associated with reproductive wastage and multilocus imprinting disorders in humans", *Nature Communications*, Vol. 6, No. 1, p. 8086, 12 2015.

31. Peng, H., B. Chang, C. Lu, J. Su, Y. Wu, P. Lv, Y. Wang, J. Liu, B. Zhang, F. Quan, Z. Guo and Y. Zhang, "Nlrp2, a Maternal Effect Gene Required for Early Embryonic Development in the Mouse", *PLoS ONE*, Vol. 7, No. 1, p. e30344, 1 2012.

32. Meyer, E., D. Lim, S. Pasha, L. J. Tee, F. Rahman, J. R. W. Yates, C. G. Woods, W. Reik and E. R. Maher, "Germline Mutation in NLRP2 (NALP2) in a Familial Imprinting Disorder (Beckwith-Wiedemann Syndrome)", *PLoS Genetics*, Vol. 5, No. 3, p. e1000423, 3 2009.

33. Nguyen, N. M. P. and R. Slim, "Genetics and Epigenetics of Recurrent Hydatidiform Moles: Basic Science and Genetic Counselling", *Current Obstetrics and Gynecology Reports*, Vol. 3, No. 1, pp. 55–64, 3 2014.

34. Lurain, J. R., "Gestational trophoblastic disease I: epidemiology, pathology, clinical presentation and diagnosis of gestational trophoblastic disease, and management of hydatidiform mole", *American Journal of Obstetrics and Gynecology*, Vol. 203, No. 6, pp. 531–539, 12 2010.

35. Beygo J. et al., "Deep Bisulfite Sequencing of Aberrantly Methylated Loci in a Patient with Multiple Methylation Defects", *PLoS ONE*, Vol. 8, No. 10, pp. 1–13, 2013.

36. Sills, E. S., A. J. Obregon-Tito, H. Gao, T. K. McWilliams, A. T. Gordon, C. A. Adams and R. Slim, "Pathogenic variant in NLRP7 (19q13.42) associated with recurrent gestational trophoblastic disease: Data from early embryo development observed during in vitro fertilization", *Clinical and Experimental Reproductive Medicine*, Vol. 44, No. 1, p. 40, 3 2017.

37. Candelier, J.-J., "The hydatidiform mole.", *Cell adhesion & migration*, Vol. 10, No. 1-2, pp. 226–35, 2016.

38. Oron, E. and N. Ivanova, "Cell fate regulation in early mammalian development", *Physical Biology*, Vol. 9, No. 4, 2012.

39. Simmons, D. G. and J. C. Cross, "Determinants of trophoblast lineage and cell subtype specification in the mouse placenta", *Developmental Biology*, Vol. 284,

No. 1, pp. 12–24, 2005.

40. Bernardo A. S. et al., "BRACHYURY and CDX2 mediate BMP-induced differentiation of human and mouse pluripotent stem cells into embryonic and extraembryonic lineages.", *Cell stem cell*, Vol. 9, No. 2, pp. 144–55, 8 2011.

41. Niwa, H., J.-i. Miyazaki and A. G. Smith, "Quantitative expression of Oct-3/4 defines differentiation, dedifferentiation or self-renewal of ES cells", *Nature Genetics*, Vol. 24, No. 4, pp. 372–376, 4 2000.

42. De Paepe, C., G. Cauffman, A. Verloes, J. Sterckx, P. Devroey, H. Tournaye, I. Liebaers and H. Van de Velde, "Human trophectoderm cells are not yet committed", *Human Reproduction*, Vol. 28, No. 3, pp. 740–749, 3 2013.

43. Horii, M., Y. Li, A. K. Wakeland, D. P. Pizzo, K. K. Nelson, K. Sabatini, L. C. Laurent, Y. Liu and M. M. Parast, "Human pluripotent stem cells as a model of trophoblast differentiation in both normal development and disease", *Proceedings of the National Academy of Sciences*, Vol. 113, No. 27, pp. E3882–E3891, 2016.

44. Velicky, P., M. Knöfler and J. Pollheimer, "Function and control of human invasive trophoblast subtypes: Intrinsic vs. maternal control", *Cell Adhesion & Migration*, Vol. 10, No. 1-2, pp. 154–162, 3 2016.

45. Rizzo, R., M. Vercammen, H. van de Velde, P. A. Horn and V. Rebmann, "The importance of HLA-G expression in embryos, trophoblast cells, and embryonic stem cells", *Cellular and Molecular Life Sciences*, Vol. 68, No. 3, pp. 341–352, 2 2011.

46. Millar, L., N. Streiner, L. Webster, S. Yamamoto, R. Okabe, T. Kawamata, J. Shimoda, E. Büllesbach, C. Schwabe and G. Bryant-Greenwood, "Early placental insulin-like protein (INSL4 or EPIL) in placental and fetal membrane growth.", *Biology of reproduction*, Vol. 73, No. 4, pp. 695–702, 10 2005.

47. Khaliq, A., X. F. Li, M. Shams, P. Sisi, C. A. Acevedo, M. J. Whittle, H. Weich and A. Ahmed, "Localisation of placenta growth factor (PIGF) in human term placenta.", *Growth factors (Chur, Switzerland)*, Vol. 13, No. 3-4, pp. 243–50, 1996.

48. Shore, V. H., T. H. Wang, C. L. Wang, R. J. Torry, M. R. Caudle and D. S. Torry, "Vascular endothelial growth factor, placenta growth factor and their receptors in isolated human trophoblast.", *Placenta*, Vol. 18, No. 8, pp. 657–65, 11 1997.

49. Camolotto, S., A. Racca, V. Rena, R. Nores, L. C. Patrito, S. Genti-Raimondi and G. M. Panzetta-Dutari, "Expression and Transcriptional Regulation of Individual Pregnancy-specific Glycoprotein Genes in Differentiating Trophoblast Cells", *Placenta*, Vol. 31, No. 4, pp. 312–319, 2010.

50. Lee, C. Q., L. Gardner, M. Turco, N. Zhao, M. J. Murray, N. Coleman, J. Rossant, M. Hemberger and A. Moffett, "What Is Trophoblast? A Combination of Criteria Define Human First-Trimester Trophoblast", *Stem Cell Reports*, Vol. 6, No. 2, pp. 257–272, 2016.

51. Takahashi, K. and S. Yamanaka, "Induction of Pluripotent Stem Cells from Mouse Embryonic and Adult Fibroblast Cultures by Defined Factors", *Cell*, Vol. 126, No. 4, pp. 663–676, 8 2006.

52. Merkle, F. and K. Eggan, "Modeling Human Disease with Pluripotent Stem Cells: from Genome Association to Function", *Cell Stem Cell*, Vol. 12, No. 6, pp. 656–668, 6 2013.

53. Onder, T. T. and G. Q. Daley, "New lessons learned from disease modeling with induced pluripotent stem cells", *Current Opinion in Genetics & Development*, Vol. 22, No. 5, pp. 500–508, 10 2012.

54. Bellin, M., M. C. Marchetto, F. H. Gage and C. L. Mummery, "Induced pluripotent stem cells: the new patient?", *Nature Reviews Molecular Cell Biology*, Vol. 13,

No. 11, pp. 713–726, 11 2012.

55. Xu, R.-H., X. Chen, D. S. Li, R. Li, G. C. Addicks, C. Glennon, T. P. Zwaka and J. A. Thomson, "BMP4 initiates human embryonic stem cell differentiation to trophoblast", *Nature Biotechnology*, Vol. 20, No. 12, pp. 1261–1264, 12 2002.

56. Gamage, T. K., L. W. Chamley and J. L. James, "Stem cell insights into human trophoblast lineage differentiation", *Human Reproduction Update*, Vol. 23, No. 1, pp. 77–103, 2016.

57. Amita, M., K. Adachi, A. P. Alexenko, S. Sinha, D. J. Schust, L. C. Schulz, R. M. Roberts and T. Ezashi, "Complete and unidirectional conversion of human embryonic stem cells to trophoblast by BMP4.", *Proceedings of the National Academy of Sciences of the United States of America*, Vol. 110, No. 13, pp. 1212–21, 3 2013.

58. Yang, Y., K. Adachi, M. A. Sheridan, A. P. Alexenko, D. J. Schust, L. C. Schulz, T. Ezashi and R. M. Roberts, "Heightened potency of human pluripotent stem cell lines created by transient BMP4 exposure", *Proceedings of the National Academy of Sciences*, Vol. 112, No. 18, pp. E2337–E2346, 2015.

59. Yabe, S., A. P. Alexenko, M. Amita, Y. Yang, D. J. Schust, Y. Sadovsky, T. Ezashi and R. M. Roberts, "Comparison of syncytiotrophoblast generated from human embryonic stem cells and from term placentas", *Proceedings of the National Academy of Sciences*, Vol. 113, No. 19, pp. E2598–E2607, 2016.

60. Chen, H.-F., C.-Y. Yu, M.-J. Chen, S.-H. Chou, M.-S. Chiang, W.-H. Chou, B.-S. Ko, H.-P. Huang, H.-C. Kuo and H.-N. Ho, "Characteristic Expression of Major Histocompatibility Complex and Immune Privilege Genes in Human Pluripotent Stem Cells and Their Derivatives", *Cell Transplantation*, Vol. 24, No. 5, pp. 845–864, 5 2015.

61. Kumar, P. and C. R. Mendelson, "Estrogen-related receptor gamma (ERRgamma)

mediates oxygen-dependent induction of aromatase (CYP19) gene expression during human trophoblast differentiation.", *Molecular endocrinology (Baltimore, Md.)*, Vol. 25, No. 9, pp. 1513–26, 9 2011.

62. Haniffa M. et al., "Human Tissues Contain CD141hi Cross-Presenting Dendritic Cells with Functional Homology to Mouse CD103+ Nonlymphoid Dendritic Cells", *Immunity*, Vol. 37, No. 1, pp. 60–73, 7 2012.

63. Kocabas, A. M., J. Crosby, P. J. Ross, H. H. Otu, Z. Beyhan, H. Can, W.-L. Tam, G. J. M. Rosa, R. G. Halgren, B. Lim, E. Fernandez and J. B. Cibelli, "The transcriptome of human oocytes", *Proceedings of the National Academy of Sciences*, Vol. 103, No. 38, pp. 14027–14032, 9 2006.

64. Ulker, V., H. Gurkan, H. Tozkir, V. Karaman, H. Ozgur, C. Numanoglu, A. Gedikbasi, O. Akbayir and Z. Uyguner, "Novel NLRP7 mutations in familial recurrent hydatidiform mole: are NLRP7 mutations a risk for recurrent reproductive wastage?", *European Journal of Obstetrics & Gynecology and Reproductive Biology*, Vol. 170, No. 1, pp. 188–192, 9 2013.

65. Reddy R. et al., "The genomic architecture of NLRP7 is Alu rich and predisposes to disease-associated large deletions", *European Journal of Human Genetics*, Vol. 24, No. 10, pp. 1445–1452, 10 2016.

66. Ben-David U. et al., "Aneuploidy induces profound changes in gene expression, proliferation and tumorigenicity of human pluripotent stem cells", *Nature Communications*, Vol. 5, No. 1, p. 4825, 12 2014.

67. Donohoe, M. E., X. Zhang, L. Mcginnis, J. Biggers, E. N. Li and Y. Shi, *Targeted Disruption of Mouse Yin Yang 1 Transcription Factor Results in Peri-Implantation Lethality*, Tech. Rep. 10, 1999.

68. Kurisaki, K., A. Kurisaki, U. Valcourt, A. A. Terentiev, K. Pardali, P. Ten Di-

jke, C.-H. Heldin, J. Ericsson and A. Moustakas, "Nuclear factor YY1 inhibits transforming growth factor beta- and bone morphogenetic protein-induced cell differentiation.", *Molecular and cellular biology*, Vol. 23, No. 13, pp. 4494–510, 7 2003.

69. Bachir Affar, E., F. Gay, Y. Shi, H. Liu, M. Huarte, S. Wu, T. Collins, E. Li and Y. Shi, "Essential Dosage-Dependent Functions of the Transcription Factor Yin Yang 1 in Late Embryonic Development and Cell Cycle Progression", *Molecular and Cellular Biology*, Vol. 26, No. 9, pp. 3565–3581, 2006.

70. Thomas, M. J. and E. Seto, "Unlocking the mechanisms of transcription factor YY1: are chromatin modifying enzymes the key?", *Gene*, Vol. 236, No. 2, pp. 197–208, 8 1999.

71. Gordon, S., G. Akopyan, H. Garban and B. Bonavida, "Transcription factor YY1: structure, function, and therapeutic implications in cancer biology", *Oncogene*, Vol. 25, No. 8, pp. 1125–1142, 2 2006.

72. Shi, Y., J. S. Lee and K. M. Galvin, "Everything you have ever wanted to know about Yin Yang 1...", *Biochimica et Biophysica Acta - Reviews on Cancer*, 1997.

73. Shrivastava, A. and K. Calame, "An analysis of genes regulated by the multifunctional transcriptional regulator Yin Yang-1.", *Nucleic acids research*, Vol. 22, No. 24, pp. 5151–5, 12 1994.

74. Reddy R. et al., "Report of four new patients with protein-truncating mutations in C6orf221/KHDC3L and colocalization with NLRP7", *European Journal of Human Genetics*, Vol. 21, No. 9, pp. 957–964, 2013.

75. Roberts, R. M., T. Ezashi, M. A. Sheridan and Y. Yang, "Specification of trophoblast from embryonic stem cells exposed to BMP4†", *Biology of Reproduction*, Vol. 99, No. 1, pp. 212–224, 7 2018.

76. Skotheim R. I. et al., "Differentiation of Human Embryonal Carcinomas In vitro and In vivo Reveals Expression Profiles Relevant to Normal Development", *Cancer Research*, Vol. 65, No. 13, pp. 5588–5598, 7 2005.

77. Qin, H., M. Hejna, Y. Liu, M. Percharde, M. Wossidlo, L. Blouin, J. Durruthy-Durruthy, P. Wong, Z. Qi, J. Yu, L. S. Qi, V. Sebastiano, J. S. Song and M. Ramalho-Santos, "YAP Induces Human Naive Pluripotency", *Cell Reports*, Vol. 14, No. 10, pp. 2301–2312, 3 2016.

78. Chen, G., Z. Ye, X. Yu, J. Zou, P. Mali, R. A. Brodsky and L. Cheng, "Trophoblast Differentiation Defect in Human Embryonic Stem Cells Lacking PIG-A and GPI-Anchored Cell-Surface Proteins", *Cell Stem Cell*, Vol. 2, No. 4, pp. 345–355, 4 2008.

79. Takeda, T., M. Sakata, A. Isobe, T. Yamamoto, F. Nishimoto, R. Minekawa, M. Hayashi, Y. Okamoto, P.-Y. Desprez, K. Tasaka and Y. Murata, "Involvement of Sp-1 in the regulation of the Id-1 gene during trophoblast cell differentiation.", *Placenta*, Vol. 28, No. 2-3, pp. 192–8, 2007.

80. Fitzgerald, J. S., T. G. Poehlmann, E. Schleussner and U. R. Markert, "Trophoblast invasion: the role of intracellular cytokine signalling via signal transducer and activator of transcription 3 (STAT3)", *Human Reproduction Update*, Vol. 14, No. 4, pp. 335–344, 4 2008.

81. Soundararajan, R. and A. J. Rao, "Trophoblast 'pseudo-tumorigenesis': Significance and contributory factors", *Reproductive Biology and Endocrinology*, Vol. 2, No. 1, p. 15, 3 2004.

82. Wen, H., E. Miao and J.-Y. Ting, "Mechanisms of NOD-like Receptor-Associated Inflammasome Activation", *Immunity*, Vol. 39, No. 3, pp. 432–441, 9 2013.

83. Sharma, D. and T.-D. Kanneganti, "The cell biology of inflammasomes: Mecha-

nisms of inflammasome activation and regulation.", *The Journal of cell biology*, Vol. 213, No. 6, pp. 617–29, 6 2016.

84. Cai, S., S. Batra, N. Wakamatsu, P. Pacher and S. Jeyaseelan, "NLRC4 inflammasome-mediated production of IL-1β modulates mucosal immunity in the lung against gram-negative bacterial infection.", *Journal of immunology (Baltimore, Md. : 1950)*, Vol. 188, No. 11, pp. 5623–35, 6 2012.

85. Man S. M. et al., "Inflammasome activation causes dual recruitment of NLRC4 and NLRP3 to the same macromolecular complex.", *Proceedings of the National Academy of Sciences of the United States of America*, Vol. 111, No. 20, pp. 7403–8, 5 2014.

86. Arlehamn, C. S. L. and T. J. Evans, "Pseudomonas aeruginosa pilin activates the inflammasome.", *Cellular microbiology*, Vol. 13, No. 3, pp. 388–401, 3 2011.

APPENDIX A: MATERIALS

A.1. Equipments Used in the Project

Table A.1: Equipments.

Equipment	Supplier
Agarose Gel Electrophoresis System	Mini-sub Cell GT, BioRad, USA
Autoclaves	Midas 55, Prior Clave, UK ASB260T, Astell, UK
Balance	DTBH 210, Sartorius, GERMANY
CO2 Cell Culture Incubator	MCO-18AC, Sanyo, Japan
Carbon dioxide Tank	Genc Karbon, Turkey
Centrifuges	Ultracentrifuge J2MC, Beckman, USA VWR CT15RE, Japan Allegra X-22, Beckman USA
Cold room	Birikim Elektrik Soğutma, Turkey
Confocal Microscope	Leica SP8, USA
Countess, Cell Counter	Invitrogen, USA
Deepfreezers	(-20) Ugur, UFR 370 SD, Turkey (-80) Sanyo Ultra Low, UK (-150) Sanyo MDF-1156, UK
Dish Washer	Mielabor G7783, Miele, Germany
Documentation System	Gel Doc XR System, Bio-Doc, ITALY Stella, Raytest, Germany G-BOX Chemi XX6, Syngene, UK
Electrophoresis Equipments	Mini-Protean III Cell, Bio-Rad, USA
Flow Cytometer	Acuri C6, Becton Dickinson, USA

Table A.1. Equipments (cont.).

Equipment	**Supplier**
Heat blocks	NDI-2E Dry Bath Block Heater (Turkey), DBI-200 Series Incubator Dry Block Heater & Cooler (Turkey)
Hemocytometer	Improved Neubauer, Weber Scientific International Ltd, UK
Ice Machine	Scotsman Inc., AF20, ITALY
Ice Maker	Scotsman Inc. AF20, Italy
Inverted Microscope	Z1 Axio Observer, Zeiss, USA
Laboratory Bottles	Isolab, Germany
Laminal Flow Cabinet	Class II B, Tezsan, Turkey
Magnetic Stirrer	IKA RCT Classic, USA
Micropipettes	Finnpipette, Thermo, USA Axygen, USA, Axypipettes, USA Gilson,USA
Microplate Reader	680, Biorad, USA
Microscopes	Inverted Microscope, Nikon, Eclipse TS100, Netherlands, Fluoroscence Microscope, Observer.Z1, Zeiss, Germany
Microwave Oven	Arçelik, Turkey
Oven	Gallenkamp 300, UK
pH Meter	Hanna Instrumentsi, USA
Pipettor	VWR, USA
Power Supply	Power Pac Universal, Bio-Rad, USA
Power Supply	Bio-Rad, USA
Real-Time Quantitative PCR System	Bioneer Exicycler, Republic of Korea

Table A.1. Equipments (cont.).

Equipment	**Supplier**
Refrigerators	Ugur, USS 300 DTK, Turkey
Shakers	Polymax 1010, USA Polymax 1040, USA Heildophl, Germany
Softwares	Quantity One, Bio-Rad, ITALY ImageJ, Image Analysis Software, NIH, USA XStella 1.0, Stella, GERMANY FlowJo, USA, Syngene-Genetools, UK Leica LASX, USA
Sonicator	Sonicator & SonoPlus, Bandelin, Germany
Spectrophotometer	Agilent 8453, USA NanoDrop 1000, USA
Thermal Cyclers	Bio-Rad, USA
Transblot Turbo Transfer System	Bio-Rad, USA
Vacuum Pump	Vacusafe, Integra, Switzerland
Vortex	VWR, USA
Water purication	WA-TECH UP Water Purication Sys. Germany
Water purification system	UTES, TURKEY

Table A.2: Disposable Equipments.

Cell Culture Petri Dishes (145mm, 100 mm, 60 mm)	TPP, Switzerland
Cell Scraper	TPP, Switzerland
Centrifuge Tubes (15 ml, 50 ml)	CAPP, Denmark
Cover Slips	VWR, USA
Cryovial Tubes (2ml)	CAPP, Denmark
Microfuge Tubes (0.5ml, 1.5ml. 2ml)	CAPP, Denmark
Micropipette Tips	Axygen, USA
Multiwell Plates (6-well, 12-well, 24-well, 96-well)	TPP, Switzerland
PCR Tubes (0.2ml)	Axygen, USA
Petri Dishes	Fırat Plastik, Turkey
Pippette Tips (Bulk)	CAPP, Denmark
Pippette Tips (filtered)	CAPP, Denmark
Serological Pipettes (5ml, 10ml, 25ml)	CAPP, Denmark
Syringe Filter Units (0.22 μm, 0.45 μm)	EMD Millipore, USA
Syringes (1ml, 5ml, 10ml, 50ml)	Set Medikal, Turkey
Test Tubes (0.2 ml, 0.5 ml, 1.5 ml, 2 ml)	CAPP, Denmark
PVDF Membrane	Roche, Switzerland
Watmann Filter Paper-Extra Thick	Thermo Scientific, USA

APPENDIX B: PLASMID MAPS

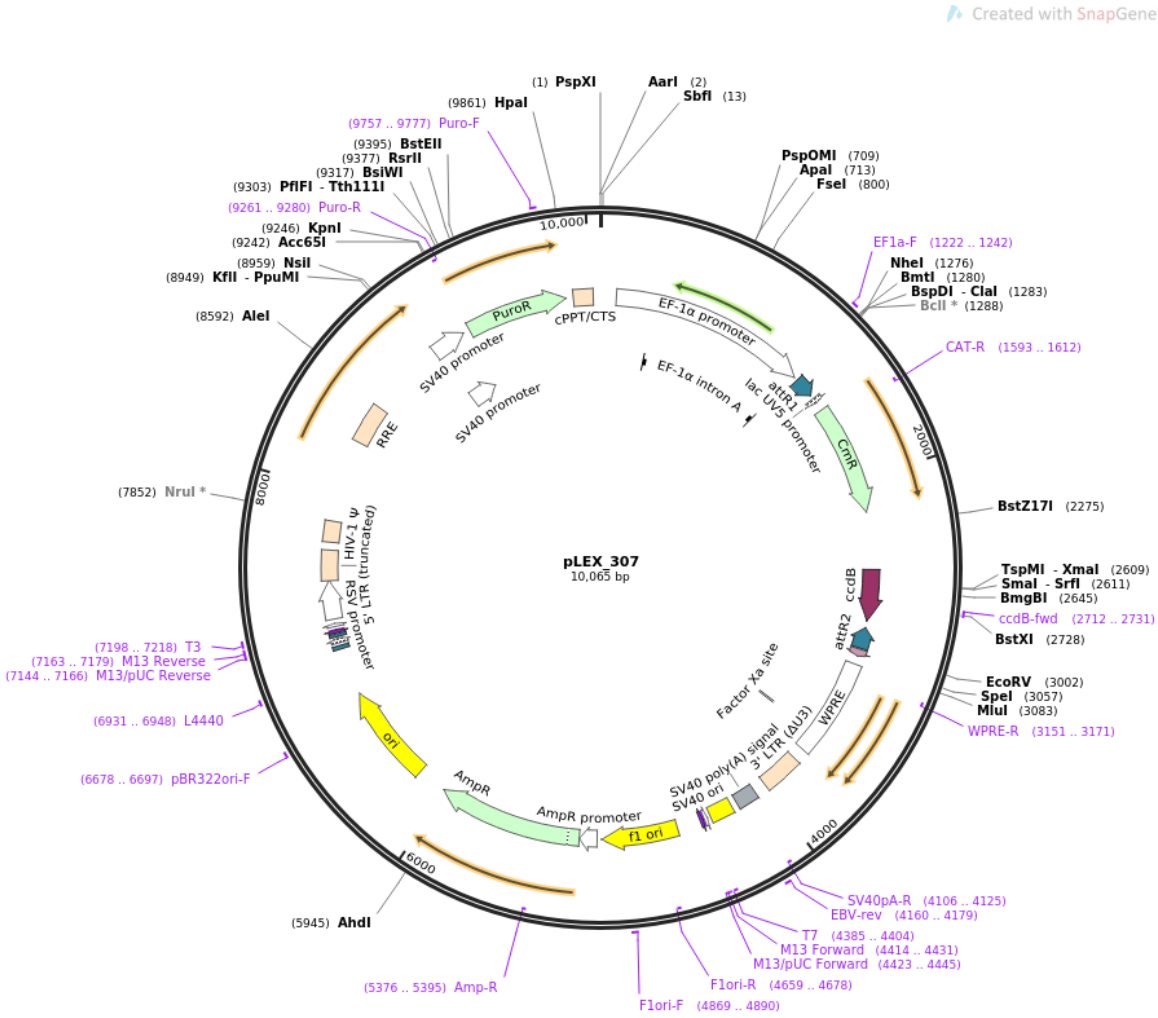

Figure B.1. Map of the pLEX-307 vector.

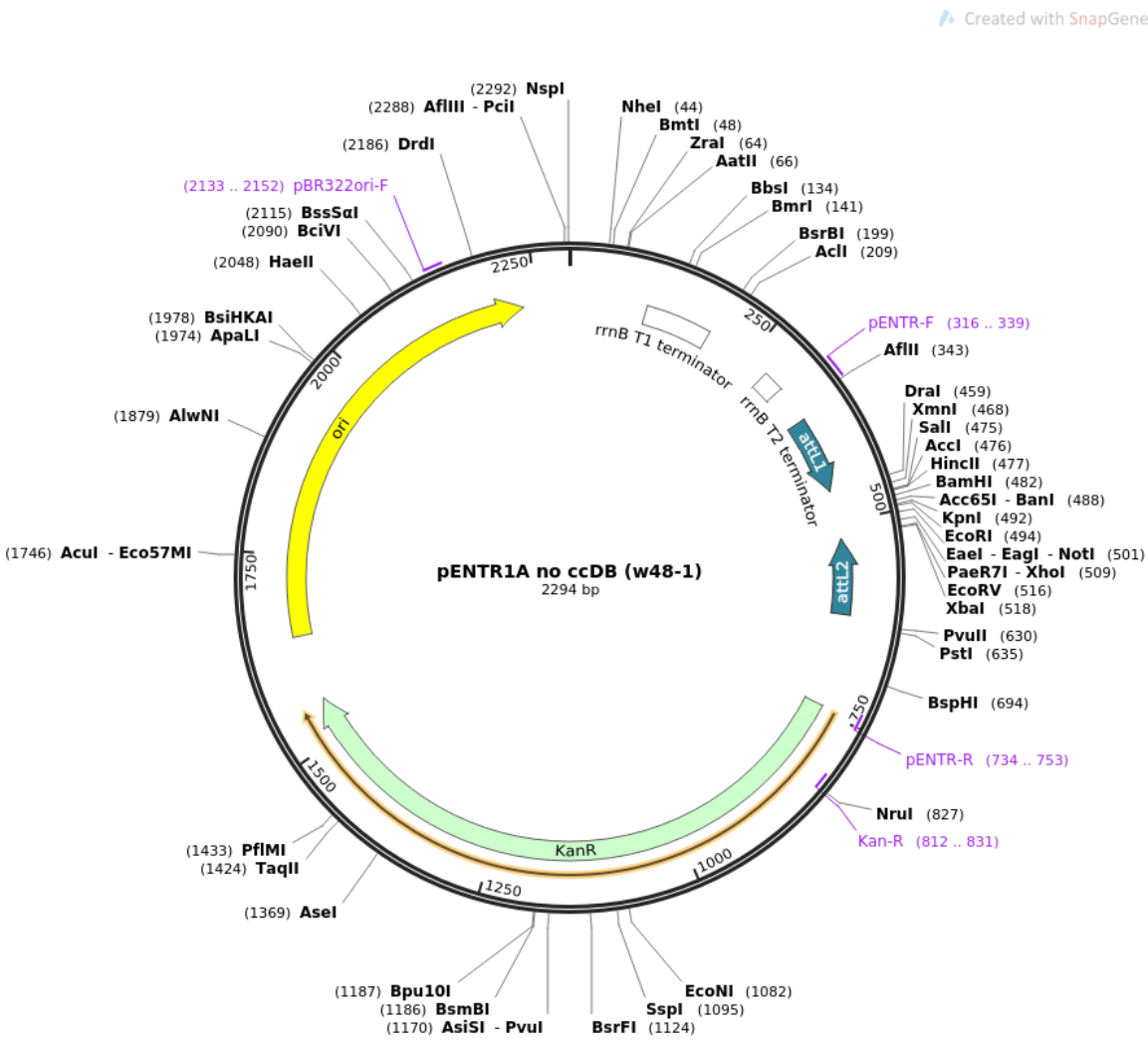

Figure B.2. Map of the pENTR1A no ccDB (w48-1) vector.

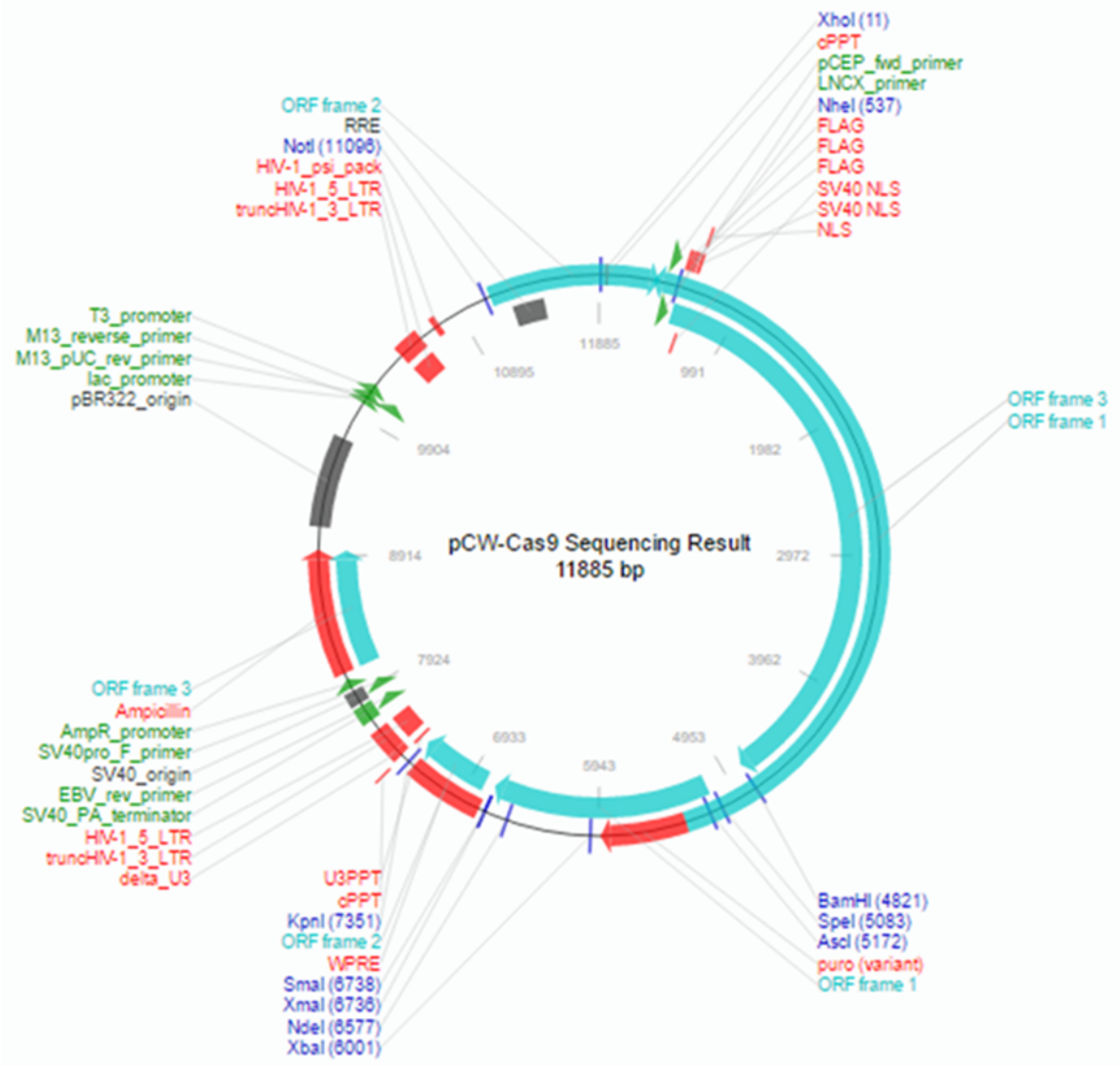

Figure B.3. Map of the pCW-Cas9 vector.

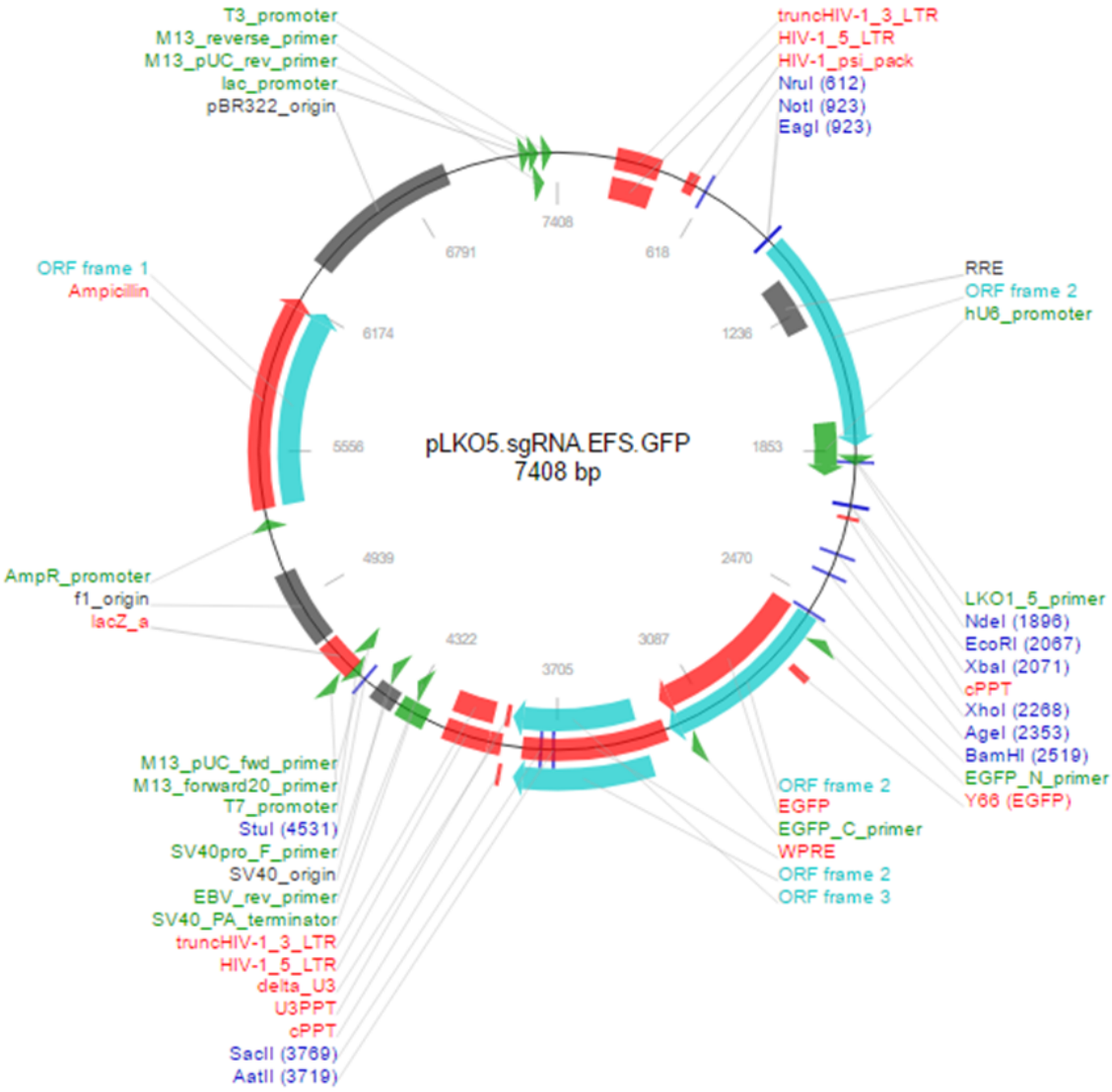

Figure B.4. Map of the pLKO5.sgRNA.EFS.GFP vector.